

**Proteomic approaches to understanding G protein beta gamma
subunit signalling networks**

Jennifer Y. Sung

Department of Pharmacology and Therapeutics
McGill University
Montreal, Quebec, Canada

December 2017

A thesis submitted to McGill University in partial fulfillment of the requirements of the degree
of Master's of Science

© Jennifer Y. Sung 2017

TABLE OF CONTENTS

TABLE OF CONTENTS.....	II
ABSTRACT.....	IV
RÉSUMÉ	V
ACKNOWLEDGEMENTS.....	VI
PREFACE AND CONTRIBUTION OF AUTHORS	VIII
LIST OF ABBREVIATIONS.....	IX
LIST OF TABLES AND FIGURES	XV
1. INTRODUCTION	1
1.1 Preface.....	1
1.2 What are GPCRs?.....	1
1.3 GPCR & Gβγ signalling.....	2
1.4 Gβγ cellular translocation across organelles	3
1.5 Gβγ non-canonical signalling at the nucleus.....	6
1.5.1 <i>Gβγ as regulators of transcriptional activity</i>	7
1.6 Gβγ non-canonical signalling at the Golgi apparatus	9
1.7 Gβγ non-canonical signalling at the mitochondria.....	11
1.7.1 <i>Gβγ involvement in mitochondria dynamics</i>	11
1.7.2 <i>Gβγ involvement in cellular respiration</i>	11
1.8 Gβγ and the cytoskeleton	12
1.8.1 <i>Chemotaxis</i>	12
1.8.2 <i>Cell adhesion</i>	13
1.8.3 <i>Microtubules</i>	13
1.9 Gβγ degradation	14
1.10 Thesis objectives and rationale	15
2. MATERIALS AND METHODS.....	18
2.1 Preface.....	18
2.2 Cell culture techniques.....	18
2.2.1 <i>Transient transfection</i>	18
2.3 Interaction validation immunoprecipitation and western blotting	19
2.3.1 <i>Anti-rabbit IgG agarose immunoprecipitation</i>	19
2.3.2 <i>Anti-HA immunoprecipitation</i>	19
2.3.3 <i>Western blotting</i>	20
2.4 KCTD5 KO HEK 293 cell line generation	20
2.4.1 <i>Cell culture</i>	20
2.4.2 <i>Mass spectrometry</i>	21
3. RESULTS	23
3.1 Preface.....	23
3.2 Pathway identification from Gβγ proteomics screen	23
3.2.1 <i>Gβγ and degradation pathways</i>	24
3.2.2 <i>Gβγ and other signalling pathways</i>	29
3.3 Validating Gβγ interactors from degradation pathways.....	42

3.3.1 <i>Gβγ</i> and the 26S proteasome.....	42
3.3.2 <i>Gβγ</i> and KCTD5.....	43
3.4 KCTD5 CRISPR knockout line generation and validation.....	45
3.4.1 <i>Background</i>	45
3.4.2 <i>Experimental design</i>	45
3.4.3 <i>Preliminary survey of KCTD5 gene indels</i>	46
3.4.4 <i>KCTD5 knockout single clone RFLP and sequencing</i>	46
3.4.5 <i>Mass spectrometry functional validation of KCTD5 knockout</i>	47
3.4.6 <i>Comparing <i>Gβγ</i> interaction landscapes between KCTD5 knockout and parental cell lines</i>	47
3.5 KCTD5 and 26S proteasome effects on <i>Gβγ</i> degradation and signalling.....	53
3.5.1 <i>Gβ1 degradation by the 26S proteasome</i>	53
3.5.2 <i>Gβ1 degradation by the 26S proteasome evaluated by LC-MS</i>	53
3.5.3 <i>KCTD5 effect on cellular <i>Gβγ</i> levels</i>	53
3.5.4 <i>KCTD5 effects on <i>Gβγ</i> and MAPK signalling</i>	54
3.5.5 <i>KCTD5 effects on <i>Gβγ</i> and the mTOR pathway</i>	54
4. DISCUSSION & CONCLUSIONS.....	58
4.1 <i>Gβγ</i> degradation as a mechanism for control of signal transduction	58
4.2 Ubiquitination of <i>Gβγ</i> for other cellular fates.....	58
4.3 Considerations for affinity purification mass spectrometry to study protein interactions ..	59
4.4 KCTD5 in modulating <i>Gβγ</i> signalling.....	61
4.4.1 <i>KCTD5 in modulating <i>Gβγ</i> degradation</i>	62
4.4.2 <i>KCTD5 and KCTD2 interactions with <i>Gβγ</i></i>	63
4.4.3 <i>KCTD interactors' known roles in GPCR signalling and therapeutic relevance</i>	63
4.5 Other areas to explore	64
4.6 Conclusions	65
REFERENCES	68
SUPPLEMENTAL MATERIAL.....	77

ABSTRACT

G protein-coupled receptors (GPCR) are the largest family of cell surface receptors and their signalling functions are important in every system in the human body. While their heterotrimeric G protein partners are key in signal transduction, within their composition of α and $\beta\gamma$ subunits the latter dimer remains relatively understudied. To expand our understanding of its roles in general, but specifically on $G\beta\gamma$ degradation and signalling effects, we used online databases of human biological pathways and functional protein association networks to analyze data previously extracted from $G\beta\gamma$ affinity purification coupled with mass spectrometry in a proteomic screen conducted in the Hébert lab. We were able to identify multiple putative degradation pathways, as well as novel pathways such as $G\beta\gamma$ interaction with the spliceosome, mitochondrial transport proteins and oxidative phosphorylation pathway components. We followed up with and validated $G\beta\gamma$ interaction with KCTD5, an adaptor for the Cullin-E3 ubiquitin ligase complex involved in protein degradation, and the 26S proteasome which degrades ubiquitinated proteins. In human embryonic kidney (HEK 293) cells, endogenous $G\beta\gamma$ was found to interact with the 26S proteasome, and expressed Flag- $G\beta 1$ protein levels accumulated when the cells were treated with the 26S proteasome inhibitor, MG132. A KCTD5 knockout HEK 293 cell line was generated and functionally validated, and preliminary results show KCTD5 knockout increases endogenous basal $G\beta\gamma$ protein levels in the cell and shifts $G\beta\gamma$ protein-protein interactor networks towards more metabolic proteins compared to the parental cell line. We found KCTD5 inhibits $G\beta\gamma$ signalling within the MAPK cascade, and discovered a novel $G\beta 1$ ubiquitination site on lysine 209 which was independent of KCTD5. This work created a basis on which future research may be done to study how degradation affects $G\beta\gamma$ and GPCR signalling, and generated multiple directions for future research in other areas including its spliceosomal and mitochondrial roles.

RÉSUMÉ

Les récepteurs couplés aux protéines G (RCPG), qui représentent la plus grande famille de récepteurs à la surface cellulaire, jouent d'importants rôles dans la signalisation cellulaire de plusieurs systèmes du corps humain. Bien que les protéines G hétérotrimériques qui leur sont associés soient au centre de la transduction de signal, le rôle spécifique des dimers $G\beta\gamma$ reste à éclaircir. Afin d'élucider cette question, et plus spécifiquement afin de mieux comprendre la fonction de la dégradation des $G\beta\gamma$ et de ses effets sur la signalisation, des bases de données sur des voies de signalisation biologiques dans les cellules humaines et des réseaux d'association de protéines fonctionnelles ont été utilisées afin d'analyser des données obtenues dans le laboratoire du Dr. Hébert suivant la purification par affinité de $G\beta\gamma$ suivie par analyse en spectrométrie de masse. Plusieurs voies de dégradation potentielles ont ainsi été identifiées, incluant de nouvelles interactions entre les protéines $G\beta\gamma$ et le spliceosome, des protéines de transport mitochondriales ou des composantes impliquées dans le processus de la phosphorylation oxydative. Nous nous sommes concentrés sur l'étude de l'interaction avec KCTD5, une protéine adaptatrice pour le complexe de l'ubiquitine ligase Cullin-E3, et le protéasome 26S, responsable de la dégradation des protéines ubiquitinées. Dans les cellules embryonniques rénales HEK 293, l'interaction de $G\beta\gamma$ endogène avec le protéasome 26S a été confirmée et il a été observé que MG132, l'inhibiteur du protéasome 26S, augmente les niveaux d'expression de la protéine Flag- $G\beta 1$. Nous avons développé une lignée HEK 293 fonctionnelle invalide pour le gène KCTD5, et nos données préliminaires démontrent que cette invalidation augmente les niveaux d'expression de base des protéines $G\beta\gamma$ et modifie leur réseau d'interaction pour des protéines dites plus métaboliques lorsque comparé à la lignée parentale. Nous avons découvert que KCTD5 inhibe la signalisation induite par les protéines $G\beta\gamma$ dans la cascade des MAPK et un nouveau site d'ubiquitination a été identifié, soit celui de la lysine 209 de $G\beta 1$, dont l'ubiquitination s'avère indépendante de la présence de KCTD5. Ce projet a permis d'établir une nouvelle avenue pour l'étude des effets de la dégradation des protéines $G\beta\gamma$ sur la signalisation induite par l'activation des RCPG et a également ouvert la voie pour d'autres domaines de recherche portant notamment sur les rôles potentiels aux niveaux de la mitochondrie et du spliceosome.

ACKNOWLEDGEMENTS

There are many people I would like to thank because without their support this thesis would not be possible. I would like to express gratitude first and foremost to my thesis supervisor Dr. Terry Hébert of the Department of Pharmacology and Therapeutics at McGill University who allowed to me complete my MSc thesis in his lab. I am grateful for his understanding and his trust in my work, and for always being available to steer me in the right direction. His door was always open for any questions I had, and his patience, guidance and optimism helped me stay motivated. Lastly I want to express my appreciation for his meticulous editorial work, giving me valuable feedback and helping editing manuscripts, presentations and last but not least, this thesis.

I would like to thank Dr. Jean-François Trempe, Department of Pharmacology and Therapeutics, McGill University for his expertise and guidance with liquid chromatography-mass spectrometry sample preparation, optimization, data extraction and analysis.

Special thank you to my thesis advisory committee, Dr. Bruce Allen, Dr. Jason Tanny, and Dr. Paul Clarke. Your input and feedback was invaluable and the experience of presenting at committee meetings has taught me to how to better organize and present my project as well as think critically to answer difficult scientific questions.

I would like to a give a huge thank you to members of the Hébert lab. Knowing I could always see a friendly face in the lab, and their knowledge and support were instrumental in helping me complete my thesis. I would like to thank Rhiannon Campden in particular, because without her mass spectrometry work on G β γ functions in the nucleus this thesis would not be possible. To Dr. Dominic Devost specifically for his expertise and guidance on experimental design and setup of the KCTD5 CRISPR knockout cell line project, but in general for always making time to answer my questions, and for all the optimistic discussions that kept me motivated. To Darlaine Pétrin for her KCTD5 and G β γ interaction validation, and her tireless and high quality work studying pAKT signalling. To Phan Trieu, without whose organization of the lab and supplies the experiments presented in this thesis would not have been possible. To

Dr. Nicolas Audet, for his knowledge and expertise on seemingly everything and for being an excellent bench mate. To Dr. Richard Wargachuk for his general helpfulness and his work on validating the KCTD5-Flag construct used in this thesis. To Ryan Martin and Dr. Rory Sleno for being great friends and lab mates, and who could always be counted on to talk or argue about science, politics and graduate student life. To Dr. Shahriar Khan for his collaboration on our co-first authored 2016 review, and his guidance on my PHAR 599 undergraduate project work. To all the Hébert lab mates who have left, passed through briefly, or are currently still there- thank you for your kindness and being great lab mates, because it made for a great experience every day in the lab.

I want to thank members of the Department of Pharmacology and Therapeutics. Thank you to Tina Tremblay, Chantal Grignon and Anna Cuccovia from the department teaching support and administrative staff for always having kind words and your helpfulness throughout my studies. To Dr. Dusica Maysinger, Dr. Lisa Munter, and Dr. Dan Bernard for being great professors to work for and making my teaching assistant experience fun and educational. To the Graduate Association of Pharmacology and Therapeutics Students (GAPTS) for a great experience as both a member of the main council and as a member and participant at your events. To all the friends I've made in the department for your encouragement and support throughout.

Last but not least, I want to thank my family and friends for their unending support and encouragement. You know who you are, but I want to specifically thank Jad Habbal and Stephanie Sung.

This thesis work was supported by grants from the Canadian Institute of Health Research (CIHR; MOP-130909 to Terry Hébert), a Natural Sciences and Engineering Research Council of Canada (NSERC) Canada Graduate Scholarship-Master's Program, and Graduate Excellence Fellowships from the Department of Pharmacology and Therapeutics, McGill University.

PREFACE AND CONTRIBUTION OF AUTHORS

Unless stated below, the chapters of this thesis are authored by Jennifer Y. Sung, and edited by Terry Hébert

Chapter 1: introduction features an adaption of our 2016 review “Gβγ subunits- different spaces, different faces” (1) authored by Shahriar M. Khan, Jennifer Y. Sung, Terence E. Hébert, where Khan and Sung were both co-first authors.

Chapter 2: materials and methods section 2.4 was based on guidance from Dr. Dominic Devost, Hébert lab. Sections 2.4.2.3- 2.4.2.4 methods were obtained from Dr. Jean-François Trempe, McGill University. The remaining methods in Chapter 4 are from the Hébert lab.

Chapter 3: In Section 3.4.2, the experimental design was designed by Dr. Dominic Devost, Hébert lab. He also optimized the experimental set-up described in Figure 8, and performed the experiment shown in Figure 3. Darlaine Pétrin, Hébert lab, performed the experiment shown in Figure 4.

LIST OF ABBREVIATIONS

AEBP1: adipocyte enhancer-binding protein
Akt: protein kinase B
AP-1: activator protein 1
APO1: optic atrophy 1
ARS2: arsenite resistance protein 2
AT1R: angiotensin II type 1 receptor
AT2R: angiotensin II receptor type 2
ATP: adenosine triphosphate
ATPase: adenosine triphosphatase
Bp: basepair
BSA: bovine serum albumin
BTB: Bric-a-brack, Tram-track, Broad complex
cAMP: cyclic AMP
cAR1: cAMP receptor 1
Cas9: CRISPR-associated 9
CB₁: Cannabinoid Receptor 1
CBC: cap-binding complex
CCh: carbachol
CCT: chaperonin containing TCP-1
Cdc42: cell division cycle 42 protein
CDK9: cyclin-dependent kinase 9
cFos: cFBJ murine osteosarcoma viral oncogene homolog B
ChIP: chromatin immunoprecipitation
Co-IP: co-immunoprecipitation
COX2: mitochondrially-encoded prostaglandin-endoperoxide synthase 2,
COX4I1: cytochrome c oxidase subunit 4I1
COX5A: cytochrome c oxidase subunit 5A
COX7A2: cytochrome c oxidase subunit 7A2
CREB: cAMP response element binding protein

CRISPR: clustered regularly interspersed short palindromic repeats

CUL: cullin

CXCR4: chemokine receptor type 4

CYC1 : cytochrome c1

D2-R: D2 dopamine receptor

DAG: diglyceride

DMEM: Dulbecco's Modified Eagle Medium

DRiP78: dopamine receptor-interacting protein 78

Drp1: dynamin 1-like

DSB : double stranded break

DTT: dithiothreitol

DUB: deubiquitinase

ElmoE: engulfment and cell motility E

Epac1: exchange factor activated by cAMP

ER: endoplasmic reticulum

ERK: extracellular signal-regulated kinase

EtBr: ethidium bromide

GABA: gamma-Aminobutyric acid

gDNA : genomic DNA

GDNF: glial cell-derived neurotrophic factor

GEF: guanine exchange factor

GEMIN: gem nuclear organelle associated protein

GGL: Gy-like

GPCR- G protein-coupled receptor

GRK2: G protein receptor kinase 2

GTP: guanosine triphosphate

GTPase: guanosine triphosphate hydrolase

GWAS: genome-wide association study

HDAC5: histone deacetylase 5

HEK: Human Embryonic Kidney

hnRNP: heterologous ribonuclear protein

HPLC: high performance liquid chromatography
IB : immunoblotting
ICAM-1: intercellular adhesion molecule 1
IGF-1: insulin growth factor-1
IL-2: interleukin-2
IMM: inner mitochondrial membrane
IP: immunoprecipitation
IP3R1: Inositol 1,4,5-trisphosphate (IP3) receptor type 1
JAK: Janus kinase
Kir3: G protein-coupled inwardly-rectifying potassium channel
LC-MS: liquid chromatograph-mass spectrometry
M3-R M3 muscarinic acetylcholine receptors
mAKAP: A kinase anchoring protein
MAPK- mitogen-activated protein kinase
MEF2: myocyte enhancer factor-2
mRNA: messenger ribonucleic acid
MRPL12: mitochondrial ribosomal protein L12
MRPL17: mitochondrial ribosomal protein L17
MRPL4: mitochondrial ribosomal protein L4
MRPL43: mitochondrial ribosomal protein L43
MRPL46: mitochondrial ribosomal protein L46
MRPL49: mitochondrial ribosomal protein L49
MRPS18B: mitochondrial ribosomal protein S18B
MRPS27: mitochondrial ribosomal protein S27
MRPS35: mitochondrial ribosomal protein S35
MRPS5: mitochondrial ribosomal protein S5
MS: mass spectrometry
mtDNA: mitochondrial DNA
mTOR: mechanistic target of rapamycin
NADH: nicotinamide adenine dinucleotide
nDNA: nuclear DNA

NDUFA4: NADH Dehydrogenase (Ubiquinone) 1 Alpha Subcomplex 4
NDUFA9: NADH Dehydrogenase (Ubiquinone) 1 Alpha Subcomplex 9
NDUFS1: NADH:Ubiquinone Oxidoreductase Core Subunit S1
NDUFS2: NADH:Ubiquinone Oxidoreductase Core Subunit S2
NDUFS3: NADH:Ubiquinone Oxidoreductase Core Subunit S3
NDUFS7: NADH:Ubiquinone Oxidoreductase Core Subunit S7
NDUFS8: NADH:Ubiquinone Oxidoreductase Core Subunit S8
NFAT: nuclear factor of activated T-cells
NFκB: nuclear factor kappa-light-chain-enhancer of activated B cells
NHEJ : non-homologous end joining
NIS: sodium-iodide transporter
P-Rex1: PIP₃-dependent Rac exchanger
P-TEFb: positive transcription elongation factor b
PAK1: p21-activated kinase 1
pAKT: phosphorylated AKT
PAM : protospacer adjacent motif
PAQR3: progestin and adipoQ receptor 3
PAR2: protease-activated-receptor 2
PAX8: paired box gene 8
PBS: phosphate-buffered saline
PCNA: proliferating cell nuclear antigen
PCR: polymerase chain reaction
pERK1/2: phosphorylated ERK1/2
Pfetin: Predominantly Fetal Expressed T1 Domain
PHAX: phosphorylated adaptor RNA export
PhLP1: phosducin-like protein 1
PI2P: phosphatidylinositol 4,5-bisphosphate
PI3K: phosphoinositide 3-kinase
PI4P: phosphatidylinositol 4-phosphate
PIP₃: phosphatidylinositol (3,4,5)-trisphosphate
PIXα: PAK-associated guanine exchange factor

PKD: protein kinase D
PLC: phospholipase C
PRMT5: Arg *N*-methyltransferase 5
PSMC1: proteasome 26S subunit ATPase 1
PSMC2: proteasome 26S subunit ATPase 2
PSMC3: proteasome 26S subunit ATPase 3
PSMC4: proteasome 26S subunit ATPase 4
PSMC6: proteasome 26S subunit ATPase 6
PSMD1: proteasome 26S subunit non-ATPase 1
PSMD11: proteasome 26S subunit non-ATPase 11
PSMD13: proteasome 26S subunit non-ATPase 13
PSMD2: proteasome 26S subunit non-ATPase 2
PSMD3: proteasome 26S subunit non-ATPase 3
PSMD7: proteasome 26S subunit non-ATPase 7
PSMD7: proteasome 26S subunit, non-ATPase 7
PTEN: phosphatase and tensin homolog
PVDF: polyvinylidene fluoride
R7BP: R7-binding protein
RACK1: receptor for activated C kinase 1
Raf: rapidly accelerated fibrosarcoma
RFLP: restriction fragment length polymorphism
RGS: regulator of G protein signalling
RNA: ribonucleooc acid
RNAi: RNA interference
RNAPII : RNA polymerase II
Rpm: revolutions per minute
RTKG: Raf kinase trapping to the Golgi apparatus
SDS-PAGE: sodium dodecyl sulfate-polyacrylamide gel electrophoresis
SDS: sodium dodecyl sulfate
sgRNA: single guide RNA
siRNA : small interfering RNA

SMN: survival motor neuron
SNP: single-nucleotide polymorphism
snRNA: small nuclear RNA
snRNP: small nuclear ribonucleo proteins
SNRPB: Small nuclear ribonucleoprotein-associated protein B
SNRPD2: Small nuclear ribonucleoprotein-associated protein D2
SNRPD3: Small nuclear ribonucleoprotein-associated protein D3
SNRPE: Small nuclear ribonucleoprotein-associated protein E
SNRPG: Small nuclear ribonucleoprotein-associated protein G
SPN: snuportin
STAT: signal transducer and activator of transcription protein
TAP: tandem affinity purification
TFA: trifluoroacetic acid
TFIIS: transcription factor IIS
TGS1: trimethylguanosine synthase 1
TIM: translocase of the inner membrane
TIMM8A: translocase of the inner mitochondrial membrane 8A
TMG: trimethylguanosine
TOM: translocase of the outer membrane
TOMM22: translocase of outer mitochondrial membrane 22
TSH: thyroid stimulating hormone
Ub: ubiquitin
UBE2N: ubiquitin conjugating enzyme E2 N
UBE2V2: ubiquitin conjugating enzyme E2 V2
UBR4: ubiquitin protein ligase E3 component N-recognin 4
UBR5: ubiquitin protein ligase E3 component N-recognin 5
WT: wildtype
XPO1: exportin 1
Zif268: zinc finger protein 225
 δ -OR: δ -opioid receptor
 β ARK: C-terminal domain (β ARK-CT) of G protein receptor kinase 2

LIST OF TABLES AND FIGURES

Figure 1: Emerging non-canonical effectors regulated by Gβγ	5
Table 1: Gβγ interacts with multiple KCTDs	25
Table 2: Gβγ interacts with 26S proteasome components in the cytosol	27
Table 3: Gβγ interacts with ubiquitin ligases in the cytosol and nucleus	29
Figure 2: Maturation of the snRNA requires nuclear and cytoplasmic regulatory steps.....	32
Table 4: Gβγ interacts with ubiquitin ligases in cytosol and nucleus.....	34
Table 5: Gβγ interacts with oxidative phosphorylation pathway components	39
Table 6: Gβγ interacts with mitochondrial protein translocation components	41
Table 7: Gβγ interacts with mitochondrial ribosomal components	42
Figure 3: Validating PSMD7, Gβ interaction using immunoprecipitation and western blot	44
Figure 4: Validating KCTD5, Gβγ interaction using immunoprecipitation and western blot.....	44
Table 8: Optimized PCR conditions for amplification of KCTD5 sgRNA gene target	48
Figure 5: Detecting DNA mutations and indels.....	49
Figure 6: RFLP screen for KCTD5 gene disruption by CRISPR/Cas9 and KCTD5 sgRNA	49
Table 9: Comparing KCTD5 CRISPR/Cas9 single clone gene sequences.....	50
Table 10: loss of KCTD5 leads to Gβγ interaction shift towards metabolic proteins	52
Figure 7: Short time course of Flag-Gβ1 turnover	55
Figure 8: KCTD5 associated with trend of decreasing endogenous Gβγ levels.....	56
Figure 9: KCTD5 effect on MAPK signalling.....	56
Figure 10: KCTD5 and Gβγ effect on AKT phosphorylation	57
Figure 11: KCTD5 effect on Flag-Gβ1 degradation by the 26S proteasome	62
Supplemental Table 1: Full names for proteins from Thesis Chapter 3.2 and 3.4	80
Supplemental Table 2: Full list of Gβγ protein interaction changes with KCTD5 KO.....	88

1. INTRODUCTION

1.1 Preface

The introduction chapter 1 of the thesis features work from an adaptation of “Gβγ subunits- different spaces, different faces” (1) authored by Shahriar M. Khan, Jennifer Y. Sung, Terence E. Hébert, where Khan and Sung are co- first authors.

1.2 What are GPCRs?

There are over 800 known and predicted diverse human G protein-coupled receptors (GPCRs) phylogenetically categorized into 5 large families: Glutamate, Rhodopsin, Adhesion, Frizzled/Taste2, and Secretin, and they play an essential role for growth and development. GPCRs may be found in various systems within the body, including endocrine, neural, paracrine, and are involved in most senses including vision, smell, and taste (2). In addition to their importance in human physiology, their ability to act as successful therapeutic targets consolidates their relevance to drug discovery. The angiotensin II type 1 receptor (AT1R) is a GPCR that is involved in the homeostasis of cardiovascular and renal systems. Its chronic overstimulation can result in cardiovascular disease states such as hypertension, cardiac hypertrophy, renal diseases among others, and these conditions can be treated with AT1R antagonists from the sartan family (3). In general GPCRs are eminently druggable, representing almost half of drug targets as discovered by an analysis of FDA-approved drugs from the past three decades (4). Approximately one third of drugs target GPCRs and in addition to their therapeutic relevance, their financial viability is an asset where for example 63 of 200 drugs with the highest grossing sales in 2009 in the United States targeted GPCRs.

GPCRs are large membrane proteins with an extracellular N-terminus, 7 transmembrane domains consisting of consecutive transmembrane helices joined through alternating intra- and extracellular loops, and an intracellular C-terminus tail. GPCR have specific ligand binding pockets which are determined by their N-terminus sequence, arrangement of extracellular loops

and transmembrane domains. This allows for reception of a ligand by the extracellular side and leads to a contraction at the binding site and opening of the cytoplasmic side, activating G proteins and subsequent signal transduction (5). The heterotrimeric G protein partner consists of a $G\alpha$ GTPase subunit that is GDP-bound to the G protein $\beta\gamma$ dimer at resting state. Change in GPCR conformation after ligand binding allows GDP exchange for GTP and leads to G protein dissociation from the receptor, disengagement of $G\alpha$ from $G\beta\gamma$, and both to independently engage downstream effectors (6). Analysis of known GPCR structures highlights the importance of the G protein as a convergence point for GPCR activation pathways despite their structural diversity and diverse signalling paradigms (5).

1.3 GPCR & $G\beta\gamma$ signalling

The ability of GPCRs to translate diverse stimuli into varied intracellular signalling events is reflected by their evolutionary success. GPCRs or similar 7-transmembrane-containing proteins have been identified in 5 of 6 kingdoms of life: Bacteria, Plantae, Protozoa, Fungi, and Animalia with the latter three having the ability to interact with G proteins as an additional signaling modality (2). GPCRs dominate as one of the key signalling modules in eukaryotes (7), and in humans they are the largest receptor family.

Despite GPCR sequence diversity, their modular components remain conserved and activation of heterotrimeric G proteins remains an important part of signalling. $G\beta\gamma$ subunits are best known as the dimer component of the heterotrimeric G protein that couples to the GPCR family. $G\beta\gamma$ subunits are obligate dimers, of which there are 5 $G\beta$ isoforms and 12 $G\gamma$ isoforms in mammals, which interact with one of 21 $G\alpha$ isoforms to form the G protein heterotrimer. In this heterotrimer state they interact with GPCRs and can transduce extracellular stimuli to various downstream signaling cascades within the cell. Although understudied compared to $G\alpha$ subunits, there is a great deal known regarding the roles that $G\beta\gamma$ subunits generally play in signal transduction (reviewed in (8-10)). One striking feature regarding mammalian $G\beta\gamma$ subunits remains their diversity. Although $G\beta$ 1-4 subunits share 78-88% identity over their approximately 340 amino acid sequences (reviewed in (9, 11)), $G\beta$ 5 is structurally distinct from the other $G\beta$ subunits, sharing only 50% sequence identity. $G\gamma$ subunits are more structurally diverse than the

G β subunits, sharing 27-76% sequence homology (9, 11). Many studies have also reported specific roles for individual G β and G γ subunits, but we still do not have a precise view of their individual functions. Roles for individual G β and G γ subunits have been suggested using antisense and RNA interference (RNAi) approaches and the roles they play in receptor signalling pathways as well as embryonic development have been characterized in animal knockout models (12-27). To date, most of these studies have focused on canonical effectors, mainly localized to the plasma membrane. However, this thesis will focus on a growing number of non-canonical effectors and pathways which have also been identified to be influenced by G $\beta\gamma$ (reviewed in (9), Figure 1). In this thesis, when we refer to a specific G β or G γ subunit- this assumes they are partnered in the context of a G $\beta\gamma$ dimer. We know of no instances where they function alone.

1.4 G $\beta\gamma$ cellular translocation across organelles

Biosynthesis of G β and G γ subunits is a tightly regulated process that involves the functions of various chaperones that include phospholipase-like protein 1 (PhLP1), chaperonin containing TCP-1 (CCT) and dopamine receptor-interacting protein 78 (DRiP78) at the endoplasmic reticulum (28-32). Upon their biosynthesis, G $\beta\gamma$ subunits interact with components of nascent signalling complexes, i.e. GPCRs, G α subunits and various effectors, at the ER and are trafficked to the cellular membrane as a complex ((33-35), reviewed in (8)). These studies describe one instance of G $\beta\gamma$ -mediated sorting of signalling complexes in the ER prior to trafficking to the plasma membrane, however, there are several instances where G $\beta\gamma$ subunits have been implicated beyond such biosynthesis-dependent, intracellular translocation events to be in other cellular compartments as part of signalling modules.

Due to the capability of G γ subunits to be isoprenylated, it was believed once that G $\beta\gamma$ subunits were localized strictly to the plasma membrane. Recent studies of G $\beta\gamma$ subcellular localization have shown that they are also present on various endomembranes and compartments that include the Golgi apparatus, ER, mitochondria and nucleus ((36) (37-41), reviewed in (8, 42, 43)). G $\beta\gamma$ translocation was previously thought to be limited to certain combinations of G $\beta\gamma$ with particular G γ subunits, but it has been found that all 12 G γ subunits are capable of supporting

Gβγ translocation, albeit with varying kinetics under basal and GPCR stimulation conditions ((44), reviewed in (42)). This suggests Gβγ translocation is a general phenomenon following receptor activation and may provide explanations for the many of the non-canonical roles Gβγ dimers play in cellular signalling. Examples of such known non-canonical roles include but are not limited to- the regulation of microtubule dynamics, control of intracellular anterograde and retrograde trafficking from the Golgi apparatus, and signalling complex assembly in the endoplasmic reticulum.

With respect to how Gβγ might be involved in the translocation of other signalling proteins and complexes, translocation of extracellular signal-regulated kinase 1/2 (ERK1/2) to the nucleus serves as an excellent example. A role for Gβγ subunits in this translocation event was described where a unique autophosphorylation event on ERK1/2 at Thr188 which results in phosphorylation of nuclear targets that lead to cardiac hypertrophy (Figure 1, Box F) (45). This novel regulatory event was found to be induced by Gβγ signalling, downstream of the activation of the Raf-Mek-ERK cascade whereby hypertrophic stimuli induced interaction of Gβγ with Raf1 and ERK1/2 that was dependent on ERK2 dimerization, resulting in autophosphorylation of and subsequent nuclear localization of ERK1/2 (45, 46). What happened to Gβγ itself in this process (i.e. whether it shuttled to the nucleus alongside the Thr188-phosphorylated ERK1/2) remains unknown.

Even the most structurally distinctive subunit in the Gβ family, Gβ5 is also capable of nuclear translocation (Figure 1G). Gβ5 preferentially forms obligate dimers with the Gγ-like (GGL) domain-containing R7- regulator of G protein signalling (R7-RGS) family of proteins (47). Cellular distribution and nuclear targeting of Gβ5-R7-RGS is believed to involve the R7-binding protein (R7BP) (48-50). Palmitoylation of R7BP anchors it to the plasma membrane, however, a recent study demonstrates that mutant R7BP lacking the N-terminal Disheveled, EGL-10, pleckstrin homology domain displays marked decreases in nuclear localization (51). Gβ5 nuclear localization was assessed in neurons and brains from R7BP knockout mice and it was found that Gβ5-R7-RGS displays 50-70% less localization (51). This suggests that R7BP is central to the nuclear localization of Gβ5-R7-RGS.

1.5 Gβγ non-canonical signalling at the nucleus

Increasing evidence suggests that GPCRs reside on the nuclear envelope where they have distinct signalling profiles compared to their counterparts at the cell surface. However, specific and distinct roles for individual Gβγ subunits in the nuclear compartments are not fully defined and mostly unknown (52). Nuclear effects of Gβγ dimers are novel in concept and are only beginning to be understood (43). We focus here on updating this story with results of more recent studies since we wrote our last review on the subject. Using a tandem affinity purification (TAP)-based proteomics screen, we noted that Gβγ subunits are present in the nucleus and change their interactions with partner proteins in response to GPCR activation. Examples of such newly defined interactors include members of the heterologous nuclear ribonucleoprotein family (hnRNP, Figure 1, Box A), proteins involved in nuclear import and export such as importin 7 and exportin 1 (Figure 1, Box B), and transcription factors such as NFκB (Figure 1, Box C) (41), reviewed in (43)). To further elucidate novel roles for Gβγ subunits in nuclear signalling, we recently demonstrated that not only is signalling downstream of endogenous M3 muscarinic acetylcholine receptors (M3-R) in human embryonic kidney (HEK) 293 cells mediated by specific Gβ and Gγ subunit types, but also that knockdown Gβ1 paradoxically resulted in increased M3-R mediated signalling outputs of proximal effectors, as well as changes to expression of effectors such as ERK1/2. Moreover, we demonstrated that Gβ1 can associate with more than 700 promoters using a chromatin immunoprecipitation (ChIP) on chip approach, including that of Gβ4 (Figure 1, Box D), further suggesting roles for Gβ1 beyond canonical signalling, alluding to roles for specific Gβ subunits in gene expression regulation (27). Furthermore, other studies have suggested nuclear action for Gβγ downstream of angiotensin II type 1 receptor (AT1R) signalling. For example, it was demonstrated Ang II-mediated activation of AT1R results in the nuclear translocation of Gβ2 subunits where it was found to interact with core histones and proteins that modulate transcription. Knockdown of Gβ2 led to a repression of AT1R-stimulated myocyte enhancer factor-2 (MEF2) transcriptional activity, via a specific interaction motif of Gβ2 found on various transcription factors (53). This latter study added significantly to our growing understanding of nuclear roles of Gβγ in GPCR-mediated regulation of gene transcription via interaction with chromatin-bound transcription factors.

1.5.1 Gβγ as regulators of transcriptional activity

GPCR signalling pathways and the effectors modulated by G proteins have previously been shown to converge on the regulation of gene expression (reviewed in (54)). In particular, Gβγ dimers are also involved in such pathways (Figure 1, Box E). Gβγ subunits have been implicated in thyroid differentiation (55). Activation of thyrotropin receptor by thyroid stimulating hormone (TSH) causes Gas activation, increases in intracellular cAMP and a subsequent increase in gene transcription of the gene for the sodium-iodide transporter (NIS) via binding of paired box gene 8 (Pax8) to the NIS promoter (55). Inhibition of Gβγ by sequestration using a membrane-localized version of the C-terminal domain (βARK-CT) of G protein receptor kinase 2 (GRK2, βARK) caused inhibition of NIS transcription whereas overexpression of Gβγ led to increases in NIS promoter activity. Mechanisms underlying these signalling events were found to be phosphoinositide 3-kinase (PI3K)-mediated, whereby inhibition of Gβγ led to exclusion of Pax8 from the nucleus (55). Gβγ dimers have also been implicated in the modulation of interleukin-2 (IL-2) levels in CD4⁺ T-helper cells. Knockdown of Gβ1 (but not Gβ2) and gallein-mediated inhibition of Gβγ resulted in increased levels of the T cell receptor-mediated IL-2 mRNA production in human naïve and memory T helper cells and Jurkat cells, whereby inhibition of Gβγ resulted in increased nuclear localization of nuclear factor of activated T cells c1 (NFATc1) and increased NFAT mediated transcriptional activity (56).

Gβγ dimers also regulate the activities of transcriptional modulators by mechanisms that include relief of transcriptional repression as in the case of interaction with adipocyte enhancer-binding protein (AEBP1) (57), or histone deacetylase 5 (HDAC5) to result in increased MEF2 mediated transcription ((58), reviewed in (9)). We have previously shown that Gβγ acts to regulate activator protein 1 (AP-1) mediated transcriptional activity via direct interaction with cFos resulting in co-localization of Gβγ and AP-1 in the nucleus, recruitment of HDACs and subsequent inhibition of AP-1 mediated gene transcription (Figure 1, Box C) (40). More recently, Mizuno et al investigated mechanisms of IP₃-R1 upregulation as a result of D2 dopamine receptor (D2-R) activation whereby inhibition of Gβγ led to abrogation of the D2-R-mediated increase in IP₃-R1 mRNA expression (59). Receptor activation by quinpirole, a selective D2 agonist, resulted in increased cFos and Jun protein expression, increased nuclear transport of NFATc4 and increased binding of AP-1 and NFATc4 to the IP₃-R1 promoter, and it

has been suggested that these events were G $\beta\gamma$ -dependent (59). Moreover, G $\beta\gamma$ subunits have been implicated in the regulation of glial cell-derived neurotrophic factor (GDNF) levels in SH-SY5Y cells and rat midbrain slices whereby stimulation of D2-R with quinpirole results in a G $\beta\gamma$ - and ERK1/2-dependent increase in zinc finger protein 225 (Zif268), a transcription factor that was also found to bind GDNF promoters, resulting in increased expression (60). Similarly, treatment of striatal neurons with corticotropin release factor was found to result in a G $\beta\gamma$ -dependent increase in phosphorylated levels of cAMP response element binding protein (CREB) that is also thought to occur through a mitogen-activated protein kinase (MAPK)-dependent pathway (61).

We have recently demonstrated that knockdown of G β_1 in HEK 293 cells resulted in an unexpected potentiation of carbachol-stimulated M3-R mediated Ca²⁺ release, decreased ERK1/2 protein expression, and increased G β_4 protein expression (27). Intriguingly, we also demonstrated that G β_1 binds the promoter of G β_4 while a proteomics screen revealed that G β_1 interacts with members of the hnRNP family of proteins – hnRNP C, hnRNP R and hnRNP D-like (Figure 1, Box A) (27). Since hnRNPs are known function as co-transcriptional modulators of mRNA processing, trafficking and nuclear retention (62, 63), our studies reveal novel roles played by G $\beta\gamma$ dimers in transcription as possible regulators of co-transcriptional modulation or as partners which allow entry of G $\beta\gamma$ subunits into the nucleus.

Further, members of the signal transducer and activator of transcription protein (STAT) protein family were demonstrated to be regulated by G protein signalling. STATs are integral components of the Janus kinase (JAK)-STAT pathway whereby JAK-mediated tyrosine phosphorylation of STAT proteins results in their nuclear translocation. Previous studies have shown that G $\alpha_q/11$, G α_{16} and G α_{14} are capable of stimulating STAT3 and STAT1 (64). Recent studies have investigated possible roles of STAT activation by G $\beta\gamma$ dimers – a comprehensive G $\beta\gamma$ overexpression screen of 48 possible dimers in HEK 293 cells demonstrated that 13 specific dimer pairs stimulated STAT3 phosphorylation to varying degrees according to the specific G β and G γ subunits assessed (64). However, it was not determined whether G $\beta\gamma$ dimers directly interacted with STAT3. Subsequent studies to describe mechanisms that lead to these phosphorylation events focused on δ -opioid receptor (δ -OR)-mediated regulation and activation

of STAT5B (65). They showed that STAT5B constitutively interacts with δ -OR and is released upon δ -OR activation, resulting in STAT5B activation in a c-src-mediated mechanism. Interestingly, this study demonstrates that $G\beta\gamma$ subunits directly bind STAT5B, serving as a scaffold to facilitate recruitment of c-Src to the δ -OR (65). These findings provide further evidence of roles played by $G\beta\gamma$ in the regulation of transcriptional events.

1.6 $G\beta\gamma$ non-canonical signalling at the Golgi apparatus

A role for $G\beta\gamma$ in regulating trafficking from the Golgi apparatus has been described whereby $G\beta\gamma$ activates protein kinase D (PKD, a resident Golgi protein), resulting in anterograde trafficking of proteins from the trans-Golgi network (Figure 1H) (reviewed in (9)). It has been found that $G\beta\gamma$ dimers bind the PH domains contained within PKD and such binding events, in conjunction with PLC β 2/3 activity, are necessary for the induction of PKD activity (66, 67). With respect to specific $G\beta$ and $G\gamma$ subunits that regulate PKD, an analysis of $G\beta$ and $G\gamma$ subunit specificity for activation of PKD reveals that $G\beta$ 1 dimers with γ 2, γ 3, γ 4, γ 5, γ 7, and γ 10 effectively activate PKD whereas the remaining $G\gamma$ subunits do not (67). Moreover, Jensen et al have recently described a role for $G\beta\gamma$ and PKD in the agonist-induced trafficking of intracellular Protease-activated-receptor 2 (PAR2) (68). Here, they demonstrate that activation of PAR2 by its agonists trypsin and 2-Furoyl-LIGRLO-NH₂ resulted in the translocation of $G\beta\gamma$ to the Golgi apparatus where it activates PKD, whereas inhibition of $G\beta\gamma$ with gallein resulted in inhibition of PKD activity (68). Furthermore, it was revealed that inhibition of PKD with CRT0066101 resulted in a loss of trypsin-stimulated translocation of PAR2 from Golgi apparatus to the plasma membrane, diminishing the mobilization of intracellular stores of PAR2 to rapidly replenish the plasma membrane with signalling-competent receptors (68). It remains to be identified what the roles of the other $G\beta$ subunits are in regulating PKD activity.

RTKG (Raf kinase trapping to the Golgi apparatus; also known PAQR3 (Progesterin and AdipoQ Receptor 3) has been found to interact with $G\beta$ in the Golgi apparatus where it sequesters $G\beta\gamma$, modulating its function at the plasma membrane (Figure 1I). Indeed, this Golgi-resident membrane protein has been found to bind the N-terminal region of $G\beta$ trapping $G\beta\gamma$ in the Golgi (69). Such interactions have been found to decrease $G\beta\gamma$ -dependent protein kinase B

(PKB also known as Akt) phosphorylation, abrogating GPCR-stimulated recruitment of GRK2 and inhibiting G $\beta\gamma$ translocation to the Golgi (69). A recent article demonstrates that PAQR3 also acts to promote G $\beta\gamma$ signalling in the Golgi apparatus (70). G β binding-deficient PAQR3 mutants displayed an inability to cause fragmentation of the Golgi apparatus compared to wild type PAQR3 while Golgi fragmentation was also inhibited by β ARK-CT, gallein and overexpression of a dominant negative PKD (70). Furthermore, the G β binding-deficient PAQR3 mutant resulted in an inhibition of the constitutive transport of VSV-G cargo protein from the Golgi apparatus to the plasma membrane (70). All in all, these findings suggest a new role for PAQR3 in regulating the functions of G $\beta\gamma$ at the Golgi apparatus and the transport of G $\beta\gamma$ from the Golgi to the plasma membrane via the G $\beta\gamma$ -PKD pathway.

Furthermore, G $\beta\gamma$ dimers have been recently implicated in the regulation of PLC ϵ in the perinuclear region. PLC ϵ is a novel form of PLC shown to be activated downstream of receptor tyrosine kinases and GPCRs via regulation by Ras, Rho, Rap and G $\beta\gamma$ (Figure 1J). Knockdown of PLC ϵ results in a loss of endothelin-1-, norepinephrine- and isoproterenol-induced cardiac hypertrophy (71). A recent study aimed to elucidate the mechanisms and functional consequences of PLC ϵ activation in cardiac failure (72). Here, it was identified that PLC ϵ is recruited to the perinuclear compartment in complex with the nuclear envelope scaffolding protein muscle-specific A kinase anchoring protein (mAKAP), Epac1 (exchange factor activated by cAMP, to which PLC ϵ directly binds), and PKD that PLC ϵ acts to activate (72). Furthermore, it was found that phosphatidylinositol 4-phosphate (PI4P) was enriched at the nuclear envelope, and that PI4P, not phosphatidylinositol 4,5-bisphosphate (PIP2), was the substrate for PLC ϵ . PLC ϵ was found to generate diglyceride (DAG) from PI4P in close proximity to the perinuclear region required for activation of nuclear PKD (72). As PKD activity is regulated by G $\beta\gamma$ binding and activation, it was suggested that G $\beta\gamma$ -dependent activation of PLCs to generate diacylglycerol (DAG) is required for Golgi PKC and PKD activity (73). These studies show that ET-1-mediated PI4P hydrolysis to DAG and subsequent PLC ϵ activation is a G $\beta\gamma$ -regulated process, leading to PKD activation and eventual development of cardiac hypertrophy (72, 73).

1.7 Gβγ non-canonical signalling at the mitochondria

1.7.1 Gβγ involvement in mitochondria dynamics

In addition to previous reports of the presence of Gαi and Gα12 in mitochondria (74, 75), Gα_{o1}, Gα₁₁, Gα_{i2-3}, Gβ1, Gβ4 and Gγ2 have recently been shown to localize there (76). The heterotrimer can be found at the outer membrane where Gβγ has a role in enhancing Gα targeting to mitochondria facilitating Gα_{q/11} entry into mitochondria through unknown mechanisms. Gβγ was only detected at the outer membrane, and the authors suggested it may not be possible for Gβγ to enter the mitochondria because of its structure. Gβ subunits contain a WD propeller domain which cannot be imported through the translocase of the outer membrane (TOM) complex of the mitochondria (77). Despite this, Gβγ subunits can affect the balance between fusion and fission by altering the activity of various mitochondrial proteins including mitofusins, dynamin 1-like (Drp1) and optic atrophy 1 (OPA1) (76). Gβ2 has been shown to specifically bind mitofusin 1 directly to affect mitochondrial fragmentation (Figure 1M) (39).

1.7.2 Gβγ involvement in cellular respiration

In addition to influencing mitochondrial dynamics, G proteins may have a role in regulating respiratory function. For example, the absence of mitochondrial Gα_{q/11} reduced dimeric form of ATPase, and oxidative phosphorylation supercomplex formation leading to reduced ATP production efficiency (76). Our own analysis following a TAP proteomic screen (data not shown) shows that Gβγ may interact with proteins in the oxidative phosphorylation pathway (Figure 1, Box N). Characterization of functional GPCR systems within the mitochondria suggests G proteins are involved in energy metabolism in the cell. Abadir et al., 2011 described a novel mitochondrial renin-angiotensin system with the angiotensin II receptor type 2 (AT2R) found at the inner membrane. Upon activation by Ang II, nitric oxide levels increased resulting in decreased mitochondrial respiration (78). Cannabinoid 1 (CB₁) receptors were also found on the mitochondrial outer membrane of mouse neurons. Stimulation of these receptors can cause changes in mitochondrial energetics which may alter endocannabinoid-dependent synaptic plasticity in the brain. These mitochondrial changes affect respiratory chain complex 1 through mitochondrial cAMP accumulation and PKA activity (79). However, the precise role of Gβγ in these events remains unclear.

1.8 Gβγ and the cytoskeleton

1.8.1 Chemotaxis

Gβγ subunits transduce signals from chemokine receptors in neutrophils to induce directional polarization and actin polymerization towards the source of the chemoattractant. Downstream of receptor activation, there are various pathways regulated by Gβγ subunits which led to chemotaxis (reviewed in (80)). Modulation of Gβγ chemotactic signalling may involve competitive binding of proteins such as the receptor for activated C kinase 1 (RACK1) to Gβγ against other effectors that stimulate cell motility. In this inhibitory pathway, after cellular chemoattractant stimulation RACK1 interacts with Gβγ moving towards the leading edge and competes with PI3Kγ and PLCβ for Gβγ (Figure 1K) (81). This decreases chemotaxis because asymmetrical GPCR stimulation by chemoattractant gradients leads to increased Gβγ activation of PI3Kγ at the leading edge and an intracellular phosphatidylinositol (3,4,5)-trisphosphate (PIP₃) gradient, inducing activation of one or more Rho GTPases (82) which have distinct and overlapping functional profiles to induce actin polymerization (83). This may be achieved through PIP₃-dependent Rac exchanger (P-Rex1), an abundant guanine exchange factor (GEF) that may be activated by both Gβγ and PIP₃ to induce Rac GTPase activity and chemotaxis (84). In *D. discoideum*, the chemokine GPCR cAMP receptor 1 (cAR1) induces engulfment and cell motility E (ElmoE) GEF association with Gβγ and translocation to the plasma membrane where it activates RacB and actin assembly at the leading edge (Figure 1L) (85). The authors also showed that ElmoE associates with “dictator of cytokinesis” (Dock)-like proteins and proposed Gβγ acts as a bridge in higher organisms between activation of chemokine-responsive GPCRs and the evolutionarily conserved Elmo/Dock180 known to lead to Rac activation in chemotaxis (86-88). This may be a potential new avenue for Gβγ to regulate cell motility. Distinct from activating Rac-GTPases is Gβγ-mediated activation of cell division cycle 42 protein (Cdc42) through p21-activated kinase (PAK) 1 and PAK-associated guanine exchange factor (PIXα) (89). This Gβγ/PAK1/PIXα/Cdc42 pathway is involved in repelling phosphatase and tensin homolog (PTEN) from the leading edge to maintain PIP₃ gradient and proper localization of F-actin formation toward chemoattractant point sources, allowing for direction sensing and maintenance of cellular polarization after GPCR stimulation in myeloid cells.

1.8.2 Cell adhesion

Using *in vitro* trans-well migration assays in human promyelocytic leukemia cells HL60 and primary neutrophils, it was shown that release of free G $\beta\gamma$ alone was sufficient to induce directional chemotaxis comparable to that mediated by chemokine receptor activation (90). Motility *in vivo*, is a different matter because such cells display ligands such as intercellular adhesion molecule 1 (ICAM-1) which bind to surface integrins on leukocytes to induce adhesion. Thus, successful directional migration on these surfaces then require cells to maintain additional mechanisms of de-adhesion. It seems that G α_i is important in facilitating de-adhesion and projecting polarized projection of pseudopods (91). This was shown using a small molecule called 12155 to displace G α -GDP from G $\beta\gamma$ which essentially activates the latter without activating G α . 12155-induced release of G $\beta\gamma$ inhibited basal neutrophil polarity and motility, while increasing neutrophil adhesion to ICAM-1 coated surfaces (91). One study suggested that G $\beta\gamma$ regulates increase of cell-matrix adhesiveness downstream of chemokine receptor activation (92) through interaction with Rap1a and its effector Radil, both involved in mediating integrin-dependent adhesion (93, 94).

Various studies using small molecule inhibitors for G $\beta\gamma$ demonstrate that in addition to its importance in chemotaxis there is potential for therapeutic targeting. *In vitro*, small molecular inhibitors gallein and M119 against G $\beta\gamma$ that disrupted its PI3K γ interaction led to inhibition of chemotaxis (95). This translates to reduced inflammation *in vivo*, where the prophylactic administration of gallein to mice showed reduced paw edema which characterized reduced neutrophil infiltration in the carrageenan paw edema model (95). Also therapeutically relevant is M119K, which reduced migration and invasion of metastatic breast cancer *in vitro* in a Rac-1- and chemokine GPCR chemokine receptor type 4 (CXCR4)-dependent manner, adding metastatic relevance to G $\beta\gamma$ chemotactic signalling (96).

1.8.3 Microtubules

G proteins have been shown to directly interact with microtubule proteins leading to various alterations in cytoskeletal processes (reviewed in (97)). G $\beta\gamma$ specifically have been

shown to bind tubulin, and stabilize microtubule polymerization with both G β and G γ subunit specificity (98, 99). Another cytoskeleton-regulated process that G $\beta\gamma$ is involved in includes spindle orientation and positioning. Studies in *C. elegans* show G β is necessary for migration of centrosome around the nucleus and mitotic spindle orientation to allow for cellular division at the early embryo stage (100, 101). G $\beta\gamma$ also seems to be important in determining asymmetrical cellular division. In *Drosophila*, G β is necessary for asymmetrical spindle positioning in neuroblasts, where it is proposed that differential G protein activation causes this asymmetry which is important in generating heterologous neural fate determination (102). This effect was similarly seen in mammals, where G $\beta\gamma$ is important for mitotic-spindle orientation in the asymmetric cell division of progenitor cells to produce one differentiating into a neuron and the other a progenitor cell in the developing mammalian cortex. Disruption of G $\beta\gamma$ causes a shift in the cell-cleavage plane resulting in both daughter cells having the same neuronal fate (103).

1.9 G $\beta\gamma$ degradation

Compared to GPCRs, relatively little is known regarding degradation of heterotrimeric G proteins in general and less about G $\beta\gamma$ subunits in particular. One of the only known instances of degradation through the proteasome is for transducin $\beta\gamma$, specific to photoreceptors. Ubiquitination of transducin G γ (G γ 1) results in transducin G $\beta\gamma$ degradation *in vitro* through a mechanism requiring ATP and the proteasome (104). Phosducin binding was found to be protective against this effect. Phosducin naturally binds transducin G $\beta\gamma$ to control levels of free G $\beta\gamma$ dimer after photoreceptor activation to regulate light sensitivity, and may also act to regulate transducin G $\beta\gamma$ degradation (104). G γ subunits in other cell types may be ubiquitinated through the N-end rule (105). This rule describes destabilizing amino acids at the N-terminus of a protein which predicts protein ubiquitination and degradation (106). A small proportion of G γ 2 isolated from the bovine brain and had an N-terminal domain variant was found to be ubiquitinated via the N-end rule (105). The regulation of G $\beta\gamma$ levels in other cell types is not well understood and further work is required to generalize such findings, but so far this shows degradation may be used as a method to regulate GPCR signalling.

1.10 Thesis objectives and rationale

We have progressed from a simplistic view of G $\beta\gamma$ subunits as regulators of GPCR signalling to a sense that there is a rich tapestry of G $\beta\gamma$ -dependent signalling throughout the cell. Broader approaches will reveal new roles for G $\beta\gamma$ signalling in different parts of the cell, in different cells and tissues and in a subunit- and species-specific manner. The overall aim of this thesis is to continue to understand roles of G $\beta\gamma$ in signalling events, specifically to further our understanding of G $\beta\gamma$ degradation because it is not a well-studied field but has potential to alter GPCR signalling. Desensitization that follows stimulation is a normal mechanism for regulating signalling. Taking GPCRs for example, one such mechanism is phosphorylation which leads to endocytosis and prevents persistent receptor signalling. Receptors can then be dephosphorylated and returned to the plasma membrane for further signalling or targeted for degradation (107). One pathway for GPCR degradation is through the 26S proteasome- the protein degradation system integral to the cell's tight regulation over proteins and cellular health. For example, phosphorylation of the β_2 -adrenergic receptor is followed by interaction with β -arrestin which is an adaptor for the E3 ligase NEDD4 (108). The E3 ligase catalyzes ubiquitin conjugation onto the substrate, targeting it for degradation by the 26S proteasome. This large macromolecular complex consists of a 19S regulatory structure that acts on both ends as a base-lid complex and functions to recognize ubiquitinated proteins, de-ubiquitinate, unfold and translocate them to the middle barrel-shaped 20S protease core for proteolysis. Regulation of G $\beta\gamma$ levels is likely to be critical in modulating GPCR signalling and evidence points to the 26S proteasome pathway as well. The best studied case of G $\beta\gamma$ degradation is transducin $\beta\gamma$ (G $\beta_1\gamma_1$) in rod photoreceptors, where the G γ is ubiquitinated leading to dimer degradation as a mechanism through which rod cells can regulate their light sensitivity in the retina (104). This demonstrates G $\beta\gamma$ degradation by the 26S proteasome is a mechanism of G $\beta\gamma$ signalling regulation within the cell, but it remains unknown whether this is a conserved mechanism in general. No specific E3 ligase or ligase adaptor has yet been identified for G $\beta\gamma$. There is potential that the potassium channel tetramerization domain (KCTD) proteins identified to interact with G $\beta\gamma$ (Hébert lab, unpublished) are involved in this mechanism through the Cullin 3 (CUL3)-E3 ligase substrate. Previous studies have suggested that KCTD5 may act alone or in concert with CUL3 to oppose

G β γ signalling (109) (110), and the KCTDs are proven substrate-specific adaptors for CUL3 although no substrate has yet been identified (111). There is previous evidence from our lab that G β γ association with KCTD5 and KCTD5 overexpression experiments lead to decreased G β levels in cells while knockdown has the opposite effect (92).

Previous work from our lab by Rhiannon Campden during her MSc studies has provided a basis from which to perform analysis to help uncover G β γ degradation pathways and other roles in the cell. The focus of Campden's MSc thesis was primarily on optimizing an affinity purification coupled with mass spectrometry approach for identifying potential G β γ nuclear interacting partners to support our lab's research into G β γ function there (112). Her work completed an *in vitro* TAP proteomics screen and mass spectrometry identified more than 400 potential G β γ interactors in different conditions such as in the nucleus or cytosol, and under basal conditions or in response to stimulation of the endogenous M3-R. The majority of these protein interactors have never been previously reported. Her methods used HEK 293 cell lines stably expressing TAP-tagged G β 1, split TAP-tagged G β 1 and G γ 7, or Flag-G β 1 which were tandem affinity purified or immunoprecipitated (IP) and their precipitates were analyzed by mass spectrometry. Her results only included proteins which were identified in 2 of 3 independent experiments, and was compared to the Contaminant Repository for Affinity Purification (CRAPome) to filter out background and non-specific interactions. Her results generated a list of potential interactors for this thesis to further study.

The objective of my thesis is to analyze Campden's G β γ protein-protein interaction data for insight into G β γ degradation and signalling, and to validate and examine their functions and effects on G β γ signalling *in vitro*. The aims of the thesis can be summarized as thus:

1. Evaluate G β γ protein-protein interactors from Campden's proteomics screen to identify signalling pathways related to degradation and other signalling paradigms of interest. This will be done by screening all protein interactors through online integrated databases for human biological pathways, such as KEGG Pathway and PathCards- Pathway Unification Database, which will analyze the proteins based on molecular interactions and functional protein association networks to identify relevant pathways. The interactors

in the pathways will be analyzed on additional factors including the type of immunoprecipitation used by Campden to identify it, the subcellular localization of the interaction and its responsiveness to upstream M3-R GPCR stimulation by carbachol. Identified proteins within the pathways and the pathways themselves will be described and their interaction with G $\beta\gamma$ in literature will be further discussed.

2. Select and validate G $\beta\gamma$ interactors within the degradation pathways identified and described in Aim 1 (PSMD7 from the 26S proteasome, and KCTD5) using immunoprecipitation and visualization by western blot.
3. Generate a KCTD5 knockout cell line model using CRISPR/Cas9 technology to target the KCTD5 gene in HEK 293 immortal cell line to study the KCTD5 and G $\beta\gamma$ interaction. Validate the functional knockout of KCTD5 by using IP and mass spectrometry of G $\beta\gamma$ precipitates.
4. Examine the influence of the interactions described in Aim 2 on signalling. For the 26S proteasome on G $\beta\gamma$ degradation this will be done by employing MG132, a 26S proteasome inhibitor to examine expressed Flag-G $\beta 1$ degradation by the proteasome and changes in protein levels visualized by western blot. For the KCTD5-G $\beta\gamma$ interaction, the knockout cell line will be used to measure changes in G $\beta\gamma$ ubiquitination and protein-protein interactor patterns using mass spectrometry, and changes in cellular endogenous G $\beta\gamma$ protein levels. It will also be used to assess KCTD5 effects on phenotypic outputs of pathways which G $\beta\gamma$ influences such as the MAPK cascade and ERK1/2 phosphorylation as well as the mTOR pathway and AKT phosphorylation using western blot.

2. MATERIALS AND METHODS

2.1 Preface

The section describes the methods and materials used to generate this thesis's results section, and are organized to loosely follow the order in which the Aims are described in Section 1.10 and in which the results are presented in Chapter 3. Section 2.2 outlines general cell culture techniques used throughout the results, and Section 2.3 outlines immunoprecipitation and western blotting techniques used to validate protein-protein interactors identified from the Campden G β γ proteomic screen. Section 2.4.1 outlines techniques used in the KCTD5 knockout cell line generation using the CRISPR/Cas9 method which were developed based on guidance from Dr. Dominic Devost, Hébert lab. Section 2.4.2.3- 2.4.2.4 Liquid Chromatography Mass Spectrometry (LC-MS) sample preparations were done according to protocols from and under the guidance of Dr. Jean-François Trempe, Department of Pharmacology and Therapeutics, McGill University, Montreal. LC-MS and data extraction were performed by Dr. Jean-François Trempe. The remaining methods were obtained from the Hébert lab.

2.2 Cell culture techniques

HEK 293 cells were grown at 37°C and 5% CO₂ in full media: Dulbecco's Modified Eagle Medium (DMEM) with 5% (v/v) fetal bovine serum and 1% (v/v) penicillin–streptomycin purchased from Wisent.

2.2.1 Transient transfection

Cells were cultured to 70% confluency prior to transfection in clear 6-well plates (Thermo Scientific, 140675). 1.5 μ g of plasmid DNA with 3 μ l Lipofectamine 2000 transfection reagent (Invitrogen) were added with DMEM and incubated for 5 hours, then media changed to full media and incubated for 48 hours. The transfection protocol for a 6-well plate was scaled up or down relative to plating surface area and as needed for experiments.

2.3 Interaction validation immunoprecipitation and western blotting

2.3.1 Anti-rabbit IgG agarose immunoprecipitation

Treated HEK 293 cells were lysed in NP40 lysis buffer (150mM NaCl, 1% NP40, 50mM Tris pH8.0, 1X protease inhibitor cocktail) and protein concentration quantified by Bradford Assay. Per unknown sample, 1mg of protein lysate was precleared with 40µl of anti-rabbit IgG agarose beads (Sigma Aldrich). The precleared lysates were then divided into two, and incubated with 0.6µg of anti-Gβ total (T-20) antibody (Santa Cruz Biotechnology) or no antibody overnight at 4°C with gentle mixing. The following day, per sample 40µl of anti-rabbit IgG agarose beads were washed and blocked in 2% bovine serum albumin (BSA), washed, then added into each overnight lysate and incubated for 3 hours at 4°C with gentle mixing. The mixtures were spun down and the supernatants saved as “unbound” for further analysis. The bead pellets were washed 3X in NP40 lysis buffer. 40µl of 2X Laemmli buffer (4% (w/v) SDS, 20% glycerol, 120mM Tris pH6.8) was added to each sample and denatured for 15min at 65°C to elute captured proteins from the beads. The eluted proteins were then loaded onto 10% acrylamide gel alongside 30µg of “unbound” and 30µg of “input” (total lysate) for comparison and subjected to SDS-PAGE western blotting.

2.3.2 Anti-HA immunoprecipitation

This method was used to IP our subcloned Flag-HA-PSMD7 plasmid-expressing protein (original Flag-HA-PSMD7 was a gift from Wade Harper [Addgene plasmid #22558] (113)). Treated HEK 293 cells were lysed in NP40 lysis buffer (150mM NaCl, 1% NP40, 50mM Tris pH8.0, 1X protease inhibitor cocktail) and protein concentration quantified by Bradford Assay. The EZview™ Red Anti-HA affinity gel (Sigma-Aldrich) adapted from manufacturer’s protocols was used. Briefly, 40µl of EZview™ Red Anti-HA affinity gel was washed and added to 500µg of protein sample and incubated overnight at 4°C with gentle mixing. The following day, the mixture was spun down and supernatant saved as “unbound” for further analysis. The pelleted beads were washed 3X with NP40 lysis buffer. To elute the captured proteins from the beads, 50µl of 2X Laemmli buffer (4% (w/v) SDS, 20% glycerol, 120mM Tris pH6.8) was added, vortexed, and incubated for 15min at 65°C. The eluted proteins were then loaded onto 10%

acrylamide gel alongside 30µg of “unbound” and 30µg of “input” (total lysate) for comparison and subjected to SDS-PAGE western blotting.

2.3.3 Western blotting

Prepared lysates were loaded onto a 10% acrylamide gel with a protein ladder and subjected to SDS-PAGE. The separated proteins were transferred onto a polyvinylidene fluoride (PVDF) membrane and blocked with 5% milk, then incubated with primary antibodies (Anti-Gβ antibody (T-20) (Santa Cruz Biotechnology); Anti-HA antibody (Roche Applied Science); Anti-phosphoERK1/2 antibody (Cell Signalling Technology); Anti-ERK1/2 total antibody (Santa Cruz Biotechnology, Inc); Anti-β-tubulin antibody, (Invitrogen); Anti-pAKT (Cell Signalling Technology); Anti-AKT total (Cell Signalling Technology); Anti-Flag (Sigma Aldrich); Anti-KCTD5 (Sigma Aldrich)). Peroxidase-conjugated secondary anti-mouse or anti-rabbit IgG antibodies (Sigma-Aldrich) were incubated at a 1/20000 dilution for one hour, then the membranes were washed. Western Lightning Plus-ECL, Enhanced Chemiluminescence substrate (Perkin Elmer) was applied to membranes for immunoblotting and visualization of proteins was done using a chemiluminescence detection system.

2.4 KCTD5 KO HEK 293 cell line generation

2.4.1 Cell culture

HEK 293 cells were plated in a 6-well plate and transiently transfected with a PX330 plasmid containing *S. pyogenes* Cas9 (SpCas9) alone as a negative control, or a PX300 plasmid containing SpCas9 and a KCTD5 single guide RNA (sgRNA, designed by Feng Zhang lab, MIT). The cultures were expanded and genomic DNA (gDNA) extracted using the Blood/Cell DNA kit (Geneaid) following manufacturer’s protocols. The region of sgRNA complementation within the KCTD5 gene was PCR-amplified (100ng gDNA, PFU Ultra DNA polymerase and buffer (Agilent), 10mM dNTP, 25mM forward primer, 25mM reverse primer) using self-designed primers and analyzed by the Surveyor Mutation Detection Kit for Standard Gel Electrophoresis (Integrated DNA Technologies- IDT) following manufacturer’s protocol and visualized on a 1% agarose gel in TAE buffer (40mM Tris, 20mM acetic acid, 1mM EDTA) with

ethidium bromide (EtBr). After positive detection of Cas9 nuclease action at the heterogeneous cell population level, the cell count of the cell cultures was measured using the TC20 Automated Cell Counter (BioRad) and subsequently plated at a rate of 1 cell/3 wells in a 96-well plate for 2 weeks to develop single cell colonies. gDNA was isolated for each colony and PCR amplified again to perform restriction fragment length polymorphism (RFLP) for the NaeI restriction enzyme site. $\frac{1}{4}$ PCR product was digested with 1X Cutsmart buffer and 1 μ l NaeI (New England Biolabs- NEB) and incubated at 37°C for 1 hour. Digested PCR product results were visualized on a 1% agarose/TAE gel with EtBr. Clones were sequenced to validate RFLP results.

2.4.2 Mass spectrometry

All samples were stored through flash freezing and in -80°C to preserve protein stability.

2.4.2.1 Whole cell lysate sample preparation

Whole cell lysate sample preparation was performed using an adapted version of a previously described protocol (114). Briefly, cells were seeded in T175 flasks and transiently transfected with Flag-G β 1 in pcDNA3.1+ plasmid. After transfection, flasks were washed and gently resuspended using a tapping motion with 10ml cold 1X phosphate buffered saline (PBS). Cells were pelleted then combined into one flask and supernatant removed. The pellet was resuspended in cold 5ml TAP lysis buffer (1mM MgCl₂, 10% glycerol, 100mM KCl, 50mM HEPES-KOH pH8.0, 0.2mM EDTA pH8.0, 2mM DTT, 0.1% NP-40, 1X protease inhibitor cocktail) and incubated on a mixing platform for 30min at 4°C, then flash frozen in liquid nitrogen and stored in -80°C freezer until anti-Flag IP. Prior to IP, lysates were thawed on ice and pelleted. Only the supernatant was used for IP.

2.4.2.2 Anti-Flag immunoprecipitation

Whole cell lysate prepared samples were quantified by Bradford assay and 12.5mg of protein was used per IP. Anti-Flag IP was performed using an adapted version of previously described protocols (114). 50 μ l Anti-Flag M2 agarose affinity gel (Sigma-Aldrich, A2220) were washed 3X in TAP lysis buffer (1mM MgCl₂, 10% glycerol, 100mM KCl, 50mM HEPES-KOH pH8.0, 0.2mM EDTA pH8.0, 2mM DTT, 0.1% NP-40, 1X protease inhibitor cocktail), and

added to 12.5mg protein of whole cell lysate and incubated overnight at 4°C with gentle shaking. On the following day, beads were pelleted at 1600 rpm (Sorvall Mach 1.6R), 10min, 4°C and unbound fraction kept for further analysis. The beads were washed 3X with TAP lysis buffer, followed by wash 3X with Flag rinsing buffer (50mM ammonium bicarbonate pH8-8.5, 75mM KCl), then washed 3X in 50mM ammonium bicarbonate. Elution of proteins off beads was done by incubating the beads in a Micro Bio-SpinTM Size Exclusion Spin Column (Bio-Rad) with 100µl of 0.5M ammonium hydroxide (pH>11.0, diluted with clean HPLC water) for 10min and repeated 5 times in total. Subsequent elutions were pooled, lyophilized, and stored at -80°C.

2.4.2.3 Protein isolation

For samples which were analyzed by LC-MS but have not gone through IP nor been lyophilized, such as the unbound and whole cell lysate samples, the proteins were isolated through this protocol. Using 100µg of protein lysate and vortexing in between each addition of solution, 4 volumes of methanol was added, followed by 1 volume chloroform, then 3 volumes H₂O were added. The solution becomes cloudy and is spun at 13,000g for 5min. The upper aqueous phase was removed and discarded, leaving a protein film at the interphase. 3 volumes of methanol were added, vortexed and centrifuged again. Pelleted protein was dried through evaporation, and stored at -80°C if not used immediately for LC-MS sample preparation.

2.4.2.4 LC-MS sample preparation

Dried protein pellet was first resuspended in denaturing buffer (6M urea, 1mM EDTA, 50mM TEAB pH8.5). Cysteine residues were reduced by 2mM TCEP pH7.0 for 10min at 37°C, then alkylated for 30min in darkness. KCTD5 CRISPR knockout validation samples were alkylated with 50mM iodoacetamide (freshly prepared, Sigma). MG132-treated Flag-Gβ1 samples looking at Gβγ ubiquitination sites were alkylated with 50mM chloroacetamide. Next, the samples were diluted with 50mM TEAB pH8.5 until a final concentration of 1µg/µl protein and 1M urea, then digested with 0.2µg trypsin (Sigma) for 3 hours at 37°C. After digestion, 1.5% TFA and 5% acetonitrile were added to stop digestion and peptides were purified using ZipTip C18 pipettes (Millipore), and resuspended in 0.05% TFA and 2% acetonitrile.

3. RESULTS

3.1 Preface

The results chapter is organized in a manner that reflects the order of the aims listed in the thesis objectives and rational, and unless stated here all tables and figures were generated by Jennifer Y. Sung. It begins with an in-depth analysis of Campden's G $\beta\gamma$ protein-protein interactions data (Section 3.2). Specifically, the section examines G $\beta\gamma$ interactions with components of the degradation pathway such as with the 26S proteasome and KCTD family members, as well as non-canonical signalling pathways identified. The next step was to validate protein interactors that pertain to G $\beta\gamma$ degradation identified in Section 3.2, namely KCTD5 and proteasome 26S subunit, non-ATPase 7 (PSMD7), using immunoprecipitation and immunoblotting (Section 3.3) where Figure 4 was generated by Darlaine Pétrin, Hébert lab. Next to study the KCTD5 and G $\beta\gamma$ interaction, in Section 3.4 are the results from the process of KCTD5 knockout (KO) HEK 293 cell line generation and validation. The experimental design was set up under the guidance of Dr. Dominic Devost, Hébert lab (Section 3.4.2), and mass spectrometry analysis under the guidance Dr. Jean-François Trempe, McGill University (Section 3.4.5). Lastly, effects of the 26S proteasome and KCTD5 on G $\beta\gamma$ degradation and signalling were examined (Section 3.5). The 26S proteasome effect on G $\beta\gamma$ degradation was studied using a 26S proteasome inhibitor MG132. Changes in G $\beta\gamma$ protein interactor partners, ubiquitination sites and protein levels with KCTD5 KO were investigated using IP and mass spectrometry, where the mass spectrometry analysis of G $\beta\gamma$ Lys209 ubiquitination site was done under the guidance Dr. Jean-François Trempe, McGill University (Section 3.5.2). KCTD5 effect on G $\beta\gamma$ signalling pathways of ERK1/2 phosphorylation within the MAPK cascade (3.5.4), and AKT phosphorylation within the mechanistic target of rapamycin (mTOR) pathway were examined (3.5.5).

3.2 Pathway identification from G $\beta\gamma$ proteomics screen

Proteins discussed within Section 3.2, Tables 1-7 are listed by their gene symbols for clarity and consistency, and their full gene names may be found in the Supplemental Table 1.

3.2.1 *Gβγ* and degradation pathways

3.2.1.1 Gβγ interaction with multiple KCTD isoforms

KCTD5 and three additional KCTD family proteins (KCTD2, 12, 17) were identified in the original proteomic screen (Table 1). KCTD proteins belong to recently discovered family of 22 (111) or more members (115) depending on the source. KCTDs are defined by a Bric-a-brac, Tram-track, Broad complex (BTB) domain also known as a POZ domain at the N-terminus which facilitate protein-protein interactions and homo- and hetero-dimerization (115). They are small proteins fairly homologous to each other, highly conserved through evolution suggesting they have an important role (116). Common among many KCTDs is their interaction directly with ubiquitin ligases and cullin (CUL)3-based E3 ubiquitin ligase complexes through their BTB domains (116). Such complexes are involved in conjugation of ubiquitin (Ub) onto specific targets which occurs in a three-step enzymatic process. The first step is ubiquitin activation by an E1 enzyme, which is secondly transferred onto an E2 ubiquitin conjugating enzyme that then interacts with an E3 ubiquitin ligase involved in target recruitment. While there are relatively few E2 enzymes within the human genome, there are hundreds of E3 ligases allowing for discrimination of specific substrate targets. E3 ligases can be categorized into three groups based on their defining motifs, and CUL3 specifically binds RING type E3 ligases. The E3 ligase-CUL3 complex catalyzes conjugation of ubiquitin by bringing the Ub-E2 ligase into close proximity to the target protein through the E3 ligase interaction with the Ub-E2, and the CUL3 which acts as an adaptor to bind a substrate-specific adaptor such as KCTD which recruits specific targets (117). Ubiquitination is an important homeostatic function, mainly in targeting proteins to the 26S proteasome for degradation, but it may also be involved in other signalling mechanisms such as transport (118). Of the four KCTDs, KCTD12 is most dissimilar and does not bind CUL3 (119), whereas KCTD2, 5 have been shown to bind to CUL3 and similarity of amino acid sequences between KCTD2, 5, 17 suggests they may have overlapping roles within the cell, both in regards to ubiquitin ligases, (116) and potentially with respect to *Gβγ* interactions. KCTD5 is discriminatory in its interaction with CUL3 only and not with the 6 other cullins. It is part of a functional Cullin-E3 ligase complex as a substrate-specific adaptor

although no substrate target has been identified, and it is not a ubiquitinated substrate itself as is possible for some adaptors (111).

G $\beta\gamma$ interaction with the 4 KCTD isoforms appear to be common because of their occurrence under all conditions tested. The interactions were identified in most cases in both basal and under upstream G $\beta\gamma$ stimulation through CCh (Table 1) suggesting a basal ubiquitous interaction presence. E3 ligases may ubiquitinate proteins in the nucleus (120) so within this paradigm it is not strange KCTDs were identified in the nucleus. However, the split TAP-G $\beta 1\gamma 7$ purification yielded more KCTD-G $\beta\gamma$ interactions overall compared to TAP-G $\beta 1$, and more in the nucleus compared to Flag-G $\beta 1$ suggesting the G γ isoform specification may increase specificity or strength of this type of interaction. No members of cullin or E3 ligases known to interact with CUL3 were identified in the Campden screen.

Name	Flag-G $\beta 1$				TAP-G $\beta 1$				Split TAP-G $\beta 1\gamma 7$			
	Cytosol		Nucleus		Cytosol		Nucleus		Cytosol		Nucleus	
	Basal	CCh	Basal	CCh	Basal	CCh	Basal	CCh	Basal	CCh	Basal	CCh
KCTD2	+	+	-	-	-	-	-	-	+	+	+	+
KCTD5	+	+	-	+	-	-	+	+	+	+	+	+
KCTD12	+	+	-	+	+	-	+	-	+	+	+	+
KCTD17	+	+	-	-	-	-	-	-	+	+	-	-

Table 1: G $\beta\gamma$ interacts with multiple KCTDs

Mass spectrometry analysis of tagged G $\beta\gamma$ immunoprecipitates as indicated in HEK 293 cells under basal or 1M CCh stimulation over 45 min. “+” indicates the interaction was identified by LC-MS, whereas “-” indicates the interaction was not.

3.2.1.2 G $\beta\gamma$ interaction with the 26S proteasome

Analysis of mass spectrometry data identified Flag-G $\beta 1$ interaction with proteasome 26S subunit ATPase (PSMC) 1-4, PSMC6, and proteasome 26S subunit non-ATPase (PSMD) 1-3,

PSMD7, PSMD11, PSMD13 (Table 2) which comprise the majority of the 19S regulatory complex of the 26S proteasome. The 19S regulatory particle is situated in a mirrored fashion on both ends of a 20S core and its functions include recognizing and receiving ubiquitinated proteins, de-ubiquitinating and translocating them to the proteolytic 20S core for degradation. The 19S complex is subcategorized into an outermost section called ‘lid’, and a ‘base’ which partially acts as a gate to the 20S core (121). Within its interactors in the lid, Flag-G β 1 notably interacts with PSMD1 which is involved in substrate recognition and binding, and PSMD7 which is a de-ubiquitinase (DUB) (113). Within the base, Flag-G β 1 interacts with PSMC1-4, 6 which compose 5 of the 6 majority of the ATPase group that have chaperone-like functions and unfold proteins as they translocate into the 20S proteolytic core for degradation (121). Flag-G β 1 being identified as an interactor for proteins involved in substrate recognition, de-ubiquitination, substrate unfolding and translocation into 20S core highly suggests G $\beta\gamma$ may be degraded by the proteasome. Additionally, G $\beta\gamma$ degradation through this pathway seems to increase after upstream GPCR signaling as seen with increased interactions post-carbachol treatment (Table 2A).

A

Name	Flag-G β 1	
	Cytosol	
	Basal	CCh
PSMD3	-	+
PSMD7	-	+
PSMD11	-	+
PSMD13	+	+
PSMD1	-	+
PSMD2	+	+
PSMC1	+	+
PSMC2	+	+
PSMC3	+	+
PSMC4	-	+
PSMC6	+	+

B

Name	Function
PSMD1	Largest non-ATPase subunit in lid complex. Involved in substrate recognition and binding
PSMD2	Component of the lid complex
PSMD3	Component of the lid complex
PSMD7	Component of the lid complex and a de-ubiquitinase
PSMD11	Component of the lid complex and required for proteasome assembly
PSMD13	Component of the lid complex
PSMC1	ATPases of the base complex, with chaperone-like function and unfolds proteins as they translocate into 20S core
PSMC2	
PSMC3	
PSMC4	
PSMC6	

Table 2: Gβγ interacts with 26S proteasome components in the cytosol

Gβγ interactors identified through the KEGG pathway database. (A) Mass spectrometry of tagged Gβγ immunoprecipitates as indicated in HEK 293 cells under basal or 1M CCh stimulation over 45 min. “+” indicates the interaction was identified by mass spectrometry, and “-” indicates the interaction was not. (B) Brief interactor roles and functions extracted from GeneCards- Human Gene Database, retrieved Nov. 2017, URL: www.genecards.org.

3.2.1.3 Gβγ and ubiquitin-mediated pathways

Multiple enzymes from the 3-step ubiquitin-conjugating pathway were identified as putative interactors of Gβγ (Table 3) including an E2 ubiquitin-conjugating enzyme from step 2 which loads ubiquitin and interacts with step 3 E3 ubiquitin ligase involved in target recruitment and catalyzing transfer of ubiquitin onto substrate. These putative Gβγ interactors have diverse roles found in literature and give insight into Gβγ degradation and nuclear functions.

Flag-Gβ1 immunoprecipitation identified two E3 ubiquitin ligases, ubiquitin protein ligase E3 component N-recogin 4 (UBR4) and 5 (UBR5, Table 3B) which participate in the N-end rule pathway for ubiquitin-dependent proteolysis. These proteins belong to a family of 7 UBR proteins which have a UBR domain box and function within a type of ubiquitin-dependent degradation system named the N-end rule pathway. Within the system, the UBR box is involved

in recognizing destabilizing N-terminal residues on target substrates which act as degradation signals leading to ubiquitination and degradation of the substrate (122). As expected UBR4 and UBR5 ubiquitin ligases which function in the cytosol were identified to interact with G β γ there. Previously G γ has been suspected to be ubiquitinated through this N-end rule pathway (106) and this may still be an instance of ubiquitin ligases interacting with the γ subunit of the $\beta\gamma$ obligate dimer as multiple G γ isoforms were also detected by Campden's mass spectrometry (data not shown). UBR4, UBR5 interactions with Flag-G β 1 under both basal or CCh stimulation suggest there is potential for the N-end rule to be involved in G $\beta\gamma$ signal transduction control as a general mechanism.

Ubiquitin conjugating enzyme E2 V2 (UBE2V2) interacted with G $\beta\gamma$ within the nucleus under CCh stimulation. Poly-ubiquitination does not always occur on Lys48 of ubiquitin and in doing so can lead to non-proteasomal fates for the ubiquitinated substrates (123). Analysis of G $\beta\gamma$ interaction with UBE2V2 suggests G $\beta\gamma$ may be involved in chromatin repair or mediating transcription. UBE2V2 is categorized as an E2 ubiquitin-conjugating enzyme due to its similarities, but lacks the cysteine residue which confers the catalytic activity to traditional E2 ligase. However, acting within a heterodimer with another E2 ubiquitin ligase named ubiquitin conjugating enzyme E2 N (UBE2N) they conjugate non-canonical Lys63-linked poly-ubiquitin chains which may act as recruitment signals for sites of post-replicative DNA repair in the nucleus (124, 125). These signals recruit proteins such as proliferating cell nuclear antigen (PCNA) which is important in DNA replication and repair and incidentally prominently identified within the Campden screen in all TAP and IP conditions (data not shown). UBE2V2 has been previously demonstrated to enhance cFos transcription from the promoter (126). G $\beta\gamma$ has also been previously suggested to increase cFos expression post D2-R -selective agonist administration of quinpirole (59). Apart from potentially mediating cFOS expression, G $\beta\gamma$ has been directly identified to interact with cFOS subunit of AP-1 to affect AP-1 mediated transcription (40). G $\beta\gamma$ -UBE2V2 interaction in the nucleus under CCh treatment (Table 3A) may suggest a receptor-inducible G $\beta\gamma$ role involved in transcription-related functions.

A

Name	Flag-Gβ1			
	Cytosol		Nucleus	
	Basal	CCh	Basal	CCh
UBE2V2	-	-	-	+
UBR4	-	+	-	-
UBR5	+	-	-	-

B

Name	Function
UBE2V2	Is an E2 ubiquitin-conjugating enzyme, and acts in heterodimer with UBE2N to catalyze synthesis of non-canonical poly-Ub chains linked through Lys63 which may lead to transcriptional activation of target genes
UBR4	Is an E3 ubiquitin ligase, and follows the N-end rule pathway
UBR5	Is an E3 ubiquitin ligase which follows the N-end rule pathway, and may cause mRNA upregulation by regulating CDK9 poly-ubiquitination

Table 3: Gβγ interacts with ubiquitin ligases in the cytosol and nucleus

Gβγ interactors identified through KEGG pathway database. (A) Mass spectrometry of tagged Gβγ immunoprecipitates as indicated in HEK 293 cells under basal or 1M CCh stimulation over 45 min. “+” indicates the interaction was identified by mass spectrometry, and “-” indicates the interaction was not. (B) Brief interactor roles and functions extracted from GeneCards- Human Gene Database, retrieved Nov. 2017, URL: www.genecards.org.

3.2.2 Gβγ and other signalling pathways

3.2.2.1 Gβγ and the spliceosome

There has been no previously ascribed function for Gβγ in relation to the spliceosome, yet the Campden screen identified interaction with multiple spliceosome components. A majority of the interactors were identified within the TAP-Gβ1 interaction purification condition, only in the cytosol and under carbachol stimulation (Table 4). Since spliceosome is only known to be in the cytoplasm during biogenesis prior to returning to the nucleus for nuclear maturation and pre-mRNA splicing functions, the following describes and analyzes Gβγ interactors in relation to spliceosome biogenesis.

Reviewed in (127), the spliceosome machinery is a multi-megadalton RNA-protein factor complex made up of an assembly of multiple small nuclear ribonucleoproteins (snRNPs). SnRNPs are composed of protein factors and a small nuclear RNA (snRNA) of which there are many- the major ones belonging to the spliceosome are U1, U2, U4, U5, U6. These snRNPs come together to locate intronic sequences in pre-mRNA transcripts and splice them in the nucleus. SnRNP biogenesis occurs over multiple steps of assembly and maturation in both the cytoplasm and nucleus (127) (Figure 2).

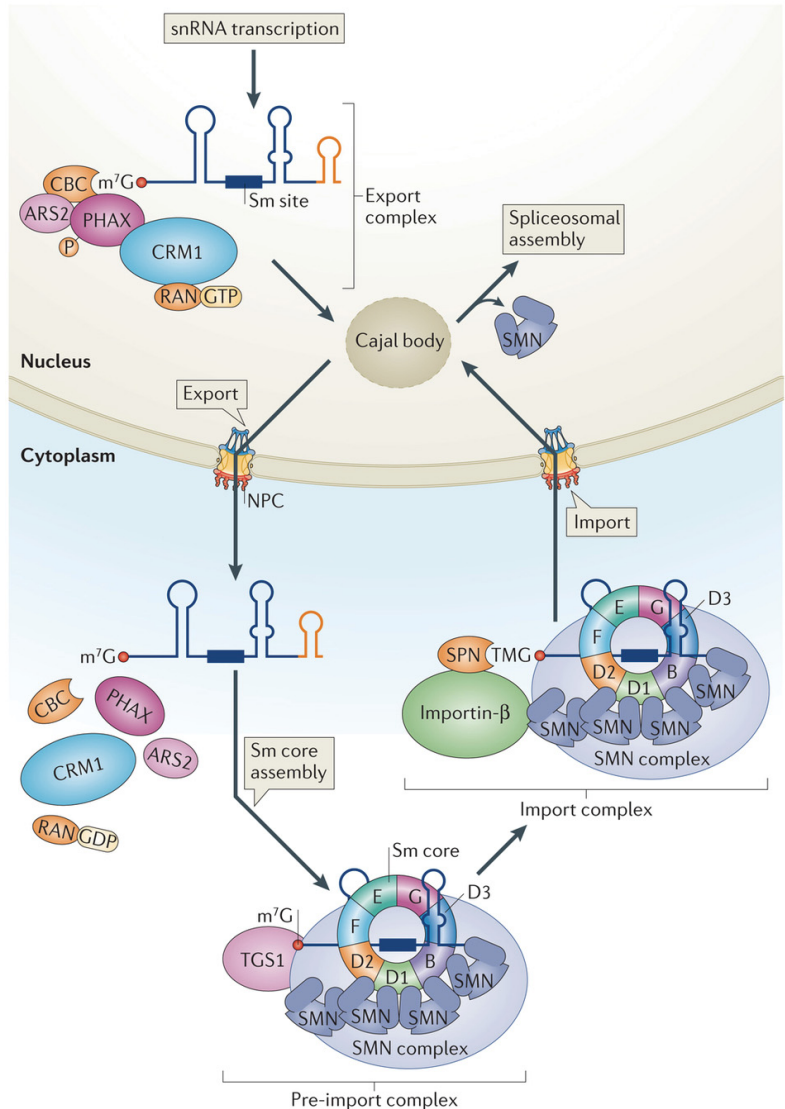
The first step in snRNP assembly is RNAPII transcription of snRNA which is exported out of the nucleus. SnRNA is exported within a large complex where its 5' cap has specific proteins linked to it such as the snRNA-specific export adaptor phosphorylated adaptor RNA export (PHAX), the cap-binding complex (CBC), arsenite resistance protein 2 (ARS2) which associate with exportin 1 (XPO1) and RAN-GTPase to be exported. Once in the cytoplasm, dephosphorylation of PHAX causes snRNA export complex to be disassembled (127). The proteomics data suggests that G $\beta\gamma$ interacts with proteins involved in general export mechanism such as XPO1 and RAN, but does not interact with the other major players of snRNA export suggesting it is not mainly involved in snRNA export.

After snRNA export to the cytoplasm comes the addition of a core component of the snRNP, the Sm heptameric protein ring, and it is at this stage that G $\beta\gamma$ involvement is the most prominent. Sm proteins are important within spliceosome function because they help align RNA-RNA pairing between the snRNA and pre-mRNA during splicing. The assembly of Sm protein onto the snRNA occurs in the cytoplasm and helps stabilize and protect the RNA from degradation. There are seven Sm proteins which are stored in the cytoplasm as partially formed rings. They associate with factors such as a protein Arg *N*-methyltransferase 5 (PRMT5) sequestering protein and a pICln assembly chaperone which helps them to not prematurely assemble. After export, snRNAs associate with the survival motor neuron (SMN) complex composed of SMN and gem nuclear organelle associated protein 2-7 (GEMIN2-GEMIN7) and trigger Sm heptamer ring assembly onto the Sm site of the snRNA through a series of steps that remain poorly understood (127). In the cytosol, the G $\beta\gamma$ proteomic screen identified interaction

with SNRPB, SNRPD2, SNRPD3, SNRPE, SNRPG, in total 5 of the 7 Sm proteins across 3 different purification techniques. The majority SNRPD2, SNRPD3, SNRPE, SNRPG were identified by TAP-G β 1, which are only known to exist together as a heptamer complex fully assembled onto the snRNA suggesting G β γ interacts with the formed Sm in this format. All the 5 G β γ -Sm protein interactions occurred specifically under CCh treatment suggesting this phenomenon is not a ubiquitous basal interaction but is regulated by a GPCR stimulus. Potentially G β γ may be involved with assembling of Sm complex onto the snRNA in the cytoplasm, although it should be noted neither PRMT5, pICln, SMN nor GEMINS proteins were identified in the proteomic screen.

The last step in the cytoplasm is the import of the snRNP and SMN complex into the nucleus. Trimethylguanosine synthase 1 (TGS1) hypermethylates the snRNA 5' end to form a trimethylguanosine (TMG) cap structure which triggers assembly of import complex including snuportin (SPN) and importin- β to the macromolecule. TMG and Sm both act as nuclear localization signals, and the whole complex is imported to Cajal body for final maturation steps (127). G β γ was not seen to associate with importin- β , SPN nor TGS1 in the screen.

G β γ in the spliceosome may participate in Sm assembly which is a critical step in the process of snRNP generation that remains poorly understood. With regards to snRNP biogenesis G β γ does not seem to be specifically involved in snRNA export or snRNP/SMN complex import. As for the other G β γ spliceosome interactors identified (Table 4), these proteins are mainly assembled onto snRNPs during the final maturation steps in the nuclear Cajal bodies. Since the majority of these G β γ interactors were identified only in the cytoplasm, this suggest G β γ may be involved in sequestering, regulating or transporting spliceosome factors in addition to Sm proteins needed for nuclear spliceosome assembly and activity.



Nature Reviews | Molecular Cell Biology

Figure 2: Maturation of the snRNA requires nuclear and cytoplasmic regulatory steps
 Figure taken from (127).

A

Name	Flag-Gβ1				TAP-Gβ1				Split TAP-Gβ1γ7			
	Cytosol		Nucleus		Cytosol		Nucleus		Cytosol		Nucleus	
	Basal	CCh	Basal	CCh	Basal	CCh	Basal	CCh	Basal	CCh	Basal	CCh
SF3A1	+	-	+	-	-	-	-	-	-	-	-	-
SF3B3	-	-	-	-	-	-	-	-	-	+	-	-

SNRPB	-	+	-	-	-	-	-	-	-	-	-	-
SNRPC	-	-	-	-	-	-	-	-	-	+	-	-
SNRPD2	-	-	-	-	-	+	-	-	-	-	-	-
SNRPD3	-	-	-	-	-	+	-	-	-	+	-	-
SNRPE	-	-	-	-	-	+	-	-	-	-	-	-
SNRPG	-	-	-	-	-	+	-	-	-	-	-	-
PRPF19	-	-	-	-	-	-	-	-	-	+	-	-
PRPF6	-	-	-	-	-	+	-	-	-	-	-	-
PRPF8	-	-	-	-	-	+	-	-	-	-	-	-
SRSF1	-	-	-	-	-	+	-	-	-	-	-	-
SRSF2	-	-	-	-	-	+	-	-	-	+	-	-
SRSF3	-	-	-	-	-	+	-	-	-	-	-	-
SRSF5	-	-	-	-	-	+	-	-	-	-	-	-
SRSF6	-	-	-	-	-	-	-	-	-	+	-	-
SRSF7	-	-	-	-	-	+	-	-	-	-	-	-
SRSF8	-	-	-	+	-	+	-	-	-	-	-	-
NAA38	+	-	-	-	-	-	-	-	-	-	-	-
TRA2A	-	-	-	-	-	-	-	-	+	-	-	-
HSPA6	+	-	-	-	+	-	+	-	-	-	+	-
DDX23	-	-	-	-	-	+	-	-	-	-	-	-
DDX46	+	-	-	-	-	-	-	-	-	-	-	-
SNRNP200	-	-	-	-	-	+	-	-	-	-	-	-
SNRNP70	-	-	-	-	-	+	-	-	-	-	-	-
HNRNPC	-	-	-	-	-	+	+	+	+	+	-	-
U2SURP	+	-	-	-	-	-	-	-	-	-	-	-
RBMX	-	-	-	-	-	-	+	-	-	-	-	-
RBM17	+	-	-	-	-	-	-	-	-	-	-	-
PPIL1	-	-	-	-	-	-	-	-	-	+	-	-
EFTUD2	-	-	-	-	-	+	-	-	-	-	-	-

B

Name	Spliceosome function
SF3A1	Component of splicing factor 3a heterotrimer of mature U2 snRNP
SF3B3	Component of splicing factor 3b and together with 3a, forms U2 snRNP
SNRPB	Common nuclear protein found in U1, U2, U4/U6 snRNPs
SNRPC	Component of U1 snRNP
SNRPD2	Component of common Sm protein core of snRNPs
SNRPD3	Component of common Sm protein core of snRNPs
SNRPE	Component of common Sm protein core of snRNPs. Plays a role in the 3' end processing of histone transcripts
SNRPG	Component of common Sm protein core of snRNPs. lays a role in the 3' end

	processing of histone transcripts
PRPF19	Ubiquitin-protein ligase part of the spliceosome and participates in its assembly, remodeling, and activity
PRPF6	Involved in pre-mRNA splicing and potentially acts as bridge between snRNPs
PRPF8	Essential for catalytic step II in pre-mRNA splicing process
SRSF1	Can act to activate or repress splicing, depending on its phosphorylation state and interactors
SRSF2	From the serine/arginine (SR)-rich family of pre-mRNA splicing factors and part of the spliceosome. Each factor contains RNA recognition motif (RRM) and a RS domain binding other proteins. SR proteins are also involved in mRNA export from nucleus for translation.
SRSF3	
SRSF5	
SRSF6	From the SR family, and involved potentially in determining alternative splicing
SRSF7	From the serine/arginine (SR)-rich family of pre-mRNA splicing factors and part of the spliceosome. Each factor contains RNA recognition motif (RRM) and a RS domain binding other proteins. SR proteins are also involved in mRNA export from nucleus for translation.
SRSF8	
NAA38	Anxillary component of N-terminal acetyltransferase C complex involved in catalyzing acetylation of M-terminal methionine residues
TRA2A	Has several RRM and plays role in pre-mRNA splicing
HSPA6	Molecular chaperone, involved in protein quality control system
DDX23	Member of DEAD box protein family. DEAD are putative RNA helicases.
DDX46	Core component of U4/U6-U5 nRNPs and part of U5 snRNP specific proteins
SNRNP200	RNA helicase and component of the U5 snRNP and U4/U6-U5 tri-snRNP complexes
SNRNP70	U1 snRNP subunit 70
HNRNPC	Part of hnRNPs which are RNA binding proteins with influence on pre-mRNA processing, metabolism, transport
U2SURP	U2 snRNP associated SURP Domain Containing.
RBMX	RNA binding protein with multiple roles in regulation of pre- and post-transcriptional processes
RBM17	RNA binding, part of spliceosome complex, and functions in second catalytic step of mRNA splicing
PPIL1	Involved in protein folding
EFTUD2	GTPase and component of the spliceosome

Table 4: G β interacts with ubiquitin ligases in cytosol and nucleus

G β interactors identified through KEGG pathway database. (A) Mass spectrometry of tagged G β immunoprecipitates as indicated in HEK 293 cells under basal or 1M CCh stimulation over 45 min. “+” indicates the interaction was identified by mass spectrometry, and “-” indicates the

interaction was not. (B) Brief interactor roles and functions extracted from GeneCards- Human Gene Database, retrieved Nov. 2017, URL: www.genecards.org.

3.2.2.2 *Gβγ*, cellular respiration and the mitochondria

The *Gβγ* proteomics screen identified multiple components of the oxidative phosphorylation pathway including central components of Complex I, III, IV and ATP synthase (Table 5). Oxidative phosphorylation is a cellular respiratory and metabolic pathway in the mitochondria used by cells to generate ATP. Reviewed in (128), there are 4 complexes within the pathway which transfer electrons in redox reactions to create a proton gradient, allowing for the ATP synthase to generate ATP. First is Complex I, also known as nicotinamide adenine dinucleotide (NADH) dehydrogenase which oxidizes two electrons from NADH that are transferred through iron-sulfur clusters to a ubiquinone molecule in the membrane. Complex I is a large enzyme complex composed of 43 subunits, and the *Gβγ* proteomics screen identified interactions with 7 core subunit components: NADH Dehydrogenase (Ubiquinone) 1 Alpha Subcomplex 4 and 9 (NDUFA4, NDUFA9) and NADH:Ubiquinone Oxidoreductase Core Subunit S1-3, S7, S8 (NDUFS1, NDUFS2, NDUFS3, NDUFS7, NDUFS8). Of those, NDUFS1, NDUFS2, NDUFS3, NDUFS7, NDUFS8 are core components believed to belong to the Complex I minimal assembly required for catalysis (129), and NDUFS1, NDUFS2, NDUFS3 are three of seven iron-sulfur proteins involved in the electron transfer. No components of complex II, or succinate dehydrogenase were identified in our screen. Next in the electron transfer chain is complex III or cytochrome c reductase. Cytochrome c1 (CYC1), one of three cytochrome subunits that go through redox reactions to transfer electrons to cytochrome c was identified to interact with *Gβγ*. Next in this chain, cytochrome c transfers electrons to Complex IV also known as cytochrome c oxidase which has a complex structure containing 13 subunits, 10 of which are nuclear DNA (nDNA)-encoded and 3 mitochondrial DNA (mtDNA)-encoded. Of all the oxidative phosphorylation pathway proteins identified in our screen, only prostaglandin-endoperoxide synthase 2 (COX2) from Complex IV comes from mitochondrial DNA. In fact mtDNA encodes only 13 genes in total while the remaining mitochondrial proteins are nDNA-encoded. Interestingly, *Gβγ* is not presently known to reside within the mitochondria itself so its interaction with COX2 remains a puzzle. COX2 is subunit 2 of three mtDNA-encoded catalytic

core subunits of Complex IV and transfers electrons from cytochrome c to subunit 1. Cytochrome c oxidase subunit 4I1, 5A, 7A2 (COX4I1, COX5A, COX7A2) were also identified in the screen, and belong to the nDNA-encoded subunits of Complex IV whose functions are unknown but believed to play roles in complex IV regulation and assembly (129). Lastly is the ATP synthase, which sits on the inner mitochondrial membrane and uses the proton gradient to generate ATP. It is composed of 2 compartments: a F1 soluble catalytic core composed of 5 distinct subunits, and a Fo membrane-spanning proton channel with 9 subunits. G β γ interactor data identified ATP Synthase, H⁺ Transporting, Mitochondrial F1 Complex, Alpha Subunit 1 (ATP5A1) and ATP Synthase, H⁺ Transporting, Mitochondrial F1 Complex, Beta Polypeptide (ATP5B), the alpha and beta subunits of F1 respectively, and another subunit ATP Synthase, H⁺ Transporting, Mitochondrial Fo Complex Subunit F2 (ATP5J2) from Fo complex. These three interactors were identified exclusively from cytosolic Flag-G β 1 immunoprecipitation under both basal and CCh treated conditions. All the proteins described here with the exception for COX2 are nDNA-encoded proteins which are transcribed within the nucleus and guided with chaperones as preproteins to enter the mitochondria's double membrane for folding. It remains unclear whether G β γ interaction is during the preprotein generation and translocation process or within the mitochondria itself.

The G β γ proteomics data also revealed multiple processes essential to the mitochondria protein translocation and generation process such as mitochondrial preprotein import from the cytoplasm, and mitochondrial ribosomes responsible for translating mtDNA. Preprotein import into the mitochondria generally occurs through the translocase of outer mitochondrial membrane (TOM) and translocase of the inner membrane (TIMM) (130), and both TOMM22 and TIMM8A subunits were identified in the screen (Table 6). While it has been previously suspected G β γ cannot enter the mitochondria due to its structure (77), GPCRs have been identified in the inner mitochondrial membrane (IMM) (78). G β γ interaction with core preprotein transport units supports the notion that G β γ may be translocated into and exist within the mitochondria. Members from the nDNA-encoded solute carrier family 25 proteins 1, 3, 10-13, 18, 25 (SLC25A1, SLC25A3, SLC25A10, SLC25A11, SLC25A12, SLC25A13, SLC25A18, SLC25A24) were also identified, and they sit mostly on the IMM (Table 6). They act to transport

metabolites such as ions and components of the citric acid cycle of across mitochondrial membranes (Table 6B) although the role of G β γ remains unclear.

Mitochondrial ribosomes, or mitoribosomes are responsible for translating mRNA from mtDNA. Similar to cytoplasmic ribosomes, they also contain small and large subunits named 28S and 39S which are mainly composed of nDNA-encoded proteins that must be shuttled into the mitochondria (131). The G β γ proteomics screen identified death-associated protein 3 (DAP3), mitochondrial ribosomal protein S5, S18B, S27, S35, (MRPS5, MRPS18B, MRPS27, MRPS35) from the 28S subunit, and mitochondrial ribosomal protein L4, L12, L17, L43, L46, L49 (MRPL4, MRPL12, MRPL17, MRPL43, MRPL46, MRPL49) from the 39S subunit (Table 7). The majority of these interactions were identified following CCh stimulation only from the cytosol (Table 7A).

Overall, G β γ interaction with these nDNA-encoded proteins may point to its involvement in preprotein generation, translocation into the mitochondria, and even interaction within the mitochondria itself. Certain cases of G β γ interactors such as with mtDNA-encoded COX2, and TOMM and TIMM even suggest G β γ could be found also within the mitochondria itself.

A

Name	Flag-G β 1				TAP-G β 1				Split TAP-G β 1 γ 7			
	Cytosol		Nucleus		Cytosol		Nucleus		Cytosol		Nucleus	
	Basal	CCh	Basal	CCh	Basal	CCh	Basal	CCh	Basal	CCh	Basal	CCh
ATP5A1	+	+	-	-	-	-	-	-	-	-	-	-
ATP5B	-	+	-	-	-	-	-	-	-	-	-	-
ATP5J2	-	+	-	-	-	-	-	-	-	-	-	-
ATP6V0A1	-	-	-	-	-	-	+	-	-	-	-	-
ATP6V0D1	-	-	-	-	-	-	-	-	-	-	-	+
ATP6V1A	-	-	-	-	-	-	-	-	-	-	-	+
ATP6V1B2	-	-	-	-	-	-	-	-	-	-	-	+
COX2	+	-	-	-	-	-	-	-	-	-	-	-
COX4I1	-	+	-	-	-	-	-	-	-	-	-	-
COX5A	-	+	-	-	-	-	-	-	-	-	-	-
COX7A2	-	-	-	-	-	-	-	-	+	-	-	-

CYC1	-	+	-	-	-	-	-	-	-	-	+	-	-
NDUFA4	-	+	-	-	-	-	-	-	-	-	-	-	-
NDUFA9	+	+	-	-	-	-	-	-	-	-	-	-	-
NDUFS1	+	+	-	-	-	-	-	-	-	-	-	-	-
NDUFS2	+	-	-	-	-	-	-	-	-	-	-	-	-
NDUFS3	-	+	-	-	-	-	-	-	-	-	-	-	-
NDUFS7	+	-	-	-	-	-	-	-	-	-	-	-	-
NDUFS8	-	+	-	-	-	-	-	-	-	-	-	-	-

B

Name	Complex	Function
ATP5A1	ATP synthase	Gene encodes the alpha subunit in the F1 soluble catalytic core
ATP5B	ATP synthase	Gene encodes the beta subunit in the F1 soluble catalytic core
ATP5J2	ATP synthase	Gene encodes the f subunit of the proton channel in the Fo complex
ATP6V0A1	V-type ATPase	One of three A subunits of the membrane peripheral V1 domain for ATP hydrolysis
ATP6V0D1	V-type ATPase	The D subunit of the membrane peripheral V1 domain for ATP hydrolysis, found ubiquitously in the cell
ATP6V1A	V-type ATPase	One of two A subunit isoforms of the membrane peripheral V1 domain for ATP hydrolysis, found in all tissues
ATP6V1B2	V-type ATPase	One of two B subunit isoforms of the membrane peripheral V1 domain for ATP hydrolysis, found in all tissues
COX2	Cytochrome c oxidase (Complex IV)	Subunit 2 of three mitochondrial-encoded catalytic core subunits involved in electron transfer function of cytochrome c oxidase, which acts to catalyze the reduction of oxygen to water. Subunit 2 transfers the electrons from cytochrome c to catalytic subunit 1
COX4I1	Cytochrome c oxidase (Complex IV)	Nuclear-encoded subunit 4 isoform 1 of thirteen subunits which make up cytochrome c oxidase. Nuclear-encoded subunit functions are unknown but may play role in regulation and assembly of complex
COX5A	Cytochrome c oxidase (Complex IV)	Nuclear-encoded subunit Va of thirteen subunits which make up cytochrome c oxidase. Nuclear-encoded subunit functions are unknown but may play role in regulation and assembly of complex
COX7A2	Cytochrome c oxidase (Complex IV)	Nuclear-encoded subunit VIIa polypeptide 2 of thirteen subunits which make up cytochrome c oxidase. Nuclear-encoded subunit functions are unknown but may play role in regulation and assembly of complex
CYC1	Cytochrome bc1	1 of 3 cytochromes subunits containing heme groups, and

	(Complex III)	as an electron carrier it transfers electrons from the Rieske iron-sulfur protein to cytochrome c
NDUFA4	NADH dehydrogenase (Complex I)	1 of 43 subunit components of complex I that transfers electrons from NADH to the respiratory chain
NDUFA9	NADH dehydrogenase (Complex I)	Is an accessory subunit not believed to be involved in catalysis. It is from the hydrophobic protein fraction and is 1 of 43 subunit components of complex I that transfers electrons from NADH to the respiratory chain
NDUFS1	NADH dehydrogenase (Complex I)	1 of 7 iron-sulfur proteins that are core components of NADH dehydrogenase, and belongs to minimal assembly required for catalysis
NDUFS2	NADH dehydrogenase (Complex I)	1 of 7 iron-sulfur proteins that are core components of NADH dehydrogenase, and belongs to minimal assembly required for catalysis
NDUFS3	NADH dehydrogenase (Complex I)	1 of 7 iron-sulfur proteins that are core components of NADH dehydrogenase, and belongs to minimal assembly required for catalysis
NDUFS7	NADH dehydrogenase (Complex I)	1 of 43 subunit components of complex I and is a core component of NADH dehydrogenase, and belongs to minimal assembly required for catalysis
NDUFS8	NADH dehydrogenase (Complex I)	1 of 43 subunit components of complex I and is a core component of NADH dehydrogenase, and belongs to minimal assembly required for catalysis

Table 5: Gβγ interacts with oxidative phosphorylation pathway components

Gβγ interactors identified through KEGG pathway database. (A) Mass spectrometry of tagged Gβγ immunoprecipitates as indicated in HEK 293 cell under basal or 1M CCh stimulation over 45 min. “+” indicates the interaction was identified by mass spectrometry, and “-” indicates the interaction was not. (B) Brief interactor roles and functions extracted from GeneCards- Human Gene Database, retrieved Nov. 2017, URL: www.genecards.org.

A

Name	Flag-Gβ1				TAP-Gβ1				Split TAP-Gβ1γ7			
	Cytosol		Nucleus		Cytosol		Nucleus		Cytosol		Nucleus	
	Basal	CCh	Basal	CCh	Basal	CCh	Basal	CCh	Basal	CCh	Basal	CCh
CHCHD3	-	+	-	-	-	-	-	-	-	-	-	-

HSPD1	+	+	-	-	-	-	-	-	-	-	-	-
SLC16A1	-	+	-	-	-	-	-	-	-	-	-	-
SLC25A1	+	+	-	-	-	-	-	-	-	-	-	-
SLC25A10	+	+	-	-	-	-	-	-	-	-	-	-
SLC25A11	+	+	-	-	-	-	-	-	-	-	-	-
SLC25A12	-	+	-	-	-	-	-	-	-	-	-	-
SLC25A13	+	+	-	-	-	-	-	-	-	-	-	-
SLC25A18	-	+	-	-	-	-	-	-	-	-	-	-
SLC25A24	+	-	-	-	-	-	-	-	-	-	-	-
SLC25A3	+	+	-	-	-	-	-	-	-	-	-	-
TIMM8A	-	-	-	-	-	-	-	-	-	-	+	-
TOMM22	-	+	-	-	-	-	-	-	-	-	-	-
VDAC1	-	-	-	+	-	-	-	-	-	-	-	-

B

Name	Function
CHCHD3	IMM scaffolding protein, involved in mitochondrial cristae integrity and part of the mitochondrial contact site and cristae organizing system (MICOS)
HSPD1	Mitochondrial chaperonin protein, and important for folding and assembling newly imported proteins in the mitochondria
SLC25A1	Member of mitochondrial solute carrier family 25. Regulates citrate across IMM
SLC25A10	Member of mitochondrial solute carrier family 25. Exchanges dicarboxylates such as malate and succinate, for phosphate, sulfate, and other small molecules
SLC25A11	Member of mitochondrial solute carrier family 25. An oxoglutarate/malate carrier and transports 2-oxoglutarate across IMM
SLC25A12	Member of mitochondrial solute carrier family 25. Involved in exchange of aspartate for glutamate across IMM
SLC25A13	Member of mitochondrial solute carrier family 25. Catalyzes exchange of aspartate for glutamate and a proton across IMM
SLC25A18	Member of mitochondrial solute carrier family 25. Involved in glutamate and a co-transported H(+) across IMM
SLC25A24	Member of mitochondrial solute carrier family 25. Transports Mg-ATP/Mg-ADP exchange for phosphate ions across IMM
SLC25A3	Member of mitochondrial solute carrier family 25. Transports phosphate groups from cytosol to mitochondria by co-transporting H(+) or exchange for hydroxyl ions
TIMM8A	Translocase of the inner mitochondrial membrane (TIMM). Involved in import and insertion of hydrophobic membrane proteins into the IMM.
TOMM22	Translocase of the outer mitochondrial membrane (TOMM). Is the central receptor to recognize mitochondrial preproteins in the cytosol and in complex with other TOMMs moves preproteins into translocation pore

VDAC1	Voltage-dependent anion channel protein that facilitates exchange of metabolites and is a major component of OMM
-------	--

Table 6: G β y interacts with mitochondrial protein translocation components

G β y interactors identified through PathCards- Pathway Unification Database. (A) Mass spectrometry of tagged G β y immunoprecipitates as indicated in HEK 293 cell under basal or 1M CCh stimulation over 45 min. “+” indicates the interaction was identified by mass spectrometry, and “-” indicates the interaction was not. (B) Brief interactor roles and functions extracted from GeneCards- Human Gene Database, retrieved Nov. 2017, URL: www.genecards.org.

A

Name	Flag-G β 1	
	Cytosol	
	Basal	CCh
DAP3	-	+
MRPL12	-	+
MRPL17	-	+
MRPL4	-	+
MRPL43	+	+
MRPL46	-	+
MRPL49	-	+
MRPS18B	-	+
MRPS27	-	+
MRPS35	-	+
MRPS5	-	+

B

Name	Ribosomal complex
DAP3	28S
MRPL12	39S
MRPL17	39S
MRPL4	39S
MRPL43	39S
MRPL46	39S
MRPL49	39S
MRPS18B	28S
MRPS27	28S
MRPS35	28S

MRPS5	28S
-------	-----

Table 7: G β γ interacts with mitochondrial ribosomal components

G β γ interactors identified through PathCards- Pathway Unification Database. (A) Mass spectrometry of tagged G β γ immunoprecipitates as indicated in HEK 293 cell under basal or 1M CCh stimulation over 45 min. “+” indicates the interaction was identified by mass spectrometry, and “-” indicates the interaction was not. (B) Brief interactor roles and functions extracted from GeneCards- Human Gene Database, retrieved Nov. 2017, URL: www.genecards.org.

3.3 Validating G β γ interactors from degradation pathways

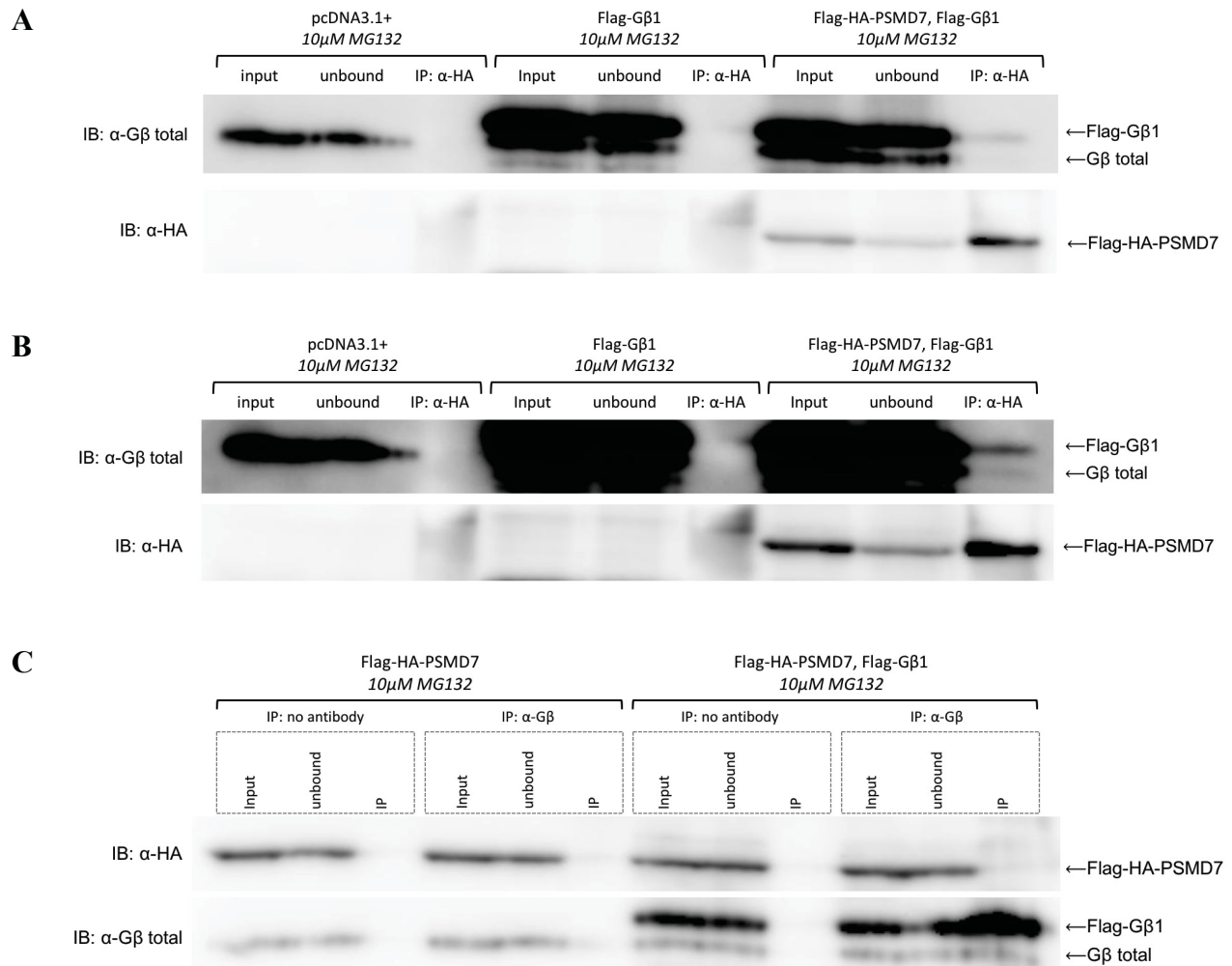
PSMD7 and KCTD5 were selected from Section 3.2 G β γ interactome analysis of degradation pathways to validate their interaction with G β γ by immunoprecipitation and western blot.

3.3.1 G β γ and the 26S proteasome

The G β γ proteomics screen identified the 26S proteasome and my analysis determined it is a likely pathway for G β γ to be involved in. We decided to study the de-ubiquitinase PSMD7, and to probe its interaction with G β γ . I first optimized Flag-HA-PSMD7 transient expression in HEK 293 cells by subcloning it into a pcDNA3.1+ vector. Due to low expression of the protein, MG132 treatment which inhibits the proteolytic activity of the 26S proteasome was added to enhance Flag-HA-PSMD7 expression after transfection, and to enrich the capture of PSMD7-G β γ interaction which under basal levels could barely, if at all, be visualized. I successfully showed interactions using IP (Figure 3) by two methods: IP HA-epitope for Flag-HA-PSMD7 and visualization of interaction using G β total antibody (Figure 3A, B), and immunoprecipitation of G β total for Flag-G β 1 and visualization of Flag-HA-PSMD7 using HA antibody (Figure 3C, D). I was able to additionally capture endogenous G β interaction with Flag-HA-PSMD7 (Figure 3B) giving evidence of endogenous G β γ and potentially other G β isoforms being degraded by the proteasome.

3.3.2 Gβγ and KCTD5

The interaction between KCTD5-Flag and TAP-Gβ1 was previously validated by the Hébert lab, as can be seen in the western blot generated by Darlaine Pétrin in Figure 4. The immunoprecipitation of Flag was clearly visualized through western blot immunoblotting of Gβ total, and the experiment shows KCTD5 interacts with both TAP-Gβ1 and endogenous Gβ total.



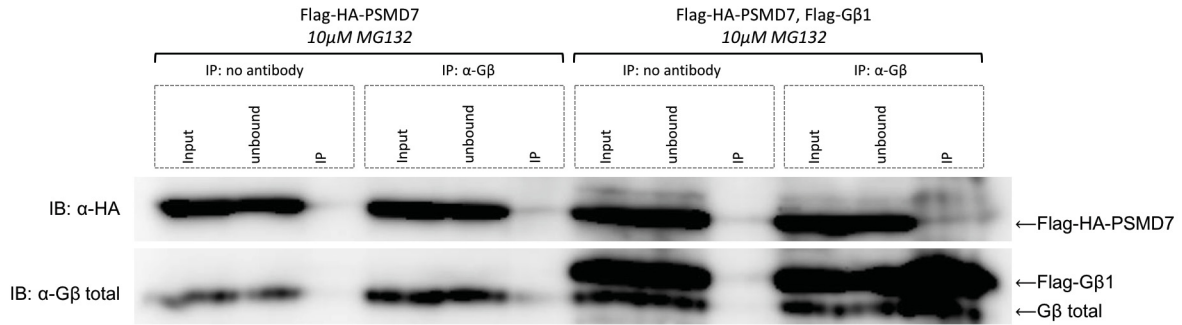
D

Figure 3: Validating PSMD7, Gβ interaction using immunoprecipitation and western blot

HEK 293 cells were transiently transfected with different plasmids (as indicated on Figures) or empty vector pcDNA3.1+ plasmid, and treated with 10μM MG132 for 12 hours to inhibit proteasomal degradation. IP was performed using two methods and visualized by western blot and immunoblotting (IB). These results are representative of 3 independent experiments. (A, B) HA epitope IP against the Flag-HA-PSMD7 protein to visualize endogenous Gβ total and Flag-Gβ1 interaction shown in a shorter (A) and longer (B) western blot chemiluminescence exposures. (C, D) Gβ total IP against endogenous Gβ and/or Flag-Gβ1 to visualize Flag-HA-PSMD7 interaction shown in shorter (C) and longer (D) chemiluminescence exposures also.

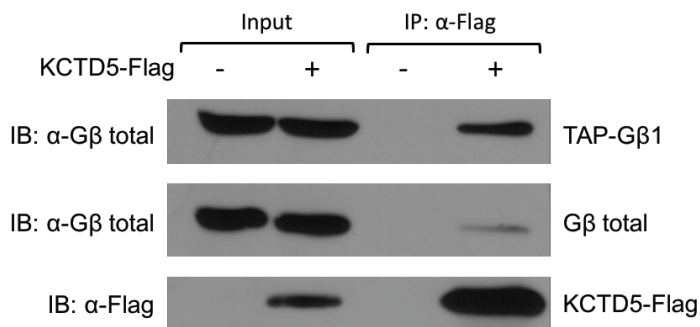


Figure 4: Validating KCTD5, Gβγ interaction using immunoprecipitation and western blot

Stable TAP-Gβ1 HEK 293 cell line was transiently transfected with KCTD5-Flag or pcDNA3.1+ empty vector plasmid. IP was performed against Flag, and co-IP of endogenous Gβ total and TAP-Gβ1 was detected by western blot immunoblotting (IB). N=2

3.4 KCTD5 CRISPR knockout line generation and validation

3.4.1 Background

Generation of a KCTD5 knockout stable cell line using Clustered Regularly Interspaced Short Palindromic Repeats (CRISPR) and CRISPR-associated 9 (Cas9) gene editing technique in HEK 293 cells will give us a tool to observe KCTD5 function and study its effect on G β γ signalling and degradation. The genome editing technique is adapted from bacterial and archaeal defense mechanisms against invasive genetic material by cleaving it and triggering their degradation and is used here as a mechanism to direct mutagenesis within the KCTD5 gene to result in non-functional proteins. Proteins discussed within Section 3.4.6 Table 10 are listed by their gene symbols for clarity and consistency, and their full gene names may be found in the Supplemental Table 1.

3.4.2 Experimental design

A plasmid with Cas9 (from the laboratory of Dr. Feng Zhang, Massachusetts Institute of Technology, MIT) and a 23 base-pair KCTD5 single guide RNA (sgRNA), were transfected into HEK 293 cells. The sgRNA contains a protospacer adjacent motif (PAM) sequence on the 3' end which helps guide Cas9 to a homologous sequence on the KCTD5 gene in exon 1. The Cas9 cleavage occurs approximately ~3 nucleotides upstream of the sgRNA PAM and was designed to coincide with a natural NaeI restriction enzyme site sequence. After directed Cas9 DNA cleavage at this site, cellular host mechanisms proceed to repair the double stranded break (DSB) by non-homologous end joining (NHEJ) which is imperfect. These new imperfections in the KCTD5 gene at the Cas9 cleavage site show up as mismatches which disrupt the NaeI restriction enzyme site and we can detect. The first step was to determine general transfection and Cas9 efficiency through the IDT Surveyor Mutation Detection Kit which uses a mismatch-specific DNA endonuclease to cleaves at DNA distortion sites and detect indels. Upon assurance of general success of the transcription, single clone colonies were cultured. Individually their gDNA was extracted, PCR amplified for the KCTD5 region of interest and subjected to restriction fragment length polymorphism (RFLP) testing for NaeI site disruption. The clones whose PCR products were not digested by NaeI enzyme meaning Cas9 genome editing and

indels occurred at that site were then validated by DNA sequencing, and functionally validated through mass spectrometry to demonstrate loss of KCTD5 interaction with Gβ1.

3.4.3 Preliminary survey of KCTD5 gene indels

This demonstrates our preliminary method of surveying the success of the CRISPR/Cas9 strategy and transfection efficiency. PCR primers were designed and optimized to amplify a 545 basepair (bp) region on the KCTD5 gene (Table 8). The PCR product encompassed the sgRNA target sequence, and the predicted region of Cas9 cleavage at the NaeI restriction enzyme site was approximately halfway through. An IDT Surveyor Mutation Detection Kit was used because it employs DNA endonucleases to cleave mismatches and identify indels. This allowed clear visualization of the contrast between non-digested samples that were predicted to appear around 545 bp, and digested samples positive for NaeI indels disruption and cleaved by the DNA endonuclease at half the size. As seen in Figure 5, there was good general efficacy of the CRISPR/Cas9 strategy as can be seen in the second band of the heterogeneous KCTD5 KO cell line.

3.4.4 KCTD5 knockout single clone RFLP and sequencing

Multiple clones were selected from the KCTD5 KO heterogeneous population to test for KCTD5 knockout by RFLP and sequencing. Using the same primers and PCR strategy (Table 8), gDNA from multiple single cell colonies were amplified at the KCTD5 gene and then digested with NaeI digestion enzyme. Within Figure 6, results demonstrated there were both single clones positive for NaeI digestion suggesting unsuccessful CRISPR/Cas9 action (clones F2, H9, A4), and clones negative for NaeI digestion (clones D2, B11). The RFLP proved to be a reliable and accurate method of assessing presence of gene disruption, because positive and negative results were validated though sequencing (Table 9) with the exception of D5 cell line which was lost prior to sequencing. The B11 clone was identified and selected as the best candidate to proceed because of its largely missense mutations within KCTD5 sgRNA target region; however one low-copy allele showed a 27 deletion which may potentially allow a functional KCTD5 to be generated. To further investigate this, mass spectrometry (MS) was used to as a last step of the validation processes.

3.4.5 Mass spectrometry functional validation of KCTD5 knockout

MS was employed to assess both the presence of KCTD5 and functional KCTD5 interactions with G β within the KCTD5 KO cell line. Using transiently-transfected Flag-G β 1 followed by α -Flag IP in parental and B11 KCTD5 KO clone method, we analyzed the IP-enriched lysate and unbound lysate to determine intensity of KCTD5 peptide presence. The MS data for Flag-G β 1 immunoprecipitates showed 1 KCTD5 peptide detected in the parental cell line and 0 peptides detected in the KCTD5 KO cell line. For comparison, 29 G β 1 peptides were identified in the parental and 21 in B11 immunoprecipitates. No KCTD5 peptides were detected in the unbound lysates for either cell line. In a separate MS experiment where the same strategy used here was employed but cells were treated with MG132 to inhibit the 26S proteasome prior to Flag immunoprecipitation, traces of KCTD5 were identified to interact with Flag-G β 1 in the KCTD5 KO cell line as well. The peptide intensity for the parental wildtype (WT) line versus B11 KCTD5 KO line (WT/KO ratio) was 2.98 for KCTD5, and as a control 0.7 for G β 1. Although this is not an absolute indicator of cellular levels of proteins, this large ratio in the case for KCTD5 suggests decreased KCTD5 presence in the B11 KCTD5 KO cell line (referred to as the KCTD5 KO cell line for the remainder of the thesis).

3.4.6 Comparing G β γ interaction landscapes between KCTD5 knockout and parental cell lines

A comparison of the data from the Flag-IP and mass spectrometry validation of KCTD5 knockout was performed. In evaluating the Flag-G β 1 interactors enriched from KCTD5 KO cell line versus the parental HEK 293 cell line, there were 118 unique proteins in common, 202 proteins lost with KCTD5 KO and unique to the parental line only, and a gain of 285 unique proteins with KCTD5 KO (Supplementary Table 2). This suggests conditions of KCTD5 KO can have significant changes to G β γ interactors. By screening these 285 unique proteins gained with KCTD5 KO through KEGG Pathway, an online integrated databases for human biological pathways, a large proportion namely 14% of those proteins were found to belong to cellular metabolic pathways (Table 10). These proteins have not been previously identified in the literature nor in our original proteomic screen, and they appear in prominent cellular metabolic pathways such as purine and pyrimidine metabolism, amino acid biosynthesis, gluconeogenesis and glycolysis. Of the 4 KCTD isoforms identified previously in the Campden proteomic screen

(KCTD2, KCTD5, KCTD12, KCTD17), KCTD17 interaction with Flag-Gβ1 was undetected in both parental and KCTD5 KO cell lines, but KCTD12 remains a common interactor in both. In contrast, with the loss of KCTD5 interaction in the KCTD5 KO cell line, Flag-Gβ1 also lost its interaction with KCTD2.

A

Name	5' to 3' nucleotide sequence	Notes
sgRNA for KCTD5	GCGAGCTCCTGTCGCCGGCCCGG	Green: NaeI restriction site. Blue: PAM sequence
gDNA forward primer	GAAGGCTAGGGTTCGAGGTCTG	Amplifies ~545bp product. sgRNA target sequence is 305bp-328bp.
gDNA reverse primer	CATCCTTGCTGAGTCCAGGTC	

B

Reagent components	Volume per reaction (μl)
10X PFU Ultra AD (Agilent)	5
10mM dNTP	2
PFU Ultra AD	1
25mM Forward primer	1
25mM Reverse primer	1
100ng gDNA	<i>variable</i>
H ₂ O	<i>variable</i>
Total	50

C

Step	Temperature (°C)	Time (min)	Repeat
1	95	5	1x
2	95	1	35x
3	65	0.5	
4	72	1	
5	72	10	1x
6	4	hold	1x

Table 8: Optimized PCR conditions for amplification of KCTD5 sgRNA gene target

(A) gDNA primer sequences and KCTD5 sgRNA target sequence. (B) PCR reaction reagents. (C) PCR cycling protocol.

Cas9	+	+	+	+
KCTD5 sgRNA	-	-	+	+
DNA endonuclease	-	+	-	+

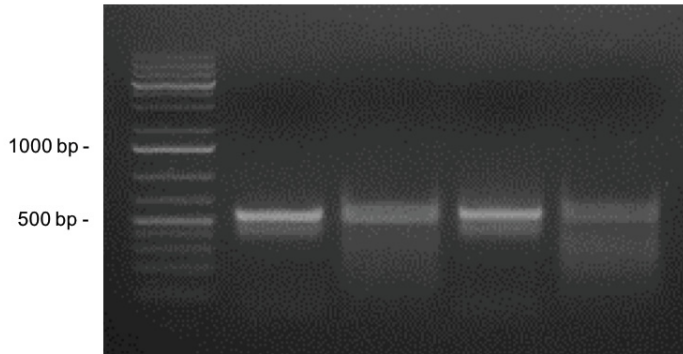


Figure 5: Detecting DNA mutations and indels

PCR-amplified 545bp products from gDNA of a heterogeneous population of Cas9-only treated (parental) cells or Cas9 and KCTD5 sgRNA treated (KCTD5 KO) cells surveyed by IDT Surveyor Mutation Detection Kit for mismatches that arise from indels.

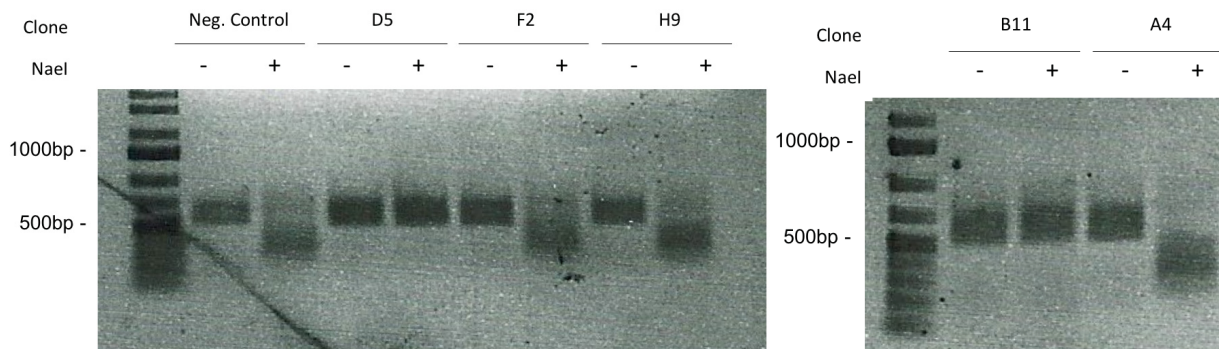


Figure 6: RFLP screen for KCTD5 gene disruption by CRISPR/Cas9 and KCTD5 sgRNA

Digestion of the KCTD5 gDNA PCR product from various clones with NaeI digestion enzyme. Negative (Neg.) control was from cell line transfected with Cas9 alone (parental), and single clones (only some shown here: D5, F2, H9, B11, A4) were from cell lines transfected with Cas9 and KCTD5 sgRNA.

Clone	Indel(s)	Sequence (5' to 3')	Frequency
WT	-	ATG GCGGAGAATCACT GCGAGCTCCTGTCGCCGGCCCGG	-
B11	27 nt deletion	ATG GCGGAGAATCACTGCGAGCTCCTGTCGCCGGCCCGG	1/10
	4 nt deletion	ATG GCGGAGAATCACT GCGAGCTCCTGTCGCCGGCCCGG	7/10
	4 nt deletion	ATG GCGGAGAATCACT GCGAGCTCCTGTCGCCGGCCCGG	2/10
F2	None	ATG GCGGAGAATCACT GCGAGCTCCTGTCGCCGGCCCGG	10/10
H9	None	ATG GCGGAGAATCACT GCGAGCTCCTGTCGCCGGCCCGG	6/6
A4	None	ATG GCGGAGAATCACT GCGAGCTCCTGTCGCCGGCCCGG	6/6

Table 9: Comparing KCTD5 CRISPR/Cas9 single clone gene sequences

Excerpts of the sequencing results of the KCTD5 gene from some clones: B11, F2, H9, A4, and of the parental line (WT) are shown. Up to 10 KCTD5 gDNA PCR products were sequenced per clone by Sanger sequencing, and frequency of indels detected are shown in column 4. Red is KCTD5 gene ATG transcription start site; yellow highlight is KCTD5 sgRNA target; green is NaeI restriction enzyme site; blue is PAM sequence; black highlight is nucleotide deletion.

A

Names				
AHCY	CTPS1	GLUL	NME2	PNPO
APIP	DUT	HPRT1	P4HA2	PRDX6
ASNS	ENO1	INPP5B	PAICS	PRPS1
BCAT1	EPRS	LDHC	PANK3	PRPS2
BLVRA	FASN	MAN2A2	PDXK	PTGES3
CMBL	GALM	NAPRT	PHGDH	QARS
COMT	GANAB	NME1	PKM	UQCRH
COX17	GART	NME1-NME2	PLCZ1	

B

Metabolic pathway	Name	Protein function
Purine metabolism	GART	A trifunctional polyprotein required for de novo purine biosynthesis
	HPRT1	Transferase converts bases into IMP and guanosine and central role in generation of purine nucleotide
	NME1	Major role in synthesis of nucleoside triphosphates other than ATP. Mutations have been identified in aggressive neuroblastomas
	NME2	Major role in synthesis of nucleoside triphosphates other than ATP. Negatively regulates Rho and is

		transcriptional activator of MYC gene
	PAICS	Catalyzes steps 6 & 7 of purine biosynthesis
	PKM	Involved in glycolysis and important to tumour cell proliferation and survival
	PRPS1	Catalyzes reaction necessary for purine metabolism and nucleotide biosynthesis.
	PRPS2	Central role in synthesis of purines and pyrimidines
Biosynthesis of amino acids	BCAT1	Cytosolic form transaminase that catalyzes the reversible transamination of branched-chain alpha-keto acids to branched-chain L-amino acids essential for cell growth
	ENO1	Role in glycolysis
	GLUL	Catalyzes synthesis of glutamine from glutamate and ammonia
	PHGDH	Involved in early steps of L-serine synthesis
	PKM	Involved in glycolysis and important to tumour cell proliferation and survival
	PRPS1	Catalyzes reaction necessary for purine metabolism and nucleotide biosynthesis.
	PRPS2	Central role in synthesis of purines and pyrimidines
Pyrimidine metabolism	CTPS1	Converts uridine triphosphate to cytidine triphosphate. Loss of function associated with immunodeficiency
	DUT	Essential for nucleotide metabolism by hydrolyzing dUTP to dUMP, providing precursor to thymine synthesis, and controlling levels of dUTP
	NME1	Major role in synthesis of nucleoside triphosphates other than ATP. Mutations have been identified in aggressive neuroblastomas
	NME2	Major role in synthesis of nucleoside triphosphates other than ATP. Negatively regulates Rho and is transcriptional activator of MYC gene
Carbon metabolism	ENO1	Role in glycolysis
	PHGDH	Involved in early steps of L-serine synthesis
	PKM	Involved in glycolysis and important to tumour cell proliferation and survival
	PRPS1	Catalyzes reaction necessary for purine metabolism and nucleotide biosynthesis.
	PRPS2	Central role in synthesis of purines and pyrimidines
Glycolysis/ gluconeogenesis	ENO1	Role in glycolysis
	GALM	An enzyme that catalyzes the epimerization of hexose sugars such as glucose and galactose
	LDHC	Catalyzes L-lactate and NAD to pyruvate and NADH in final step of anaerobic glycolysis.

	PKM	Involved in glycolysis and important to tumour cell proliferation and survival
Cysteine and methionine metabolism	AHCY	Involved in first step of biosynthesis of L-homocystein biosynthesis
	APIP	Functions in methionine salvage pathway and in step 2 of subpathway that synthesizes L-methionine into S-methyl-5-thio-alpha-D-ribose 1-phosphite
	BCAT1	Cytosolic form transaminase that catalyzes the reversible transamination of branched-chain alpha-keto acids to branched-chain L-amino acids essential for cell growth
	LDHC	Catalyzes L-lactate and NAD to pyruvate and NADH in final step of anaerobic glycolysis.
Glucagon signaling pathway, and pyruvate metabolism	LDHC	Catalyzes L-lactate and NAD to pyruvate and NADH in final step of anaerobic glycolysis.
	PKM	Involved in glycolysis and important to tumour cell proliferation and survival
Phosphatidylinositol signaling system, and inositol phosphate metabolism	INPP5B	Enzyme which inactivates inositol phosphates to regulate calcium signalling
	PLCZ1	Belongs to family of phosphoinositide-specific phospholipase C which mediates production of second messengers DAG, IP3
Oxidative phosphorylation	COX17	Terminal component of mitochondrial respiratory chain and catalyzes electron transfer from reduced cytochrome C to oxygen
	UQCRH	Component of ubiquinol-cytochrome c reductase complex in complex III or cytochrome b-c1 complex in respiratory chain
Alanine, aspartate and glutamate metabolism	ASNS	Involved in synthesis of asparagine
	GLUL	Catalyzes synthesis of glutamine from glutamate and ammonia

Table 10: loss of KCTD5 leads to G β 1 interaction shift towards metabolic proteins

Comparison of mass spectrometry data from Flag-G β 1 immunoprecipitates from parental versus KCTD5 CRISPR KO cell line is shown here. Identified proteins are listed by their corresponding gene names. (A) Full list of proteins present only in KCTD5 KO cell line involved in metabolic pathways identified by KEGG pathway analysis online. (B) Metabolic pathways identified by KEGG pathway analysis online and proteins from (A) involved within each pathway and their respective roles and functions extracted from GeneCards- Human Gene Database, retrieved Nov. 2017, URL: www.genecards.org.

3.5 KCTD5 and 26S proteasome effects on G β γ degradation and signalling

3.5.1 G β 1 degradation by the 26S proteasome

To investigate G β γ degradation, MG132 used was as a tool to inhibit the 26S proteasome and evaluate changes in G β γ levels. Transient transfection of Flag-G β 1 results in constitutive expression of the protein, and optimization shows more than 5 hours of MG132 treatment was required to visually see the accumulation of Flag-G β 1 targeted for degradation after 26S proteasome inhibition (Figure 7). Results showed clear accumulation of Flag-G β 1 in the cell after 10 μ M MG132 treatment over 12 hours. Within the same time frame, there was no identifiable change in endogenous G β total levels. G β γ is a relatively stable protein, so it is possible that the lack of endogenous G β γ change seen after 12-hour treatment of MG132 was due to insufficient time for accumulation to produce an effect as drastic as seen with the transiently transfected Flag-G β 1. It was not possible to test this as extending the MG132 treatment time past 12 hours led to massive cell death.

3.5.2 G β 1 degradation by the 26S proteasome evaluated by LC-MS

As an alternate method of approaching G β γ degradation by the proteasome, an LC-MS experiment was performed to identify ubiquitination sites on Flag-G β 1 in both parental, and KCTD5 KO cells under MG132 treatment to preserve ubiquitinated proteins. One ubiquitination site Lys209 was identified on G β 1 in both parental and KCTD5 KO cell lines confirmed by MaxQuant computational platform for mass spectrometry analysis performed by our collaborator Dr. Jean-François Trempe, McGill University. Peptide intensity of the ubiquitination site between the wildtype versus KCTD5 KO HEK 293 (WT/KO ratio) was 0.58. Given the large variability that is present for intensity ratios, this change most likely indicates a ubiquitination site independent of the presence of KCTD5.

3.5.3 KCTD5 effect on cellular G β γ levels

We next wanted to understand if G β γ degradation by the 26S proteasome was affected by KCTD5. When analyzing basal G β γ , there was a trend of decreased protein levels with

increasing KCTD5 overexpression (Figure 8A, B) by transient transfection. Basally G $\beta\gamma$ levels were lower in the KCTD5 knockout cell line compared to parental HEK 293 cells (Figure 8C).

3.5.4 KCTD5 effects on G $\beta\gamma$ and MAPK signalling

A common signalling output that is measured downstream of GPCR signalling is the MAPK cascade. Our lab has previously established protocols to measure MAPK activity by measuring downstream ERK1/2 phosphorylation after stimulation of endogenous M3-R in HEK 293 cells with CCh. Here the previously observed phenomena was replicated (Figure 9A) in HEK 293 parental cells, where ERK1/2 phosphorylation downstream of CCh signal was strongest at 5 min. The same conditions were applied to KCTD5 KO cells and a stronger ERK1/2 phosphorylation and MAPK signalling effect can be seen in comparison. To demonstrate this effect was due to KCTD5 KO, KCTD5 was re-supplemented in the KO cells and a reversal can be seen of the increased MAPK signalling whose phosphorylated ERK1/2 levels becomes comparable to that of parental cells (Figure 9B).

3.5.5 KCTD5 effects on G $\beta\gamma$ and the mTOR pathway

One paper has explored G $\beta\gamma$ signalling in depth in relation to KCTD5 and the PI3K/AKT/mTOR signalling pathway involved in cell cycle and proliferation, and suggested that basal AKT phosphorylation was negatively affected by KCTD5 and CUL3, and G $\beta\gamma$ could rescue this change (109). We decided to test this in our hands, and used the KCTD5 KO cell line with re-expression of KCTD5 and overexpression of Flag-G β 1 to determine effect on pAKT (Figure 10A). The results were inconclusive and difficult to replicate. We also tested this signalling pathway using insulin-like growth factor 1 (IGF-1) which stimulates AKT phosphorylation. While generally it seemed there could be a trend of KCTD5 KO increasing IGF-1 stimulated AKT phosphorylation (Figure 10B, C), there were significant variation between independent experiments and it was difficult to capture a consistent effect of KCTD5 and G $\beta\gamma$ on IGF-1 mediated AKT phosphorylation. A caveat of these comparative studies is that the authors of the paper (109) used haploid HAP1 cells derived from a patient with chronic myeloid leukemia and our experiments used HEK 293 cells derived from human embryonic kidney cell cultures. It is well known that different immortal cell lines may have varying

signalling pathways and homeostasis states, and even the act of serial passage of cell lines can cause phenotypic variation and genetic drift (132). Therefore it is unsurprising that translation of the research done on a HAP1 cell line to another HEK 293 cell line may not be direct.

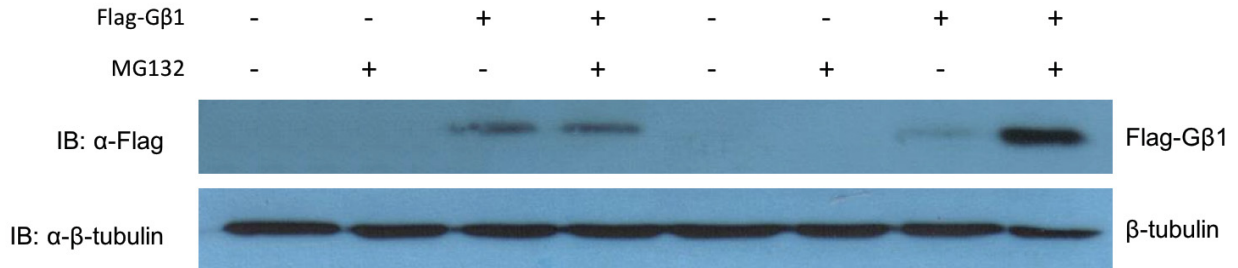
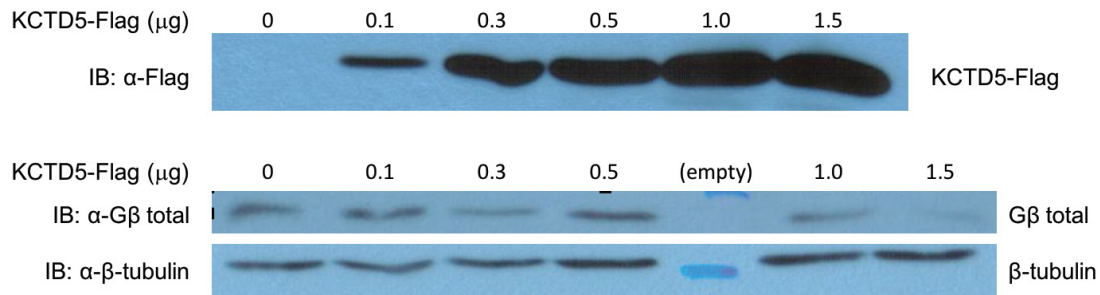


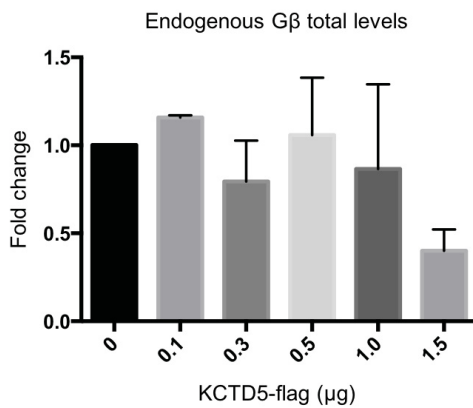
Figure 7: Short time course of Flag-Gβ1 turnover

Immunoblotting visualization of HEK 293 cells transiently expressing Flag-Gβ1 treated with 10μM MG132 for 5 or 12 hours. Experiment representative of N=3.

A



B



C

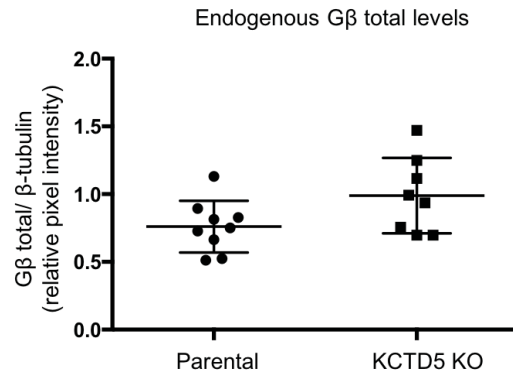
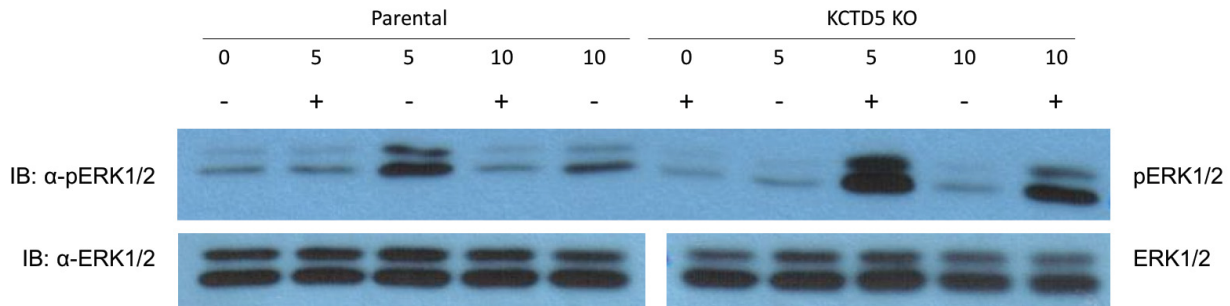


Figure 8: KCTD5 associated with trend of decreasing endogenous Gβγ levels

(A) Transient transfection of incremental concentrations of KCTD5-Flag DNA in HEK 293 cells over 48 hours and samples run on western blot, and its (B) western blot quantifications by densitometry and normalized to β-tubulin, represented by mean± standard deviation (SD) of n=2. (C) Trend of increased basal endogenous Gβ total levels in KCTD5 KO HEK 293 cells, represented by mean ± SD, n=3, unpaired t-test p=0.0642.

A



B

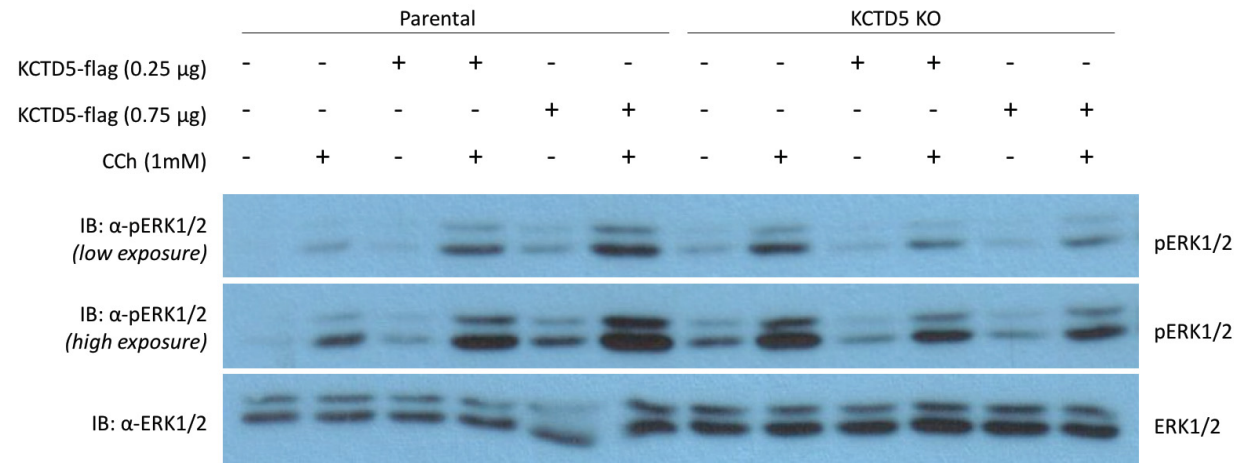


Figure 9: KCTD5 effect on MAPK signalling

Parental or KCTD5 KO HEK 293 cells under various conditions as indicated on figure were stimulated with CCh and Gβγ influence on downstream effectors for MAPK signalling was assessed. (A) Both cell lines are stimulated with 1mM CCh for 5 or 10 min and lysates run on western blot, N=1. KCTD5 loss was associated with increased ERK1/2 phosphorylation. (B)

KCTD5 re-supplementation in KO cell line shows decreased ERK1/2 phosphorylation. Both cell lines were transiently transfected as indicated and treated with 1mM CCh for 5 min. Sample lysates are run on western blot N=1.

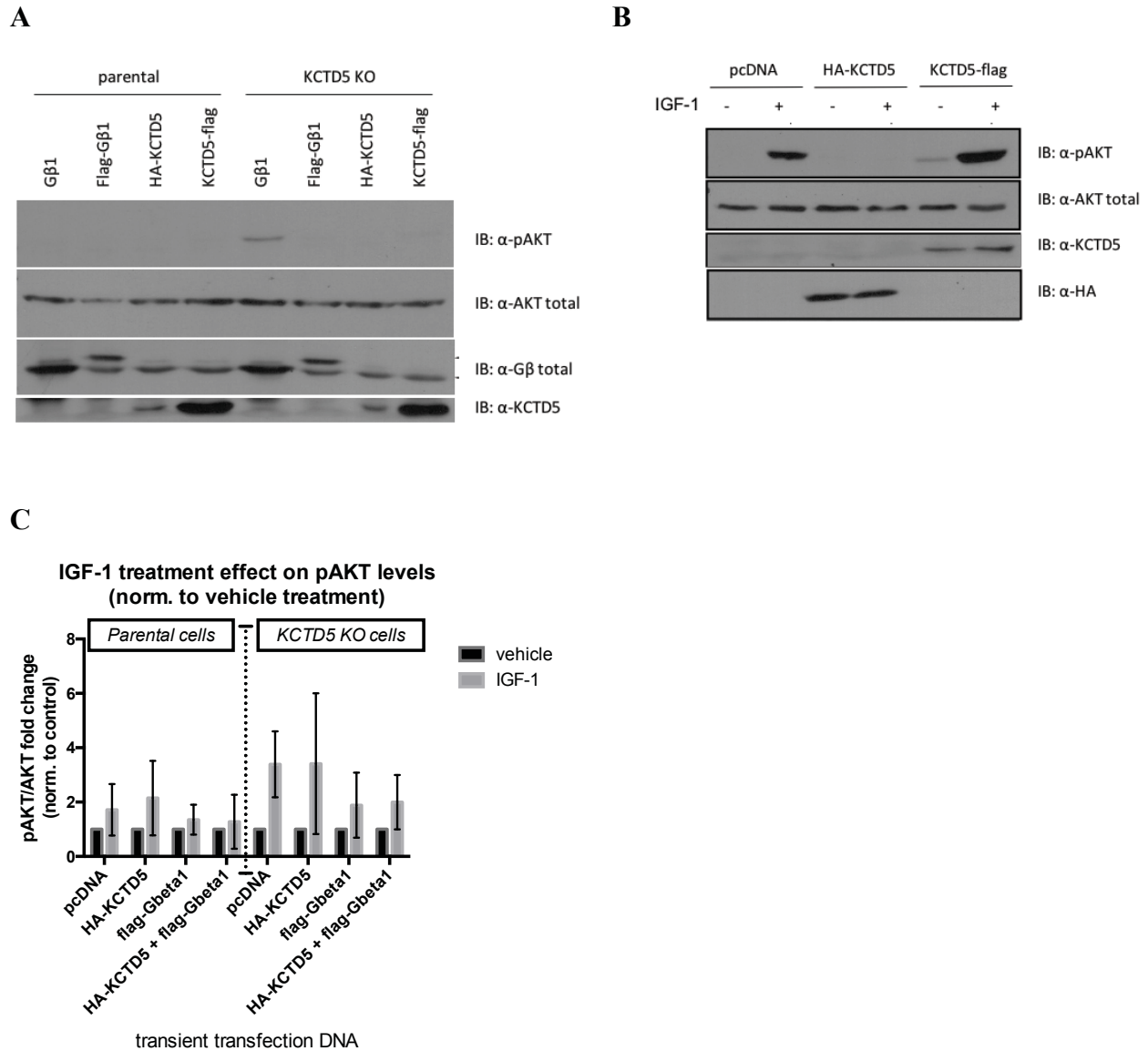


Figure 10: KCTD5 and Gβγ effect on AKT phosphorylation

Plasmid DNA were transiently transfected into parental or KCTD5 KO HEK 293 cells as indicated over 48 hours and the effect on pAKT levels was measured by immunoblotting. (B, C) IGF-1 treatment was performed for 5 minutes at 100ng/ml previously optimized to capture the optimum pAKT signal.

4. DISCUSSION & CONCLUSIONS

4.1 G $\beta\gamma$ degradation as a mechanism for control of signal transduction

The Campden G $\beta\gamma$ proteomics screen analysis revealed an increased G $\beta\gamma$ interaction with subunits of the 26S proteasome under carbachol stimulation (Section 3.2.1.3). This could be a mechanism which complements the GPCR desensitization pathway which allows the cell to control signal transduction. Increased G $\beta\gamma$ degradation after signal transduction has been previously seen as method of controlling and desensitizing transducin $\beta\gamma$ signalling in the retina (104). Given time and resource limitations, this was not further explored in this thesis, however there are simple experiments which may explore this question. For example, experiments aimed at elucidating the effect of upstream GPCR stimulation on G $\beta\gamma$ degradation rate, or measuring changes to signalling duration and responsiveness when the 26S proteasome is inhibited may help establish whether 26S proteasome is part of a ubiquitous cellular mechanism for GPCR and G $\beta\gamma$ signal desensitization.

4.2 Ubiquitination of G $\beta\gamma$ for other cellular fates

Ubiquitination does not always lead to substrate degradation by the proteasome. Poly-ubiquitination chains on Lys48 of ubiquitin usually lead to protein degradation, but in cases of non-canonical ubiquitination on Lys63, this may lead to non-proteasomal fates (123). Analysis of Campden's interactors shows G $\beta\gamma$ within ubiquitin-mediated pathways does not always occur in the cytoplasm, and this may not necessarily lead to proteasomal degradation. The G $\beta\gamma$ and E2 ubiquitin conjugating enzyme UBE2V2 interaction was only identified in the nucleus after CCh stimulation (Table 3). In the literature, UBE2V2 is known to function in the nucleus, where it may poly-ubiquitinate on Lys63 which acts as signals to recruit factors for DNA repair instead of leading to protein degradation (124, 125). UBE2V2 is also known to stimulate transcription of cFOS (126), which is a gene that G $\beta\gamma$ also stimulates expression of after upstream GPCR stimulation of D2-R (59). These factors suggest UBE2V2 and G $\beta\gamma$ interaction in the nucleus only after CCh stimulation may be involved in a signalling cascade or transcription processes.

Another protein from the Campden screen that may result in other cellular fates is the E3 ligase UBR5 interacting with Flag-G β 1 basally in the cytoplasm (Table 3). Apart from one of its roles which is to ubiquitinate substrates following the N-end pathway for protein degradation (122), its substrate ubiquitination function can lead to increased gene transcription. It has been previously suggested that UBR5 and factors which regulate transcription: transcription factor IIS (TFIIS) and positive transcription elongation factor b (P-TEFb), act together within a ternary complex to regulate transcription (120). Specifically, TFIIS was identified to recruit UBR5 which poly-ubiquitinates a subunit of P-TEFb, cyclin-dependent kinase 9 (CDK9), and instead of leading to degradation the poly-ubiquitination potentiates CDK9 loading onto chromatin and ultimately stimulates transcription elongation. While G β γ 's direct impact on transcription is not well studied, the Hébert lab has been studying G β γ roles in the nucleus, including its interaction with over 800 genes, RNA polymerase II (RNAPII), and its involvement in transcription elongation. It should be noted that G β γ interaction with UBR5 was not identified in the nucleus, but in considering UBR5 alternate roles it reminds us that ubiquitination of G β γ may not purely be for proteasomal degradation and may have other consequences including transcriptional functions.

4.3 Considerations for affinity purification mass spectrometry to study protein interactions

There are limitations of using affinity purification coupled with mass spectrometry to study protein-protein interactions that must be considered. Firstly, the strength of the interaction cannot be defined by the parameters of mass spectrometry, so prominent versus peripheral interactions cannot be distinguished. It could be argued that by comparing the tandem affinity purification versus the immunoprecipitation techniques for mass spectrometry analysis there may be an indirect way to evaluate strength of interactions. As discussed in Campden's MSc thesis (112), the TAP method was employed because by having a G β γ with both a calmodulin binding domain and the streptavidin binding domain and subsequently using 2 separate rounds of purification steps this method can eliminate non-specific contaminants. Campden also used a Flag immunoprecipitation, reasoning the Flag epitope tag is considerably smaller than the TAP tag, approximately 8 versus more than 150 amino acids respectively and with only 1 round of purification it should considerably reduce steric hindrance to allow more dynamic interactors to

be identified (112). By comparison TAP is a harsher method and only more stable G $\beta\gamma$ complexes can survive, eliminating more dynamic interactors which cannot be identified (133). It could be argued then that strong interactors would appear in both TAP and Flag, but the latter would also have more interactors in total. This seems to be the case observed, where unique interactors for either TAP-G β 1 and Flag-G β 1 identified by mass spectrometry were 88 and 259 respectively. As well, all G α and G γ subunits identified in either TAP-G β 1 or TAP-G β 1 γ 7 were also identified in the Flag-G β 1 immunoprecipitates, but overall there were more G α and G γ isoform variety detected in the Flag-IP than TAP conditions combined. Knowing this, perhaps this can be another added dimension when analyzing the proteomics data presented in this thesis results. However, this indirect way of evaluating interaction strength should be used with caution when interpreting data, as it's not always consistent. Taking the analysis of G $\beta\gamma$ and the spliceosome for example (Table 4), the majority of Sm proteins interacting with G $\beta\gamma$ was identified in the TAP-G β 1 purification. Of the total 5 identified, 1 protein SNRPB was identified in the Flag-G β 1 IP and the remaining SNRPD2, SNRPD3, SNRPE, SNRPG were from TAP-G β 1 only. It should also be taken into consideration that with differentially tagged proteins there may be false positives and negatives associated with the tags, so further interaction validation is needed.

Another consideration for this technique is the evaluation can only measure quality not quantity. Taking this into consideration, the thesis made sure to analyze number of unique proteins identified per complex or pathway between conditions and within each TAP or immunoprecipitation results. For example, in G $\beta\gamma$ interaction with the 26S proteasome (Table 2), within the Flag-IP data there were more unique subunits identified after carbachol stimulation than basally. This suggests Flag-G β 1 interaction with the 26S proteasome was more prominent after carbachol stimulation but this has yet to be directly verified.

Lastly, as with all experiments there are general false positives and false negatives that may be present in the data. One such way in which this is known to occur is through the overexpression and the tagging of bait protein which may interfere with *in vivo* functions of the protein (133). Campden took stringent precautions to ensure relevancy of her data (described in

her thesis (112)) by reducing overexpression artifacts through the use of HEK 293 cell lines stably expressing the tagged protein, by performing up to 3 independent experiments and only including proteins identified at minimum in two of three experiments, and by comparing her data to the CRAPome to filter out known background and non-specific interactions. While her results generated a list of viable interactors to analyze in Results 3.2, the considerations stated here remind us it is important to validate interactors through a secondary method which was done in this thesis (Section 3.3).

4.4 KCTD5 in modulating G β γ signalling

This thesis began to explore G β γ signalling and the role that KCTD5 may play within it. Analysis of Campden's G β γ proteomics screen suggests G β γ interaction with KCTD2, 5, 12, 17 are prominent interactions. Preliminary experiments suggest KCTD5 can alter G β γ signalling and decreases ERK1/2 phosphorylation after CCh stimulation of M3-R (Figure 9). Additional mass spectrometry experiments showed loss of KCTD5 shifted more than 50% of G β γ interactor partners identified in the parental cells to other unique proteins, and we identified a large group of these proteins being highly involved in prominent cellular metabolic processes (Table 10). While the prominence of G β γ interaction with metabolic pathway components does not indicate what influence G β γ may have on the processes, it should be noted imbalances of anabolic and catabolic pathways and cellular metabolic systems are involved in pathology of many diseases (134). As well, accompanied with the loss of KCTD5 interaction with G β γ in the KO cell line was the loss of KCTD2 interaction, whereas the other KCTDs (KCTD12, KCTD17) were unaffected. In fact, the KCTD2 identified to interact with G β γ has been previously shown to be regulate glycolysis (135, 136) which was one of the pathways we identified to be altered with the KCTD5 KO and subsequent loss of the KCTD2-G β γ interaction (discussed in 4.4.2, 4.4.3). Overall these observations suggest KCTD5 and KCTDs may have a significant effect on G β γ cellular functions.

4.4.1 KCTD5 in modulating Gβγ degradation

Within the scope of Gβγ degradation specifically, the mass spectrometry data measuring Gβγ Lys209 ubiquitination site changes due to KCTD5 KO suggests the site is independent of KCTD5. To study KCTD5 impact on Gβγ degradation by the 26S proteasome *in cellulo*, I used the KCTD5 KO cell line and repeated the experiment from Figure 7 to measure changes in accumulation of Flag-Gβ1 after treating the cells with a 26S proteasome inhibitor MG132. Preliminarily the experiment did not show any changes in the rate of Flag-Gβ1 degradation due to KCTD5 KO, overexpression, or re-supplementation (Figure 11). However, it should be noted that due to time limitations this experiment was not fully optimized, and this negative result could easily have been due to saturation of Flag-Gβ1 accumulation and the western blot method not being sensitive enough to detect smaller changes. Overall, KCTD5 may alter Gβγ signalling, but our experiments have not yet determined what role KCTD5 may play within Gβγ ubiquitination or degradation by the 26S proteasome. This is worth further investigation, because KCTD5 and other KCTDs identified to interact with Gβγ are CUL3 E3 ligase adaptors, therapeutically relevant and have a history of altering GPCR signalling.

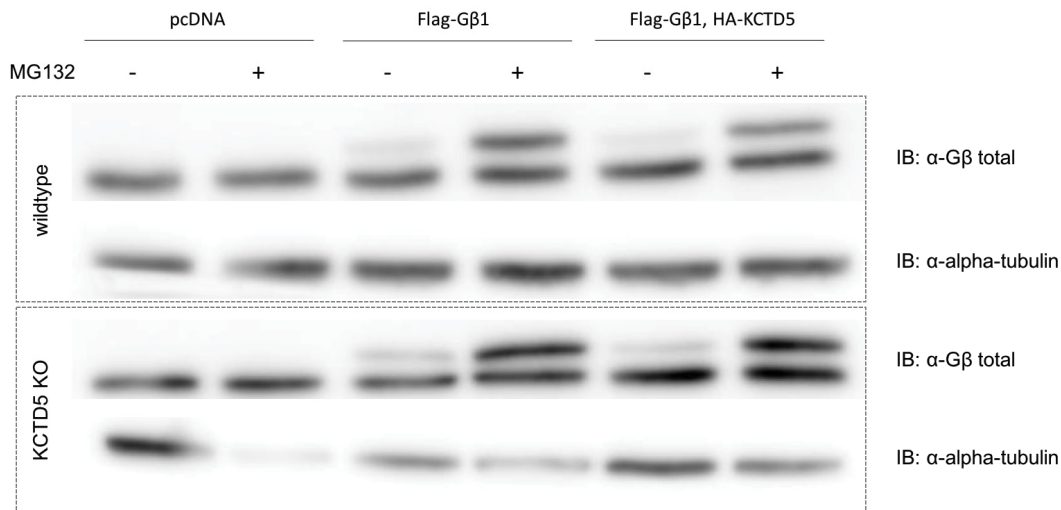


Figure 11: KCTD5 effect on Flag-Gβ1 degradation by the 26S proteasome

12 hour treatment of 10μM MG132 was applied to HEK 293 parental or KCTD5 KO cell lines transiently expressing Flag-Gβ1 ± HA-KCTD5. Sample lysates are run on western blot. N=1.

4.4.2 KCTD5 and KCTD2 interactions with Gβγ

The loss of KCTD2 with KCTD5 KO identified in our mass spectrometry experiments (Supplementary Table 2) suggests there may be cooperativity involved in their interaction with Gβγ. In fact, the evolutionary tree of the KCTD family proteins and amino acid sequence comparisons show KCTD2 and KCTD5 to be the closest to each other compared to the other 20+ KCTDs suggesting similar and overlapping molecular functions (115). Within the loss of KCTD5 in the KO cell line we also observed loss of KCTD2 interaction with Gβγ, which overall resulted in a shift of Gβγ interactors to metabolic proteins (Table 10). The loss of KCTD2 may have a role in here, because KCTD2 has been previously identified to be involved in glycolysis and altering mitochondrial energy production (135, 136), both of which were identified as metabolic processes gained after KCTD5 KO and KCTD2 interaction loss (Table 10). While it remains unclear how Gβγ may be specifically affecting these metabolic processes, these gained interactors may be resulting in irregular and compensatory energy, and metabolic homeostasis change. In fact, we have previously tried on multiple occasions in the KCTD5 KO cell line to knockdown Gβ1 using transiently transfected small interfering RNA (siRNA) to no avail (data not shown). Those cells could not survive the knockdown process despite this siRNA protocol having been optimized for HEK 293 cells and worked successfully in the parental line control.

4.4.3 KCTD interactors' known roles in GPCR signalling and therapeutic relevance

While current evidence of KCTD function remains limited, the 4 KCTDs identified to interact with Gβγ are involved in altering GPCR and G protein signalling, in the cullin-E3 ligase ubiquitin pathway, and in the progression of various diseases. KCTD2 is not well studied, but has been identified as an adaptor for the CUL3 E3 ubiquitin ligase and may be involved in Alzheimer's disease. As a CUL3 adaptor, it can regulate c-Myc and glycolysis-associated gene expression and consequently aerobic glycolysis, potentially providing a method of targeting c-Myc in glioma therapies (135). KCTD2 is associated with Alzheimer's disease, discovered through genome-wide association studies (GWAS) where its genetic locus was known for being important in regulating mitochondrial energy production, neuronal hyperpolarization in response to stress which are known factors that affect stress tolerance in Alzheimer's (136). KCTD5 and KCTD12 are better understood. KCTD5 is discriminatory in its interaction with CUL3 only and

not with the 6 other cullins. It is part of a functional Cullin-E3 ligase complex as a substrate-specific adaptor although no substrate target has been identified, and it is not a ubiquitinated substrate itself as is possible for some adaptors (111). As for KCTD5's role in directly impacting cellular phenotype, it may be a negative regulator in AKT phosphorylation within the PI3K/AKT/mTOR signalling pathway involved in cell cycle and proliferation. While it is unclear exactly how KCTD5 is involved in this signalling, the authors show the negative effect is dependent upon CUL3, and specific G $\beta\gamma$ isoforms were able to rescue the effect (109) suggesting that this might be related to KCTD5 interaction with G $\beta\gamma$. KCTD12 is the most dissimilar to the other KCTDs identified as G $\beta\gamma$ interactors. KCTD12 has been shown to directly impact GPCR and G $\beta\gamma$ responses and signalling kinetics. Tetramer KCTD12 proteins act as auxiliary subunits to the GABA-B receptor, where it tightly assembles at the C-terminus of the receptor in the brain favouring increased receptor agonist potency and more rapid desensitization kinetics (137) (138). Oligomeric KCTD12 can also stabilize G $\beta\gamma$ at the GABA-B receptor reducing the rate of G protein activation, downstream G $\beta\gamma$ activation of the G protein-coupled inwardly-rectifying potassium channel (Kir3) channel, and attenuating GABA-B receptor signalling (110, 139). KCTD12, also known as Predominantly Fetal Expressed T1 Domain (Pfetin) has been linked to various diseases although its mechanism of action within the pathology remains unclear. There is evidence for KCTD12 single-nucleotide polymorphisms (SNP) association to bipolar disorder I in the Han Chinese population (140). KCTD12 confers risk of neuropsychiatric disorders (141) and colorectal cancer (142, 143), and is a potential marker for bone marrow stromal cells. Clinical data shows KCTD12 might be an important prognostic for gastrointestinal stromal tumours (144) (145-148) (149) suggesting KCTDs have important clinical and therapeutic roles. As for the function of the last G $\beta\gamma$ interactor, little is known about KCTD17.

4.5 Other areas to explore

This thesis has generated many future directions to explore and delved further into KCTD5 effects on G $\beta\gamma$ degradation and signalling using the KCTD5 KO cell line and tools such as MG132. Other signalling paradigms would be of interest to follow up and were described within the pathways identified from Campden's G $\beta\gamma$ proteomics screen such as G $\beta\gamma$ and the

spliceosome, cellular respiration and mitochondria. G $\beta\gamma$ interactors included many spliceosome components, and in particular the Sm proteins interacting with G $\beta\gamma$ in the cytoplasm in response to carbachol which suggested G $\beta\gamma$ may have a role in spliceosome generation whereas not so much nuclear splicing itself. In other cases, the analysis identified interactors such as those in the oxidative phosphorylation chain, and proteins encoded within mitochondrial DNA such as COX2. It is not clear as to what capacity G $\beta\gamma$ interacts with these proteins as no specific function of G $\beta\gamma$ in the mitochondria has yet been identified in literature. However, GPCR systems have been identified within the mitochondria such as AT2R and CB₁ receptors which upon activation can respectively decrease mitochondrial respiration (78) and directly affect complexes within the respiratory chain (79). Within the G $\beta\gamma$ mitochondrial protein interactors (Table 5-8), only COX2 is encoded by mitochondrial DNA whereas the other mitochondrial proteins identified are encoded in nuclear DNA. This means the latter group of proteins need to first be translated in the cytoplasm prior to being transported into the mitochondria. It is only logical then, that in addition to the possibility that G $\beta\gamma$ interaction with these mitochondrial proteins are within the mitochondria itself, they may very well be occurring prior to entering the mitochondria and during preprotein transport. Interestingly to this point, G $\beta\gamma$ interact with TIMM8A, TOMM22 which are part of TIM/TOM complexes integral to transport of nuclear-encoded proteins into the mitochondria for oxidative phosphorylation. As we learn more about G $\beta\gamma$ functions in the cell, it becomes interesting to explore novel roles such as spliceosome, cellular respiration, and mitochondrial protein transport.

4.6 Conclusions

G $\beta\gamma$ roles in the cell have not been sufficiently characterized, and it remains important to further study G $\beta\gamma$ signalling. In an effort to do so, this thesis analyzed G $\beta\gamma$ protein-protein interactions to identify degradation and other signalling pathways within the cell, and attempted to validate these roles using IP, a protein-knock out HEK 293 cell line model, and cellular signalling experiments. Within the analysis of the Campden proteomics data, G $\beta\gamma$ was discovered to interact with multiple components involved in protein degradation. Within this scope, G $\beta\gamma$ interacted with 26S proteasome subunits involved in ubiquitinated substrate

identification, with KCTD5 and other members of the KCTD family which are CUL3 E3 ligase adaptors, as well as directly with E2 ubiquitin conjugation enzymes and E3 ligases. We validated and followed up with two of these interactors. Firstly, using IP and western blot it was demonstrated that both Flag-G β 1 and endogenous G β γ interact with a de-ubiquitinase of the 26S proteasome, PSMD7. The consequences of G β γ interaction with the proteasome was degradation, and treatment of cells with a 26S proteasome inhibitor MG132 caused G β γ protein levels to accumulate over time. Secondly, G β γ interaction with KCTD5 and signalling consequences were investigated. We validated the TAP-G β 1 and KCTD5-Flag interaction using IP and western blot. Then, a KCTD5 KO HEK 293 cell line was generated so it may be used as a tool in this thesis and future experiments to investigate KCTD5 effects on G β γ degradation and signalling. We briefly studied KCTD5 effects on G β γ degradation, where using this cell line a G β γ ubiquitination site was discovered on Lys209 under MG132 treatment. Upon further investigation however, the ubiquitination site was determined to be independent of KCTD5. Despite this, we have some evidence showing endogenous G β γ levels incrementally decrease with incremental increase of KCTD5-Flag overexpression, and endogenous G β γ protein levels are generally lower in KCTD5 KO cells than in parental cells.

We studied consequences on G β γ signalling after KCTD5 KO. The landscape of G β γ interaction partners shifts drastically towards more metabolic protein partners such as those involved in amino acid and nucleotide biosynthesis and metabolism, and gluconeogenesis and glycolysis. While it remains unclear what this indicates, it is well known that alterations in cellular homeostasis can lead to pathology and disease, suggesting loss of KCTD5 and change in G β γ interaction partners may have therapeutic relevance. We do see in preliminary experiments that KCTD5 may alter G β γ signalling pathway within the M3-R carbachol-stimulated MAPK cascade, where KCTD5 KO decreases subsequent ERK1/2 phosphorylation. Interesting to note also is that within the KCTD5 KO cell line, our mass spectrometry analysis shows the loss of G β γ interaction with KCTD5 is accompanied by loss of the KCTD2 interaction also. As KCTD2 is known to be involved in cellular metabolic processes, its loss could be contributing to the shift in G β γ interactors towards metabolic proteins we see. These two KCTDs are also very similar to

each other and the KCTD2 interaction loss with KCTD5 KO may indicate they have overlapping functions with regards to interaction with G β γ and its effects.

This thesis provides a good starting point to identify G β γ interactors for further exploration such as within the ubiquitin-mediated pathways and in the mitochondria, and I generated a KCTD5 KO cell line for future experimental evaluation. Given the emerging therapeutic relevance of G β γ we discussed in the introduction, where G β γ is becoming relevant to cancer treatment developments due to its roles in cellular chemotaxis (95, 96), it remains important to learn more about G β γ functions in the cell and how degradation relates to altering its signalling.

REFERENCES

1. Khan SM, Sung JY, Hebert TE. Gbetagamma subunits-Different spaces, different faces. *Pharmacol Res.* 2016;111:434-41.
2. Lagerstrom MC, Schioth HB. Structural diversity of G protein-coupled receptors and significance for drug discovery. *Nat Rev Drug Discov.* 2008;7(4):339-57.
3. Takezako T, Unal H, Karnik SS, Node K. Current topics in angiotensin II type 1 receptor research: Focus on inverse agonism, receptor dimerization and biased agonism. *Pharmacological Research.* 2017;123:40-50.
4. Rask-Andersen M, Almen MS, Schioth HB. Trends in the exploitation of novel drug targets. *Nat Rev Drug Discov.* 2011;10(8):579-90.
5. Venkatakrishnan AJ, Deupi X, Lebon G, Heydenreich FM, Flock T, Miljus T, et al. Diverse activation pathways in class A GPCRs converge near the G-protein-coupling region. *Nature.* 2016;536(7617):484-7.
6. Oldham WM, Hamm HE. Heterotrimeric G protein activation by G-protein-coupled receptors. *Nat Rev Mol Cell Biol.* 2008;9(1):60-71.
7. de Mendoza A, Seb e-Pedr s A, Ruiz-Trillo I. The Evolution of the GPCR Signaling System in Eukaryotes: Modularity, Conservation, and the Transition to Metazoan Multicellularity. *Genome Biology and Evolution.* 2014;6(3):606-19.
8. Dupr  DJ, Robitaille M, Rebois RV, H bert TE. The role of G $\beta\gamma$ subunits in the organization, assembly, and function of GPCR signaling complexes. *Annu Rev Pharmacol Toxicol.* 2009;49.
9. Khan SM, Sleno R, Gora S, Zylbergold P, Laverdure J-P, Labb  J-C, et al. The Expanding Roles of G $\beta\gamma$ Subunits in G Protein-Coupled Receptor Signaling and Drug Action. *Pharmacological Reviews.* 2013;65(2):545-77.
10. Smrcka AV. G protein $\beta\gamma$ subunits: central mediators of G protein-coupled receptor signaling. *Cell Mol Life Sci.* 2008;65.
11. Schwindinger WF, Robishaw JD. Heterotrimeric G-protein $\beta\gamma$ -dimers in growth and differentiation. *Oncogene.* 2001;20(13):1653-60.
12. Ching-Kang C E-C, Zhang H, Mancino V, Chen Y, He W, Wensel TG, Simon MI. Instability of GGL domain-containing RGS proteins in mice lacking the G protein β -subunit G β 5. *Proc Natl Acad Sci USA.* 2003;100(11):6604-9.
13. Hosohata K LJ, Varga E, Burkey TH, Vanderah TW, Porreca F, Hrubby VJ, Roeske WR, Yamamura HI. The role of G protein γ 2 subunit in opioid antinociception in mice. *European Journal of Pharmacology.* 2000;392:R9-R11.
14. Kalkbrenner F, Degtiar VE, Schenker M, Brendel S, Zobel A, Heschler J, et al. Subunit composition of G(o) proteins functionally coupling galanin receptors to voltage-gated calcium channels. *Embo J.* 1995;14(19):4728-37.
15. Kleuss C SH, Hescheler J, Schultz G, Wittig B. Selectivity in signal transduction determined by γ subunits of heterotrimeric G proteins. *Science.* 1993;259:832-4.
16. Krispel CM CC, Simon MI, Burns ME. Prolonged photoresponses and defective adaptation in rods of G β 5 $-/-$ mice. *The Journal of Neuroscience.* 2003;23(18):6965-71.
17. Lobanova ES FS, Herrmann R, Chen YM, Kessler C, Michaud NA, Trieu LH, Strissel KJ, Burns ME, Arshavsky VY. Transducin γ -subunit sets expression levels of α - and β -

- subunits and is crucial for rod viability. *The Journal of Neuroscience*. 2008;28(13):3510-20.
18. Okae H IY. Neural tube defects and impaired neural progenitor cell proliferation in G β 1-deficient mice. *Developmental Dynamics*. 2010(239):1089-101.
 19. Schwindinger WF, Betz KS, Giger KE, Sabol A, Bronson SK, Robishaw JD. Loss of G protein γ 7 alters behavior and reduces striatal α olf level and cAMP production. *J Biol Chem*. 2003;278.
 20. Schwindinger WF, Giger KE, Betz KS, Stauffer AM, Sunderlin EM, Sim-Selley LJ, et al. Mice with deficiency of G protein γ 3 are lean and have seizures. *Mol Cell Biol*. 2004;24.
 21. Schwindinger WF, Mirshahi UL, Baylor KA, Sheridan KM, Stauffer AM, Usef of S, et al. Synergistic roles for G-protein γ 3 and γ 7 subtypes in seizure susceptibility as revealed in double knockout mice. *J Biol Chem*. 2011;287.
 22. Schwindinger WF BB, Waldman LC, Robishaw JD. Mice lacking the G protein γ 3-subunit show resistance to opioids and diet induced obesity. *Am J Physiol Regul Integr Comp Physiol*. 2009;297(R1494-R1502).
 23. Varga EV HK, Borys Dariusz, Navratilova E, Nylen A, Vanderah TW, Porreca F, Roeske WR, Yamamura HI. Antinociception depends on the presence of G protein γ 2-subunits in brain. *European Journal of Pharmacology*. 2005;508:93-8.
 24. Wang Q LK, Chanturiya T, Dvorientchikova G, Anderson KL, Bianco SDC, Ueta CB, Molano RD, Slepak VZ. Targeted deletion of one or two copies of the G protein β subunit G β 5 gene has distinct effects on body weight and behavior in mice. *The FASEB Journal*. 2011;25.
 25. Xie K, Masuho I, Brand C, Dessauer CW, Martemyanov KA. The Complex of G Protein Regulator RGS9-2 and G β 5 Controls Sensitization and Signaling Kinetics of Type 5 Adenylyl Cyclase in the Striatum. *Sci Signal*. 2012;5(239):ra63-.
 26. Zhang JH PM, Seigneur EM, Panicker LM, Koo L, Schwartz OM, Chen W, Chen CK, Simonds WF. Knockout of G protein β 5 impairs brain development and causes multiple neurological abnormalities in mice. *Journal of Neurochemistry*. 2011;119:544-54.
 27. Khan SM, Min A, Gora S, Houranieh GM, Campden R, Robitaille M, et al. G β 4 γ 1 as a modulator of M3 muscarinic receptor signalling and novel roles of G β 1 subunits in the modulation of cellular signalling. *Cellular Signalling*. 2015;27(8):1597-608.
 28. Knol JC, Engel R, Blaauw M, Visser AJ, van Haastert PJ. The phosducin-like protein PhLP1 is essential for G{beta}{gamma} dimer formation in *Dictyostelium discoideum*. *Mol Cell Biol*. 2005;25(18):8393-400.
 29. Lukov GL, Hu T, McLaughlin JN, Hamm HE, Willardson BM. Phosducin-like protein acts as a molecular chaperone for G protein betagamma dimer assembly. *EMBO J*. 2005;24(11):1965-75.
 30. Lukov GL, Baker CM, Ludtke PJ, Hu T, Carter MD, Hackett RA, et al. Mechanism of assembly of G protein betagamma subunits by protein kinase CK2-phosphorylated phosducin-like protein and the cytosolic chaperonin complex. *J Biol Chem*. 2006;281(31):22261-74.
 31. Wells CA, Dingus J, Hildebrandt JD. Role of the chaperonin CCT/TRiC complex in G protein betagamma-dimer assembly. *J Biol Chem*. 2006;281(29):20221-32.
 32. Dupre DJ, Robitaille M, Richer M, Ethier N, Mamarbachi AM, Hebert TE. Dopamine receptor-interacting protein 78 acts as a molecular chaperone for G γ subunits before assembly with G β *J Biol Chem*. 2007;282(18):13703-15.

33. Dupre DJ, Robitaille M, Ethier N, Villeneuve LR, Mamarbachi AM, Hebert TE. Seven transmembrane receptor core signalling complexes are assembled prior to plasma membrane trafficking. *J Biol Chem*. 2006;281(45):34561-73.
34. Dupre DJ, Baragli A, Rebois RV, Ethier N, Hebert TE. Signalling complexes associated with adenylyl cyclase II are assembled during their biosynthesis. *Cell Signal*. 2007;19:481-9.
35. Robitaille M, Ramakrishnan N, Baragli A, Hebert TE. Intracellular trafficking and assembly of specific Kir3 channel/G protein complexes. *Cell Signal*. 2009;21(4):488-501.
36. Garcia-Regalado A, Guzman-Hernandez ML, Ramirez-Rangel I, Robles-Molina E, Balla T, Vazquez-Prado J, et al. G protein-coupled receptor-promoted trafficking of G β 1 γ 2 leads to AKT activation at endosomes via a mechanism mediated by G β 1 γ 2 -Rab11a interaction. *Mol Biol Cell*. 2008;19(10):4188-200.
37. Saini DK, Chisari M, Gautam N. Shuttling and translocation of heterotrimeric G proteins and Ras. *Trends in pharmacological sciences*. 2009;30(6):278-86.
38. Saini DK, Karunarathne WK, Angaswamy N, Saini D, Cho JH, Kalyanaraman V, et al. Regulation of Golgi structure and secretion by receptor-induced G protein $\beta\gamma$ complex translocation. *Proc Natl Acad Sci USA*. 2010;107.
39. Zhang J, Liu W, Liu J, Xiao W, Liu L, Jiang C, et al. G-protein β 2 subunit interacts with mitofusin 1 to regulate mitochondrial fusion. *Nat Commun*. 2010;1:101.
40. Robitaille M, Gora S, Wang Y, Goupil E, Petrin D, Del Duca D, et al. G $\beta\gamma$ is a negative regulator of AP-1 mediated transcription. *Cell Signal*. 2010;22(8):1254-66.
41. Campden R, Pétrin D, Robitaille M, Audet N, Gora S, Angers S, et al. Tandem Affinity Purification to Identify Cytosolic and Nuclear G $\beta\gamma$ -Interacting Proteins. In: Allen BG, Hébert TE, editors. *Nuclear G-Protein Coupled Receptors*. *Methods in Molecular Biology*. 1234: Springer New York; 2015. p. 161-84.
42. Hewavitharana T, Wedegaertner PB. Non-canonical signaling and localizations of heterotrimeric G proteins. *Cell Signal*. 2012;24(1):25-34.
43. Campden R, Audet N, Hébert TE. Nuclear G Protein Signaling: New Tricks for Old Dogs. *Journal of Cardiovascular Pharmacology*. 2015;65(2):110-22.
44. Ajith Karunarathne WK, O'Neill PR, Martinez-Espinosa PL, Kalyanaraman V, Gautam N. All G protein $\beta\gamma$ complexes are capable of translocation on receptor activation. *Biochemical and Biophysical Research Communications*. 2012;421(3):605-11.
45. Lorenz K, Schmitt JP, Schmitteckert EM, Lohse MJ. A new type of ERK1/2 autophosphorylation causes cardiac hypertrophy. *Nat Med*. 2009;15(1):75-83.
46. Vidal M, Wieland T, Lohse MJ, Lorenz K. β -Adrenergic receptor stimulation causes cardiac hypertrophy via a G $\beta\gamma$ /Erk-dependent pathway. *Cardiovascular Research*. 2012;96(2):255-64.
47. Witherow DS, Slepak VZ. A novel kind of G protein heterodimer: the G β 5-RGS complex. *Receptors & channels*. 2003;9(3):205-12.
48. Hepler JR. R7BP: A Surprising New Link Between G Proteins, RGS Proteins, and Nuclear Signaling in the Brain. *Science Signaling*. 2005;2005(294):pe38-pe.
49. Drenan RM, Doupnik CA, Boyle MP, Muglia LJ, Huettner JE, Linder ME, et al. Palmitoylation regulates plasma membrane–nuclear shuttling of R7BP, a novel membrane anchor for the RGS7 family. *The Journal of Cell Biology*. 2005;169(4):623-33.

50. Song JH, Waataja JJ, Martemyanov KA. Subcellular Targeting of RGS9-2 Is Controlled by Multiple Molecular Determinants on Its Membrane Anchor, R7BP. *Journal of Biological Chemistry*. 2006;281(22):15361-9.
51. Panicker LM, Zhang J-H, Posokhova E, Gastinger MJ, Martemyanov KA, Simonds WF. Nuclear localization of the G protein $\beta 5/R7$ -regulator of G protein signaling protein complex is dependent on R7 binding protein. *Journal of Neurochemistry*. 2010;113(5):1101-12.
52. Vaniotis G, Gora S, Nantel A, Hébert TE, Allen BG. Examining the Effects of Nuclear GPCRs on Gene Expression Using Isolated Nuclei. In: Allen GB, Hébert ET, editors. *Nuclear G-Protein Coupled Receptors: Methods and Protocols*. New York, NY: Springer New York; 2015. p. 185-95.
53. Bhatnagar A, Unal H, Jagannathan R, Kaveti S, Duan Z-H, Yong S, et al. Interaction of G-Protein $\beta\gamma$ Complex with Chromatin Modulates GPCR-Dependent Gene Regulation. *PLoS ONE*. 2013;8(1):e52689.
54. Dorsam RT, Gutkind JS. G-protein-coupled receptors and cancer. *Nat Rev Cancer*. 2007;7(2):79-94.
55. Zaballos MA, Garcia B, Santisteban P. $G\beta\gamma$ Dimers Released in Response to Thyrotropin Activate Phosphoinositide 3-Kinase and Regulate Gene Expression in Thyroid Cells. *Molecular Endocrinology*. 2008;22(5):1183-99.
56. Yost EA, Hynes TR, Hartle CM, Ott BJ, Berlot CH. Inhibition of G-Protein $\beta\gamma$ Signaling Enhances T Cell Receptor-Stimulated Interleukin 2 Transcription in CD4⁺ T Helper Cells. *PLoS ONE*. 2015;10(1):e0116575.
57. Park JG, Muise A, He GP, Kim SW, Ro HS. Transcriptional regulation by the gamma5 subunit of a heterotrimeric G protein during adipogenesis. *Embo J*. 1999;18(14):4004-12.
58. Spiegelberg BD, Hamm HE. G betagamma binds histone deacetylase 5 (HDAC5) and inhibits its transcriptional co-repression activity. *J Biol Chem*. 2005;280(50):41769-76.
59. Mizuno K, Kurokawa K, Ohkuma S. Regulation of type 1 IP3 receptor expression by dopamine D2-like receptors via AP-1 and NFATc4 activation. *Neuropharmacology*. 2013;71:264-72.
60. Ahmadiantehrani S, Ron D. Dopamine D2 receptor activation leads to an up-regulation of glial cell line-derived neurotrophic factor via $G\beta\gamma$ -Erk1/2-dependent induction of Zif268. *Journal of Neurochemistry*. 2013;125(2):193-204.
61. Stern CM, Luoma JI, Meitzen J, Mermelstein PG. Corticotropin Releasing Factor-Induced CREB Activation in Striatal Neurons Occurs via a Novel $G\beta\gamma$ Signaling Pathway. *PLoS ONE*. 2011;6(3):e18114.
62. Jean-Philippe J, Paz S, Caputi M. hnRNP A1: The Swiss Army Knife of Gene Expression. *International Journal of Molecular Sciences*. 2013;14(9):18999.
63. Krecic AM, Swanson MS. hnRNP complexes: Composition, structure, and function. *Current Opinion in Cell Biology*. 1999;11(3):363-71.
64. Yuen JWF, Poon LSW, Chan ASL, Yu FWY, Lo RKH, Wong YH. Activation of STAT3 by specific $G\alpha$ subunits and multiple $G\beta\gamma$ dimers. *The International Journal of Biochemistry & Cell Biology*. 2010;42(6):1052-9.
65. Georganta E-M, Agalou A, Georgoussi Z. Multi-component signaling complexes of the δ -opioid receptor with STAT5B and G proteins. *Neuropharmacology*. 2010;59(3):139-48.

66. Jamora C, Yamanouye N, Van Lint J, Laudenslager J, Vandenheede JR, Faulkner DJ, et al. G $\beta\gamma$ -mediated regulation of Golgi organization is through the direct activation of protein kinase D. *Cell*. 1999;98.
67. Lau WW, Chan AS, Poon LS, Zhu J, Wong YH. G $\beta\gamma$ -mediated activation of protein kinase D exhibits subunit specificity and requires G $\beta\gamma$ -responsive phospholipase C β isoforms. *Cell Communication and Signaling*. 2013;11(1):1-17.
68. Jensen D, Zhao P, Jimenez-Vargas NN, Lieu T, Gerges M, Yeatman HR, et al. Protein Kinase D and G $\beta\gamma$ Mediate Agonist-Evoked Translocation of Protease-activated Receptor-2 from the Golgi Apparatus to the Plasma Membrane. *Journal of Biological Chemistry*. 2016.
69. Jiang Y, Xie X, Zhang Y, Luo X, Wang X, Fan F, et al. Regulation of G-Protein Signaling by RKTG via Sequestration of the G $\beta\gamma$ Subunit to the Golgi Apparatus. *Molecular and Cellular Biology*. 2010;30(1):78-90.
70. Hewavitharana T, Wedegaertner PB. PAQR3 regulates Golgi vesicle fission and transport via the G $\beta\gamma$ -PKD signaling pathway. *Cellular Signalling*. 2015;27(12):2444-51.
71. Zhang L, Malik S, Kelley GG, Kapiloff MS, Smrcka AV. Phospholipase C ϵ Scaffolds to Muscle-specific A Kinase Anchoring Protein (mAKAP β) and Integrates Multiple Hypertrophic Stimuli in Cardiac Myocytes. *The Journal of Biological Chemistry*. 2011;286(26):23012-21.
72. Zhang L, Malik S, Pang J, Wang H, Park Keigan M, Yule David I, et al. Phospholipase C ϵ Hydrolyzes Perinuclear Phosphatidylinositol 4-Phosphate to Regulate Cardiac Hypertrophy. *Cell*. 2013;153(1):216-27.
73. Malik S, deRubio RG, Trembley M, Irannejad R, Wedegaertner PB, Smrcka AV. G protein $\beta\gamma$ subunits regulate cardiomyocyte hypertrophy through a perinuclear Golgi phosphatidylinositol 4-phosphate hydrolysis pathway. *Molecular Biology of the Cell*. 2015;26(6):1188-98.
74. Lyssand JS, Bajjalieh SM. The heretotrimeric G protein subunit G α_i is present on mitochondria. *FEBS Letters*. 2007;581(30):5765-8.
75. Andreeva AV, Kutuzov MA, Voyno-Yasenetskaya TA. G α_{12} is targeted to the mitochondria and affects mitochondrial morphology and motility. *The FASEB Journal*. 2008;22(8):2821-31.
76. Beninca C, Planaguma J, de Freitas Shuck A, Acin-Perez R, Munoz JP, de Almeida MM, et al. A new non-canonical pathway of G $\alpha(q)$ protein regulating mitochondrial dynamics and bioenergetics. *Cell Signal*. 2014;26(5):1135-46.
77. Dagda RK, Barwacz CA, Cribbs JT, Strack S. Unfolding-resistant Translocase Targeting: A NOVEL MECHANISM FOR OUTER MITOCHONDRIAL MEMBRANE LOCALIZATION EXEMPLIFIED BY THE B β 2 REGULATORY SUBUNIT OF PROTEIN PHOSPHATASE 2A. *Journal of Biological Chemistry*. 2005;280(29):27375-82.
78. Abadir PM, Foster DB, Crow M, Cooke CA, Rucker JJ, Jain A, et al. Identification and characterization of a functional mitochondrial angiotensin system. *Proceedings of the National Academy of Sciences*. 2011;108(36):14849-54.
79. Benard G, Massa F, Puente N, Lourenco J, Bellocchio L, Soria-Gomez E, et al. Mitochondrial CB1 receptors regulate neuronal energy metabolism. *Nat Neurosci*. 2012;15(4):558-64.
80. Wu D. Signaling mechanisms for regulation of chemotaxis. *Cell Res*. 2005;15(1):52-6.

81. Chen S, Lin F, Shin ME, Wang F, Shen L, Hamm HE. RACK1 Regulates Directional Cell Migration by Acting on G $\beta\gamma$ at the Interface with Its Effectors PLC β and PI3K γ . *Molecular Biology of the Cell*. 2008;19(9):3909-22.
82. Wang F, Herzmark P, Weiner OD, Srinivasan S, Servant G, Bourne HR. Lipid products of PI(3)Ks maintain persistent cell polarity and directed motility in neutrophils. *Nat Cell Biol*. 2002;4(7):513-8.
83. Sun CX, Magalhães MAO, Glogauer M. Rac1 and Rac2 differentially regulate actin free barbed end formation downstream of the fMLP receptor. *The Journal of Cell Biology*. 2007;179(2):239-45.
84. Welch HCE, Coadwell WJ, Ellson CD, Ferguson GJ, Andrews SR, Erdjument-Bromage H, et al. P-Rex1, a PtdIns(3,4,5)P3- and G $\beta\gamma$ -Regulated Guanine-Nucleotide Exchange Factor for Rac. *Cell*. 2002;108(6):809-21.
85. Yan J, Mihaylov V, Xu X, Brzostowski Joseph A, Li H, Liu L, et al. A G $\beta\gamma$ Effector, ElmoE, Transduces GPCR Signaling to the Actin Network during Chemotaxis. *Developmental Cell*. 2012;22(1):92-103.
86. Brugnera E, Haney L, Grimsley C, Lu M, Walk SF, Tosello-Tramont AC, et al. Unconventional Rac-GEF activity is mediated through the Dock180-ELMO complex. *Nature Cell Biology*. 2002;4(8):574-82.
87. Côté JF, Vuori K. GEF what? Dock180 and related proteins help Rac to polarize cells in new ways. *Trends in Cell Biology*. 2007;17(8):383-93.
88. Reddien PW, Horvitz, Robert H. . The Engulfment Process of Programmed Cell Death In *Caenorhabditis Elegans*. *Annual Review of Cell and Developmental Biology*. 2004;20(1):193-221.
89. Li Z, Hannigan M, Mo Z, Liu B, Lu W, Wu Y, et al. Directional Sensing Requires G $\beta\gamma$ -Mediated PAK1 and PIX α -Dependent Activation of Cdc42. *Cell*. 2003;114(2):215-27.
90. Surve CR, Lehmann D, Smrcka AV. A Chemical Biology Approach Demonstrates G Protein $\beta\gamma$ Subunits Are Sufficient to Mediate Directional Neutrophil Chemotaxis. *The Journal of Biological Chemistry*. 2014;289(25):17791-801.
91. Surve CR, To JY, Malik S, Kim M, Smrcka AV. Dynamic regulation of neutrophil polarity and migration by the heterotrimeric G protein subunits G α i-GTP and G $\beta\gamma$. *Science Signaling*. 2016;9(416):ra22-ra.
92. Ahmed SM, Daulat AM, Meunier A, Angers S. G Protein $\beta\gamma$ Subunits Regulate Cell Adhesion through Rap1a and Its Effector Radil. *Journal of Biological Chemistry*. 2010;285(9):6538-51.
93. Kinbara K, Goldfinger LE, Hansen M, Chou F-L, Ginsberg MH. Ras GTPases: integrins' friends or foes? *Nat Rev Mol Cell Biol*. 2003;4(10):767-78.
94. Liu L, Aerbajinai W, Ahmed SM, Rodgers GP, Angers S, Parent CA. Radil controls neutrophil adhesion and motility through β 2-integrin activation. *Molecular Biology of the Cell*. 2012;23(24):4751-65.
95. Lehmann DM, Seneviratne AMPB, Smrcka AV. Small Molecule Disruption of G Protein $\beta\gamma$ Subunit Signaling Inhibits Neutrophil Chemotaxis and Inflammation. *Molecular Pharmacology*. 2008;73(2):410-8.
96. Kirui JK, Xie Y, Wolff DW, Jiang H, Abel PW, Tu Y. G $\beta\gamma$ Signaling Promotes Breast Cancer Cell Migration and Invasion. *The Journal of Pharmacology and Experimental Therapeutics*. 2010;333(2):393-403.

97. Dave RH, Saengsawang W, Yu JZ, Donati R, Rasenick MM. Heterotrimeric G-Proteins Interact Directly with Cytoskeletal Components to Modify Microtubule-Dependent Cellular Processes. *Neurosignals*. 2009;17(1):100-8.
98. Roychowdhury S, Rasenick MM. G Protein $\beta_1\gamma_2$ Subunits Promote Microtubule Assembly. *Journal of Biological Chemistry*. 1997;272(50):31576-81.
99. Wu H-C, Huang P-H, Chiu C-Y, Lin C-T. G protein β_2 subunit antisense oligonucleotides inhibit cell proliferation and disorganize microtubule and mitotic spindle organization. *Journal of Cellular Biochemistry*. 2001;83(1):136-46.
100. Zwaal RR, Ahringer J, van Luenen HG, Rushforth A, Anderson P, Plasterk RH. G proteins are required for spatial orientation of early cell cleavages in *C. elegans* embryos. *Cell*. 1996;86(4):619-29.
101. Gotta M, Ahringer J. Distinct roles for $G\alpha$ and $G\beta\gamma$ in regulating spindle position and orientation in *Caenorhabditis elegans* embryos. *Nat Cell Biol*. 2001;3(3):297-300.
102. Fuse N, Hisata K, Katzen AL, Matsuzaki F. Heterotrimeric G proteins regulate daughter cell size asymmetry in *Drosophila* neuroblast divisions. *Curr Biol*. 2003;13(11):947-54.
103. Sanada K, Tsai L-H. G Protein $\beta\gamma$ Subunits and AGS3 Control Spindle Orientation and Asymmetric Cell Fate of Cerebral Cortical Progenitors. *Cell*. 2005;122(1):119-31.
104. Obin M, Lee BY, Meinke G, Bohm A, Lee RH, Gaudet R, et al. Ubiquitylation of the Transducin $\beta\gamma$ Subunit Complex: REGULATION BY PHOSDUCIN. *Journal of Biological Chemistry*. 2002;277(46):44566-75.
105. Hamilton MH, Cook LA, McRackan TR, Schey KL, Hildebrandt JD. γ_2 subunit of G protein heterotrimer is an N-end rule ubiquitylation substrate. *Proceedings of the National Academy of Sciences*. 2003;100(9):5081-6.
106. Gonda DK, Bachmair A, Wüning I, Tobias JW, Lane WS, Varshavsky A. Universality and structure of the N-end rule. *Journal of Biological Chemistry*. 1989;264(28):16700-12.
107. Dores MR, Trejo J. Ubiquitination of G Protein-Coupled Receptors: Functional Implications and Drug Discovery. *Molecular Pharmacology*. 2012;82(4):563-70.
108. Shenoy SK, Xiao K, Venkataramanan V, Snyder PM, Freedman NJ, Weissman AM. Nedd4 mediates agonist-dependent ubiquitination, lysosomal targeting, and degradation of the beta2-adrenergic receptor. *J Biol Chem*. 2008;283(32):22166-76.
109. Brockmann M, Blomen VA, Nieuwenhuis J, Stickel E, Raaben M, Bleijerveld OB, et al. Genetic wiring maps of single-cell protein states reveal an off-switch for GPCR signalling. *Nature*. 2017;546(7657):307-11.
110. Adelfinger L, Turecek R, Ivankova K, Jensen AA, Moss SJ, Gassmann M, et al. GABAB receptor phosphorylation regulates KCTD12-induced $K(+)$ current desensitization. *Biochem Pharmacol*. 2014;91(3):369-79.
111. Bayon Y, Trinidad AG, de la Puerta ML, Del Carmen Rodriguez M, Bogetz J, Rojas A, et al. KCTD5, a putative substrate adaptor for cullin3 ubiquitin ligases. *FEBS J*. 2008;275(15):3900-10.
112. Campden R. Investigating G protein beta gamma subunit interactions with nuclear proteins: McGill University; 2015.
113. Sowa ME, Bennett EJ, Gygi SP, Harper JW. Defining the human deubiquitinating enzyme interaction landscape. *Cell*. 2009;138(2):389-403.
114. Campden R, Petrin D, Robitaille M, Audet N, Gora S, Angers S, et al. Tandem affinity purification to identify cytosolic and nuclear gbetagamma-interacting proteins. *Methods in molecular biology (Clifton, NJ)*. 2015;1234:161-84.

115. Liu Z, Xiang Y, Sun G. The KCTD family of proteins: structure, function, disease relevance. *Cell Biosci.* 2013;3(1):45.
116. Skoblov M, Marakhonov A, Marakasova E, Guskova A, Chandhoke V, Birerdinc A, et al. Protein partners of KCTD proteins provide insights about their functional roles in cell differentiation and vertebrate development. *Bioessays.* 2013;35(7):586-96.
117. Ardley HC, Robinson PA. E3 ubiquitin ligases. *Essays in biochemistry.* 2005;41:15-30.
118. Hershko A, Ciechanover A. The ubiquitin system. *Annu Rev Biochem.* 1998;67:425-79.
119. Smaldone G, Pirone L, Balasco N, Di Gaetano S, Pedone EM, Vitagliano L. Cullin 3 Recognition Is Not a Universal Property among KCTD Proteins. *PLoS One.* 2015;10(5):e0126808.
120. Cojocar M, Bouchard A, Cloutier P, Cooper JJ, Varzavand K, Price DH, et al. Transcription factor IIS cooperates with the E3 ligase UBR5 to ubiquitinate the CDK9 subunit of the positive transcription elongation factor B. *J Biol Chem.* 2011;286(7):5012-22.
121. Bedford L, Paine S, Sheppard PW, Mayer RJ, Roelofs J. Assembly, Structure and Function of the 26S proteasome. *Trends Cell Biol.* 2010;20(7):391-401.
122. Tasaki T. The Substrate Recognition Domains of the N-end Rule. 2009;284(3):1884-95.
123. Pickart CM. Ubiquitin enters the new millennium. *Molecular cell.* 2001;8(3):499-504.
124. Sato Y, Yamagata A, Goto-Ito S, Kubota K, Miyamoto R, Nakada S, et al. Molecular basis of Lys-63-linked polyubiquitination inhibition by the interaction between human deubiquitinating enzyme OTUB1 and ubiquitin-conjugating enzyme UBC13. *J Biol Chem.* 2012;287(31):25860-8.
125. McKenna S, Spyropoulos L, Moraes T, Pastushok L, Ptak C, Xiao W, et al. Noncovalent interaction between ubiquitin and the human DNA repair protein Mms2 is required for Ubc13-mediated polyubiquitination. *J Biol Chem.* 2001;276(43):40120-6.
126. Xiao W, Lin SL, Broomfield S, Chow BL, Wei YF. The products of the yeast MMS2 and two human homologs (hMMS2 and CROC-1) define a structurally and functionally conserved Ubc-like protein family. *Nucleic Acids Res.* 1998;26(17):3908-14.
127. Matera AG, Wang Z. A day in the life of the spliceosome. *Nature Reviews Molecular Cell Biology.* 2014;15:108.
128. Cooper GM. *The Mechanism of Oxidative Phosphorylation.* 2nd edition ed: Sunderland (MA): Sinauer Associates; 2000.
129. Gene [Internet]. Bethesda (MD): National Library of Medicine (US), National Center for Biotechnology Information; 2004.
130. Wiedemann N, Frazier AE, Pfanner N. The protein import machinery of mitochondria. *J Biol Chem.* 2004;279(15):14473-6.
131. Greber BJ, Ban N. Structure and Function of the Mitochondrial Ribosome. *Annu Rev Biochem.* 2016;85:103-32.
132. Kaur G, Dufour JM. Cell lines: Valuable tools or useless artifacts. *Spermatogenesis.* 2012;2(1):1-5.
133. Meyer K, Selbach M. Quantitative affinity purification mass spectrometry: a versatile technology to study protein–protein interactions. *Frontiers in Genetics.* 2015;6:237.
134. DeBerardinis RJ, Thompson CB. Cellular metabolism and disease: what do metabolic outliers teach us? *Cell.* 2012;148(6):1132-44.

135. Kim EJ, Kim SH, Jin X, Jin X, Kim H. KCTD2, an adaptor of Cullin3 E3 ubiquitin ligase, suppresses gliomagenesis by destabilizing c-Myc. *Cell Death Differ.* 2017;24(4):649-59.
136. Boada M, Antunez C, Ramirez-Lorca R, DeStefano AL, Gonzalez-Perez A, Gayan J, et al. ATP5H/KCTD2 locus is associated with Alzheimer's disease risk. *Mol Psychiatry.* 2014;19(6):682-7.
137. Bartoi T, Rigbolt KT, Du D, Kohr G, Blagoev B, Kornau HC. GABAB receptor constituents revealed by tandem affinity purification from transgenic mice. *J Biol Chem.* 2010;285(27):20625-33.
138. Ivankova K, Turecek R, Fritzius T, Seddik R, Prezeau L, Comps-Agrar L, et al. Up-regulation of GABA(B) receptor signaling by constitutive assembly with the K⁺ channel tetramerization domain-containing protein 12 (KCTD12). *J Biol Chem.* 2013;288(34):24848-56.
139. Turecek R, Schwenk J, Fritzius T, Ivankova K, Zolles G, Adelfinger L, et al. Auxiliary GABAB receptor subunits uncouple G protein betagamma subunits from effector channels to induce desensitization. *Neuron.* 2014;82(5):1032-44.
140. Lee MT, Chen CH, Lee CS, Chen CC, Chong MY, Ouyang WC, et al. Genome-wide association study of bipolar I disorder in the Han Chinese population. *Mol Psychiatry.* 2011;16(5):548-56.
141. Cathomas F, Stegen M, Sigrist H, Schmid L, Seifritz E, Gassmann M, et al. Altered emotionality and neuronal excitability in mice lacking KCTD12, an auxiliary subunit of GABAB receptors associated with mood disorders. *Transl Psychiatry.* 2015;5:e510.
142. Li L, Duan T, Wang X, Zhang RH, Zhang M, Wang S, et al. KCTD12 Regulates Colorectal Cancer Cell Stemness through the ERK Pathway. *Sci Rep.* 2016;6:20460.
143. Uzozie AC, Selevsek N, Wahlander A, Nanni P, Grossmann J, Weber A, et al. Targeted Proteomics for Multiplexed Verification of Markers of Colorectal Tumorigenesis. *Mol Cell Proteomics.* 2017;16(3):407-27.
144. Suehara Y, Kondo T, Seki K, Shibata T, Fujii K, Gotoh M, et al. Pfetin as a prognostic biomarker of gastrointestinal stromal tumors revealed by proteomics. *Clin Cancer Res.* 2008;14(6):1707-17.
145. Kikuta K, Gotoh M, Kanda T, Tochigi N, Shimoda T, Hasegawa T, et al. Pfetin as a prognostic biomarker in gastrointestinal stromal tumor: novel monoclonal antibody and external validation study in multiple clinical facilities. *Jpn J Clin Oncol.* 2010;40(1):60-72.
146. Kubota D, Orita H, Yoshida A, Gotoh M, Kanda T, Tsuda H, et al. Pfetin as a prognostic biomarker for gastrointestinal stromal tumor: validation study in multiple clinical facilities. *Jpn J Clin Oncol.* 2011;41(10):1194-202.
147. Kubota D, Okubo T, Saito T, Suehara Y, Yoshida A, Kikuta K, et al. Validation study on pfetin and ATP-dependent RNA helicase DDX39 as prognostic biomarkers in gastrointestinal stromal tumour. *Jpn J Clin Oncol.* 2012;42(8):730-41.
148. Kubota D, Mukaihara K, Yoshida A, Suehara Y, Saito T, Okubo T, et al. The prognostic value of pfetin: a validation study in gastrointestinal stromal tumors using a commercially available antibody. *Jpn J Clin Oncol.* 2013;43(6):669-75.
149. Orita H, Ito T, Kushida T, Sakurada M, Maekawa H, Wada R, et al. Pfetin as a risk factor of recurrence in gastrointestinal stromal tumors. *Biomed Res Int.* 2014;2014:651935.

SUPPLEMENTAL MATERIAL

Gene symbol	Full name
AHCY	Adenosylhomocysteinase
APIP	APAF1 interacting protein
ASNS	Asparagine synthetase (glutamine-hydrolyzing)
ATP5A1	ATP Synthase, H ⁺ Transporting, Mitochondrial F1 Complex, Alpha Subunit 1, Cardiac Muscle
ATP5B	ATP Synthase, H ⁺ Transporting, Mitochondrial F1 Complex, Beta Polypeptide
ATP5J2	ATP Synthase, H ⁺ Transporting, Mitochondrial Fo Complex Subunit F2
ATP6V0A1	ATPase H ⁺ Transporting V0 Subunit A1
ATP6V0D1	ATPase H ⁺ Transporting V0 Subunit D1
ATP6V1A	ATPase H ⁺ Transporting V1 Subunit A
ATP6V1B2	ATPase H ⁺ Transporting V1 Subunit B2
BCAT1	Branched chain amino acid transaminase 1
BLVRA	Biliverdin reductase A
CHCHD3	Coiled-Coil-Helix-Coiled-Coil-Helix Domain Containing 3
CMBL	Carboxymethylenebutenolidase homolog
COMT	Catechol-o-methyltransferase
COX17	Cytochrome c oxidase copper chaperone
COX2	Mitochondrially Encoded Cytochrome C Oxidase II
COX4I1	Cytochrome C Oxidase Subunit 4I1
COX5A	Cytochrome C Oxidase Subunit 5A
COX7A2	Cytochrome C Oxidase Subunit 7A2
CTPS1	CTP synthase 1
CYC1	Cytochrome C1
DAP3	Death Associated Protein 3
DDX23	DEAD-Box Helicase 23
DDX46	DEAD-Box Helicase 46
DUT	Deoxyuridine triphosphate
EFTUD2	Elongation Factor Tu GTP Binding Domain Containing 2
ENO1	Enolase 1
EPRS	Glutamyl-prolyl-TRNA synthetase
FASN	Fatty acid synthase
GALM	Galactose mutarotase
GANAB	Glucosidase II alpha subunit

GART	Trifunctional purine biosynthetic protein adenosine-3
GLUL	Glutamate-ammonia ligase
HNRNPC	Heterogeneous Nuclear Ribonucleoprotein C (C1/C2)
HPRT1	Hypoxanthine phosphoribosyltransferase 1
HSPA6	Heat Shock Protein Family A (Hsp70) Member 6
HSPD1	Heat Shock Protein Family D (Hsp60) Member 1
INPP5B	Inositol polyphosphate-5-phosphatase B
KCTD12	Potassium Channel Tetramerization Domain Containing 12
KCTD17	Potassium Channel Tetramerization Domain Containing 17
KCTD2	Potassium Channel Tetramerization Domain Containing 2
KCTD5	Potassium Channel Tetramerization Domain Containing 5
LDHC	Lactate dehydrogenase C
MAN2A2	Mannosidase alpha class 2A member 2
MRPL12	Mitochondrial Ribosomal Protein L12
MRPL17	Mitochondrial Ribosomal Protein L17
MRPL4	Mitochondrial Ribosomal Protein L4
MRPL43	Mitochondrial Ribosomal Protein L43
MRPL46	Mitochondrial Ribosomal Protein L46
MRPL49	Mitochondrial Ribosomal Protein L49
MRPS18B	Mitochondrial Ribosomal Protein S18B
MRPS27	Mitochondrial Ribosomal Protein S27
MRPS35	Mitochondrial Ribosomal Protein S35
MRPS5	Mitochondrial Ribosomal Protein S5
NAA38	N(alpha)-Acetyltransferase 38, NatC Auxiliary Subunit
NAPRT	Nicotinate phosphoribosyltransferase
NDUFA4	NADH Dehydrogenase (Ubiquinone) 1 Alpha Subcomplex , 4
NDUFA9	NADH Dehydrogenase (Ubiquinone) 1 Alpha Subcomplex , 9
NDUFS1	NADH:Ubiquinone Oxidoreductase Core Subunit S1
NDUFS2	NADH:Ubiquinone Oxidoreductase Core Subunit S2
NDUFS3	NADH:Ubiquinone Oxidoreductase Core Subunit S3
NDUFS7	NADH:Ubiquinone Oxidoreductase Core Subunit S7
NDUFS8	NADH:Ubiquinone Oxidoreductase Core Subunit S8
NME1	NME/NM23 nucleoside diphosphate kinase 1
NME2	NME/NM23 nucleoside diphosphate kinase 2
P4HA2	Prolyl 4-hydroxylase subunit alpha 2
PAICS	Phosphoribosylaminoimidazole Carboxylase And Phosphoribosylaminoimidazolesuccinocarboxamide Synthase

PANK3	Pantothenate kinase 3
PDXK	Pyridoxal kinase
PHGDH	Phosphoglycerate dehydrogenase
PKM	Pyruvate kinase 2/3
PLCZ1	Phospholipase c zeta 1
PNPO	Pyridoxamine 5'-phosphate oxidase
PPIL1	Peptidylprolyl Isomerase Like 1
PRDX6	Peroxiredoxin 6
PRPF19	pre-mRNA processing factor 19
PRPF6	pre-mRNA processing factor 6
PRPF8	pre-mRNA processing factor 8
PRPS1	Phosphoribosyl pyrophosphate synthetase 1
PRPS2	Phosphoribosyl pyrophosphate synthetase 2
PSMC1	Proteasome 26S Subunit, ATPase 1
PSMC2	Proteasome 26S Subunit, ATPase 2
PSMC3	Proteasome 26S Subunit, ATPase 3
PSMC4	Proteasome 26S Subunit, ATPase 4
PSMC6	Proteasome 26S Subunit, ATPase 6
PSMD1	Proteasome 26S Subunit, Non-ATPase 1
PSMD11	Proteasome 26S Subunit, Non-ATPase 11
PSMD13	Proteasome 26S Subunit, Non-ATPase 13
PSMD2	Proteasome 26S Subunit, Non-ATPase 2
PSMD3	Proteasome 26S Subunit, Non-ATPase 3
PSMD7	Proteasome 26S Subunit, Non-ATPase 7
PTGES3	Prostaglandin E synthase 3
QARS	Glutaminyl-TRNA synthetase
RBM17	RNA Binding Motif Protein 17
RBMX	RNA Binding Motif Protein, X-Linked
SF3A1	Splicing Factor 3a Subunit 1
SF3B3	Splicing Factor 3b Subunit 3
SLC16A1	Solute Carrier Family 16 Member 1
SLC25A1	Solute Carrier Family 25 Member 1
SLC25A10	Solute Carrier Family 25 Member 10
SLC25A11	Solute Carrier Family 25 Member 11
SLC25A12	Solute Carrier Family 25 Member 12
SLC25A13	Solute Carrier Family 25 Member 13

SLC25A18	Solute Carrier Family 25 Member 18
SLC25A24	Solute Carrier Family 25 Member 24
SLC25A3	Solute Carrier Family 25 Member 3
SNRNP200	Small Nuclear Ribonucleoprotein U5 Subunit 200
SNRNP70	Small Nuclear Ribonucleoprotein U1 Subunit 70
SNRPB	Small Nuclear Ribonucleoprotein Polypeptides B And B1
SNRPC	Small Nuclear Ribonucleoprotein Polypeptide C
SNRPD2	Small Nuclear Ribonucleoprotein D2 Polypeptide
SNRPD3	Small Nuclear Ribonucleoprotein D3 Polypeptide
SNRPE	Small Nuclear Ribonucleoprotein Polypeptide E
SNRPG	Small Nuclear Ribonucleoprotein Polypeptide G
SRSF1	Serine and Arginine Rich Splicing Factor 1
SRSF2	Serine and Arginine Rich Splicing Factor 2
SRSF3	Serine and Arginine Rich Splicing Factor 3
SRSF5	Serine and Arginine Rich Splicing Factor 5
SRSF6	Serine and Arginine Rich Splicing Factor 6
SRSF7	Serine and Arginine Rich Splicing Factor 7
SRSF8	Serine and Arginine Rich Splicing Factor 8
TIMM8A	Translocase of Inner Mitochondrial Membrane 8A
TOMM22	Translocase of Outer Mitochondrial Membrane 22
TRA2A	Transformer 2 Alpha Homolog
U2SURP	U2 SnRNP Associated SURP Domain Containing
UBE2V2	Ubiquitin Conjugating Enzyme E2 V2
UBR4	Ubiquitin Protein Ligase E3 Component N-Recognin 4
UBR5	Ubiquitin Protein Ligase E3 Component N-Recognin 5
UQCRH	Ubiquinol-cytochrome c reductase hinge protein
VDAC1	Voltage Dependent Anion Channel 1

Supplemental Table 1: Full names for proteins from Thesis Chapter 3.2 and 3.4

Gene symbols and full names extracted from GeneCards- Human Gene Database, retrieved Nov. 2017, URL: www.genecards.org.

Flag-Gβ1 interactors in KCTD5 KO cell line only	Flag-Gβ1 interactors common in both cell lines	Flag-Gβ1 interactors in parental cell line only
AMOT*	CAD	ALB
BANF1*	CCT2	ATP5A1
CDK1*	CCT3	GNB2
EEF1G*	CCT4	GNG12
EEF2*	CCT5	HSPA6
FLNA*	CCT6A	KCTD2
PHGDH*	CCT7	KCTD5
RRP1	DNAJA1	42800
TAGLN2*	DNAJA2	ACTG1
YWHAQ*	DSP	ADAMTS6
ABCA7	GNAI1	ADGRF2
ABCB1	GNB1	AGPAT1
ACTB	GNG5	AGTRAP
ACTG2	HSPD1	AMD1
ACTR1A	KCTD12	ANKEF1
ADARB1	PDCL	ANKRD24
AFDN	PFDN4	AP3B1
AHCY	TCP1	APC2
AKNA	TRIM28	APOC2
ANKRD28	TUBA1A	ARHGAP21
APIP	TUBB3	ARHGEF11
ARHGDIA	TUBB4A	ARIH1
ASNS	UBR5	ATP5B
ATP12A	VBPI	AZGP1
ATXN7L2	ARL6IP4	B3GALT1
BCAT1	BAG2	BAHCC1
BLVRA	BAG6	BRCA1
BNC2	CCDC25	C17orf47
BOLA2; BOLA2B	CCT8	C20orf204
C10orf95	CHD6	C7orf72
C11orf84	CLNS1A	CABP5
C16orf92	CTSB	CACNA1B
C1QBP	DDB1	CALML5
CACYBP	DENND5B	CASP14
CALM	DNAJC7	CCDC154
calm1	DOCK3	CCDC155
Calm2	EAF2	CCDC186

calm2-a	EEF1A1	CCDC39
calm2-b	EFTUD2	CCDC88A
Calm3	EIF3B	CCDC88C
CALN1	EIF3D	CDAN1
CALR	ERH	CENPA
CAMK1	GAPDH	CEP97
CAPZB	GEMIN4	CFAP43
CCDC87	HECTD1	CFTR
CD3E	HNRNPH1	CLDN23
CDC42BPG	HNRNPK	CLK3
CDKL1	HNRNPM	CLUAP1
CENPF	HSP90AA1	CNGA3
CEP164	HSP90AB1	CPQ
CEP170	HSPA1A	CTSD
CFL1	HSPA1L	CYCS
CLCF1	HSPA2	DCD
CLCNKA	HSPA5	DCLK2
CLIP1	HSPA8	DDX20
CLTC	HSPA9	DMRT2
CMBL	HUWE1	DNAJA3
CNBP	IGKV2D-28	DNAJB1
COA4	IRS4	DOCK4
COL11A1	IVNS1ABP	DOCK7
COMT	KIF11	DPYSL5
CORO2A	KRT1	DSC3
COX17	KRT10	DSG1
CRELD2	KRT14	E2F7
CRIM1	KRT16	EIF3G
CTNNB1	KRT2	EMC10
CTPS1	KRT9	EPAS1
CUL9	LONP1	EPHA4
DCAF8	NAP1L1	EXOC3
DDX5	NCL	FAM78A
DNAH1	NPM1	FAM92A
DNAJA4	P4HA1	FLG2
DNASE2B	PFDN1	FOXK2
DOCK8	PFDN2	FPGT
DOPEY1	PFDN5	FRYL

DSCAML1	PFDN6	GAL3ST4
DSTN	PLOD1	GEMIN2
DUT	PRDX1	GEMIN5
DYNLL2	PRDX2	GEMIN6
DYNLRB2	PRKDC	GEMIN8
EEF1B2	PRMT5	GNAT1
EEF1D	PRPF31	GNB4
EFCAB14	PRPSAP1	GNG10
EIF2S1	RACK1	GOLGA2
EIF3A	RBBP7	GPR179
EIF3CL	RCN2	GREB1L
EIF3E	RNF126	GSX1
EIF3F	RPL11	HDX
EIF3I	RPL5	HMGN5
EIF3K	RPLP0	HNRNPU
EIF3L	RPLP1	HSPA12B
EIF4A1	RPLP2	IGHG4
EIF5AL1	RPS10	ILF2
EIF6	RPS18	IMPG2
EMILIN1	RPS8	IQCB1
ENO1	RPSA	IQUB
EPB41L5	RUVBL1	KCNJ16
EPM2AIP1	RUVBL2	KDM1B
ERBB4	SNRPB	KDM8
ERP29	SNRPD1	KIAA1328
FAM208A	SNRPD2	KMT2C
FARSB	SNRPD3	KMT2D
FASN	SNRPE	KPRP
FAT4	STIP1	KRT5
FEM1C	STK38	KRT6C
FGD6	STRAP	LMTK2
FLOT2	STUB1	LRIG3
FRMPD1	TUBA1B	LRRC49
FSTL1	TUBA1C	LTBP1
GALM	TUBB	LUC7L2
GANAB	TUBB2B	MAB21L2
GART	TUBB4B	MAP3K11
GHDC	TUBB6	MAP7D3

GLO1	TXNDC12	MAST4
GLUL	WDR77	MERTK
GOLGA4	XRCC6	MIB2
GORAB	ZSCAN25	MMRN2
GSTM3		MTA3
GSTP1		NAB2
GVINP1		NHSL2
H2AFV		NLGN2
HERC2P3		NOX1
HEY1		NSD1
HISTONE H4		NUMA1
HNRNPF		PGM1
HPRT1		PHACTR1
HSPA4		PIWIL3
HSPA4L		PLEKHA6
HSPBP1		PPARGC1B
HSPH1		PPM1L
IGBP1		PRAG1
INPP5B		PROB1
JAKMIP2		PRPF19
KIAA1161		PRPF40B
KIF3A		PRSS1
KNDC1		RALGAPA1
KPNB1		RBM12B
KRT6A		RILP
LANCL1		RINT1
LANCL2		RNF219
LCP1		ROR2
LDHC		RPAP1
LUZP1		RPL10
LVRN		RPL12
LY6G6F		RPL13
MAN2A2		RPL14
MED12		RPL18
MED13L		RPL23
MED27		RPL26L1
MIF		RPL38
MIOX		RPL4
MIS18A		RPL6

MLLT11		RPL7A
MPC2		RPS11
MSANTD4		RPS14
MTPN		RPS15
MYL6		RPS16
N4BP3		RPS19
NAPA		RPS2
NAPRT		RPS27A
NASP		RPS4X
NDFIP2		RPUSD2
NDRG1		RYR2
NF1		S100A7
NHLRC2		S100A8
NISCH		S100A9
NLRP12		SCAMP3
NME1		SHPRH
NME2		SLC1A1
NOD1		SMC3
NPR3		SMN1; SMN2
NSF		SPATA21
NT5DC2		SPDYC
NUDC		SPTBN2
NUP210L		SRGAP1
ORC6		STX6
P2RX7		SYTL5
P4HA2		TBC1D1
P4HB		TBC1D31
PABPC1		TBR1
PAICS		TIGIT
PANK3		TIRAP
PARK7		TMEM30B
PCBP1		TNNI1
PCMT1		TP53TG5
PCNX2		TRHDE
PCTP		TRIM66
PDCD5		TTC28
PDCL3		TTC3
PDE8A		TYK2

PDIA6		USP9Y
PDXK		VAMP3
PDZK1P1		WDR37
PFN2		YWHAZ
PGBD3		ZBTB8A
PHF2		ZFAT
PHLPP1		ZHX2
PIGG		ZNF281
PKM		ZNF806
PLBD2		ZNF83
PLCZ1		ZRANB3
PNPO		
POU3F1		
PPA1		
PPIA		
PPM1B		
PPM1G		
PPP2CB		
PPP6C		
PPP6R3		
PRDM2		
PRDX3		
PRDX4		
PRDX6		
PRMT1		
PRPF8		
PRPS1		
PRPS2		
PRPSAP2		
PSMD1		
PSMD6		
PTGES3		
QARS		
RAN		
RAX		
RC3H2		
RCC2		
RNF32		

RNF41		
RPL10L		
RPL22		
RPL24		
RPL7		
RPS12		
RPS21		
RPS28		
RPS3A		
RTEL1		
RUNX1T1		
SBF1		
SCN11A		
SCNN1D		
SF3B3		
SIGLEC11		
SKP1		
SLC11A2		
SLC27A4		
SLC35F3		
SNRNP200		
SNRPF		
SNRPG		
SPC24		
SPTAN1		
SSBP1		
SUB1		
SYK		
SYNM		
SYT3		
TACC2		
TANC2		
THOP1		
TMEM50A		
TMEM78		
TNRC18		
TNRC6B		
TOP1		

TPM1		
TRAPPC1		
TRIM21		
TRPC6		
TRPM5		
TRRAP		
TSKS		
TTC38		
TXN		
TXNDC5		
UBA52		
UCHL1		
UQCRH		
USP15		
VPS13D		
VPS36		
VPS39		
VPS54		
WARS		
WIPF2		
WRNIP1		
WWC3		
XRCC1		
XRCC5		
YWHAE		
YWHAG		
ZCCHC6		
ZNF75CP		
ZNRF4		
ZRANB2		

Supplemental Table 2: Full list of Gβγ protein interaction changes with KCTD5 KO

All interactors identified from MS screen of Flag-Gβ1 IP in parental and KCTD5 KO HEK 293 cell lines categorized as indicated within columns 1-3. Red font indicates interactors were identified in the Campden basal Flag-Gβ1 IP MS proteomic screen. In column 1, the red font indicates the interactors were identified in Campden screen whereas they were absent in the

parental IP. * indicates the interactors were present in parental Flag-G β 1 unbound lysate screen demonstrating proteins are detectable by MS, but were not found to be bound to Flag-G β 1.